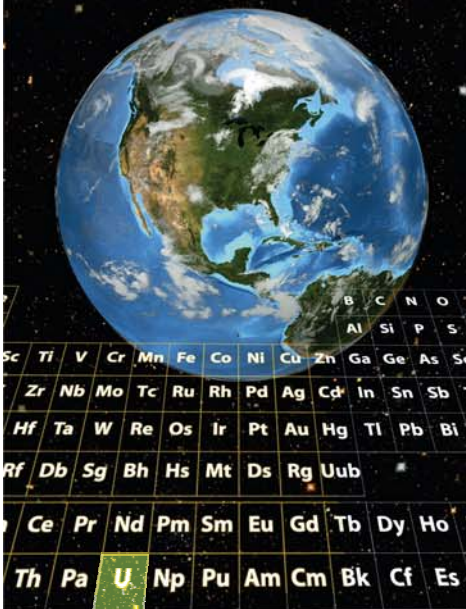# Environmental Sciences Laboratory

Natural Contamination from the Mancos Shale

April 2011

Prepared for

U.S. DEPARTMENT OF ENERGY

Legacy
Management

Cover Photo: Mancos Shale Near Loutsenhizer Arroyo.

Natural Contamination from the Mancos Shale

April 2011

This page intentionally left blank

Contents

Figures

Tables

Appendixes

Abbreviations

General

AR	activity ratio (of U-234 to U-238)
DOC	dissolved organic carbon
DOE	U.S. Department of Energy
g/cm^3	grams per cubic centimeter
gpm	gallons per minute
ICP	inductively coupled plasma
kg	kilogram
KPA	kinetic phosphorescence analysis
m^2/g	square meters per gram
meq/100 g	milliequivalents per hundred grams
mg/L	milligrams per liter
mg/kg	milligrams per kilogram
μg/L	micrograms per liter
μS/cm	microsiemens per centimeter
NURE	National Uranium Resource Evaluation
NWIS	National Water Information Service
pCi/L	picocuries per liter
SC	specific conductivity
USGS	U.S. Geological Survey

Sampling Locations

BAS	Bert Avery Spring
BCWL	Bostwick Canal West Lateral
BGS	Blue Gate Spring
BPS	Buen Pastor Spring
BSCS	Bitter Spring Creek Seep
BSCUS	Bitter Spring Creek Upper Spring
BWS	Browns Wash Seep
CAS	Cato Springs
CCS	Cedar Creek Seep
CIS	Cisco Springs

CWCS	Cottonwood Creek Spring
D9S	Ditch 9 Spring
DAR	Daly Reservoir
DARS1	Daly Reservoir Spring 1
DARS2	Daly Reservoir Spring 2
DR	Delta Reservoir
DRDS	Delta Reservoir Dam Spring
DRS1	Delta Reservoir Seep 1
DRS3	Delta Reservoir Seep 3
DTS1	Devils Thumb Seep 1
DTS2	Devils Thumb Seep 2
DTS3	Devils Thumb Seep 3
DWS	Dutchmans Wash Seep
EF-22	Many Devils Wash EF-22
ETFW	East Tributary Floy Wash
ETFWD	East Tributary Floy Wash Downstream
GRCRS	Green River Canal Return Seep
HGRP	Houston Gulch Red Pool
HGS	Houston Gulch Seep
HGSE	Houston Gulch Seep East
KCFS	Kannah Creek Flowline Spring
LGW	Little Grand Wash
LGWS	Little Grand Wash Seep
LOUT3	Loutsenhizer 3
LOUT8	Loutsenhizer 8
LUOT9	Loutsenhizer 9
LOUT11	Loutsenhizer 11
LOUT11W	Loutsenhizer 11 in Wash
LOUT12L	Loutsenhizer 12 Lower
LOUT12U	Loutsenhizer 12 Upper
LOUT13	Loutsenhizer 13
LOUT14	Loutsenhizer 14
MS	Mud Spring
MWS	Mathis Wash Seep

PCS	Point Creek Seep
S36	Section 36 Spring
SCWS	Salt Creek Wash Seep
SL	Sweitzer Lake
SNGC	Sweitzer Lake NE Garnet Canal
SNS	Sweitzer NE Seep
SNS1	Sweitzer NE Seep 1
SNS2	Sweitzer NE Seep 2
SNS3	Sweitzer NE Seep 3
SRP	Sweitzer Red Pool
TWS	Town Wash Spring
TWSP	Town Wash Spring Pool
UENAS	Upper Eagle Nest Arroyo Spring
UFWS	Upper Floy Wash Spring
UFWS1	Upper Floy Wash 30 ft from Spring
UFWS2	Upper Floy Wash 50 ft from Spring
US1	USGS Seep 1
WCTS	Whitewater Creek Tributary Seep
WCTSP1	Whitewater Creek Tributary Seep Pool 1
WCTSP2	Whitewater Creek Tributary Seep Pool 2
WD2S	Whitewater Ditch No. 2 Seep
WD2	Whitewater Ditch No. 2
WFFW	West Fork Floy Wash
YHS	Yucca House Spring

This page intentionally left blank

Executive Summary

Uranium mill tailings disposal cells in Colorado and New Mexico have been constructed on dark-gray shale bedrock of the Upper Cretaceous Mancos Shale, and a new disposal cell is being constructed on Mancos Shale in Utah. It has long been known and discussed by many researchers that the Mancos Shale is a source of salts, selenium, and trace metals. These constituents can in turn contribute to groundwater contamination. There is a need to consider the release of potential contaminants by natural processes when evaluating the progress of groundwater remediation efforts at disposal sites built on Mancos Shale.

We sampled Mancos Shale groundwater at 51 locations in Colorado, New Mexico, and Utah, mostly from shale beds but also from some sandstones and alluvial gravels. Because the Mancos Shale does not typically yield much groundwater, most samples were collected from seeps and springs. Many of the groundwater samples were highly saline, as indicated by specific conductivity values ranging from 418 to 70,002 microsiemens per centimeter (µS/cm) with a geometric mean of 9,226 µS/cm. Samples collected at nine locations had specific conductivity values of more than 30,000 µS/cm. Nitrate concentrations exceeded 250 milligrams per liter (mg/L) at 13 locations, and selenium concentrations exceeded 1,000 micrograms per liter (µg/L) in eight samples. Uranium concentrations were also high, having a range of 0.2 to 1,922 µg/L with a geometric mean of 48.8 µg/L, and samples from 18 locations had concentrations more than 100 µg/L. At several locations, seep water was colored yellow to red; the coloration was caused by dissolved organic carbon concentrations up to 280 mg/L. Boron concentrations exceeding 1,000 µg/L were common in groundwater from shale beds, but lower values were found in groundwater from sandstone.

All uranium-234 to uranium-238 activity ratios (ARs) were greater than the secular equilibrium value of 1.0. All but three of the AR values were more than 1.5, and about half of the values exceeded 2.0. Thus, high AR values may be a common characteristic of groundwater that has interacted with Mancos Shale.

The results indicate that high concentrations of boron, major ions, nitrate, selenium, and uranium are likely to occur as a natural process of interaction between groundwater and Mancos Shale. The high concentrations are apparently limited to groundwater associated with shale beds, and concentrations of these constituents in groundwater associated with sandstone were much lower. High contaminant concentrations occurred throughout the study areas and were not correlated with geographic area, stratigraphic position, or source of water. Some of the samples were influenced by irrigation, but others were collected from locations in remote areas with no significant anthropogenic input.

In a few well-characterized areas, it was possible to define the source of recharge water and the groundwater flow path to the seeps. Seeps in several areas were fed from man-made ponds or reservoirs, and had historical documentation that allowed accurate assessments of the timing of the formation of the seeps. At one area, historical data were sufficient to determine that the groundwater flow rate through the shale beds of Mancos exceeded 8 feet per day.

A literature review of the solid-phase composition of Mancos Shale indicated that the shale is composed of quartz, feldspar, illite, smectite, interlayered clays, carbonates, sulfates, organic matter, and pyrite. Uranium and nitrate likely reside in or are closely associated with organic

matter, and selenium substitutes for sulfur in pyrite. Conceptually, major ion chemical reactions are dominated by calcite dissolution following proton release from pyrite oxidation and subsequent exchange by calcium for the sodium residing on clay mineral exchange sites. This conceptual model was tested numerically using a reaction progress approach. The modeling indicated that these reactions were able to explain the general features of groundwater chemical evolution.

1.0   Introduction

We define natural contamination as a process by which constituents are transferred from geologic materials (in this case, rock of the Mancos Shale) to groundwater in concentrations that could be harmful to human health or the environment. For this definition, the source of the groundwater may be anthropogenic but the water must be of a reasonably high quality prior to contacting the geologic source of the natural contamination. Although there are many factors that should be considered when relating concentrations of a dissolved constituent to the risks to human health or the environment, in this study we consider contaminants as concentrations that exceed regulated standards. Contaminants with concentrations that exceed standards by an order of magnitude or more, which for this study included uranium, selenium, and nitrate, are of special interest (Table 1). Although Table 1 presents national drinking water standards, other standards exist. For example, an aquatic life standard of 4.6 micrograms per liter (µg/L) has been established for selenium (Thomas 2009) and the State of New Mexico has a livestock drinking water standard of 100 µg/L for vanadium (Thomas et al. 1998).

Table 1. Contaminants Exceeding 10 Times the Maximum Contaminant Levels for Drinking Water in Seep and Spring Samples Analyzed for This Study(40 E-CFR 141)

	Drinking Water Standard	Range Measured In This Study	Geometric Mean
Uranium (µg/L)	30	0.2–1,922	49.7
Selenium (µg/L)	50	0.14–4,700	51.5
Nitrate (mg/L)	44	0.5–3,614	33.7

mg/L = milligrams per liter

Natural contamination of surface drainages, including the Colorado River, by salts and selenium from irrigation on marine shale formations in semiarid lands is well known (Laronne 1977; Wagenet and Jurinak 1978; Whittig et al. 1982, 1983, 1986; Laronne and Schumm 1982; Jackson and Julander 1982; Deyo 1984; Rao et al. 1984; Evangelou 1981; Evangelou et al. 1984; Wright and Butler 1993; Butler et al. 1991, 1994, 1996; Zielinski et al. 1995; Butler and Leib 2002; Kakouros et al. 2006; Thomas et al. 2008; Tuttle and Grauch 2009). A study of natural contamination was conducted by Littke et al. (1991) on black shale of the Jurassic Posidonia Shale in Germany. They developed a mass and volume balance that estimated constituent loss (potentially transferred to groundwater) during the weathering process and concluded that shale may significantly increase sulfur and organic carbon concentrations in the groundwater over those levels derived from local anthropogenic sources.

A goal of this project was to determine the distribution of natural contamination in Mancos Shale groundwater by measuring chemical concentrations in Mancos Shale seeps and springs from samples collected throughout much of its depositional basin. This information is directly relevant to evaluation of groundwater contamination at uranium mill tailings disposal sites that were constructed on the Mancos Shale. Because uranium is an important contaminant at U.S. Department of Energy (DOE) former uranium milling sites and tailings disposal sites, it is a contaminant of principal interest to this study. It is important to understand the possible contribution of natural uranium to background concentrations at these cleanup sites to ensure realistic cleanup standards and to evaluate the progress of site cleanup. Relatively few data exist on uranium concentrations in surface water or groundwater influenced by Mancos Shale.

Uranium mill tailings disposal cells were built on Mancos Shale near Grand Junction, Colorado, and Shiprock, New Mexico. These sites are administered by DOE's Office of Legacy Management. Under another program, DOE is currently (2011) relocating uranium tailings from a former milling site near Moab, Utah, to a disposal cell built on Mancos Shale at Crescent Junction, Utah (Figure 1).

Less-direct reasons for studying Mancos Shale groundwater chemistry include its role in the understanding of (1) contaminant loading to surface water, particularly the Colorado River, (2) uranium ore genesis, and (3) influence of natural carbon releases on the global carbon budget. These three secondary objectives are discussed briefly as follows:

(1)   Many studies have focused on the release of salt and selenium from the Mancos Shale and its effects on salt loading to the Colorado River. Notable research has been conducted by personnel at the U.S. Geological Survey (USGS) (Butler et al. 1991, 1994, 1996; Wright 1995, 1999; Butler and Leib 2002; Grauch et al. 2005; Tuttle et al. 2005, 2007; Thomas et al. 2008; Tuttle and Grauch 2009; Stillings et al. 2005), University of California, Davis, (Whittig et al. 1982, 1983, 1986; Deyo 1984; Evangelou et al. 1984, 1985), Utah State University (Jurinak et al. 1977; Wagenet and Jurinak 1978; Rao et al. 1984), Colorado State University (Laronne 1977; Ponce and Hawkins 1978; Sunday 1979; Laronne and Shen 1982; Laronne and Schumm 1982), and others (Jackson and Julander 1982). These studies are important because of issues with deteriorating water quality for downstream users, particularly in California and Mexico. Data collected for most of these studies are predominantly from samples of surface waters (streams, lakes, and canals) that flow to the Colorado River. Groundwater contribution of salt and selenium have also been investigated (e.g. Butler et al. 1994), but to a far lesser extent.

(2)   Although most theories of the origin of sandstone-type uranium ore deposits in the Colorado Plateau Province do not invoke a contribution from the Mancos Shale, Shawe (1976) proposed that uranium ore deposits in the Slick Rock District in southwest Colorado were formed by uranium-bearing groundwater that flowed downward from the Mancos Shale during burial compaction, depositing uranium in the organic-carbon-rich Morrison Formation. Shawe (1976) suggested that the fluids migrating from the Mancos were reducing, with uranium kept in solution by dissolved carbonate.

(3)   Petsch et al. (2000) determined that between 60 and 100 percent of the total organic carbon present in black shale can be released during weathering. Oxidation during weathering depletes oxygen from and adds carbon dioxide to the atmosphere. As shown in Figure 1, the Mancos Shale crops out over approximately 1,250 square miles in the Four Corners states. The vast area of Mancos and equivalent gray marine shale outcrops that are in Arizona, Colorado, Kansas, Montana, Nebraska, New Mexico, North Dakota, South Dakota, Utah, and Wyoming may provide sufficient carbon dioxide release to have an impact on the global carbon budget.
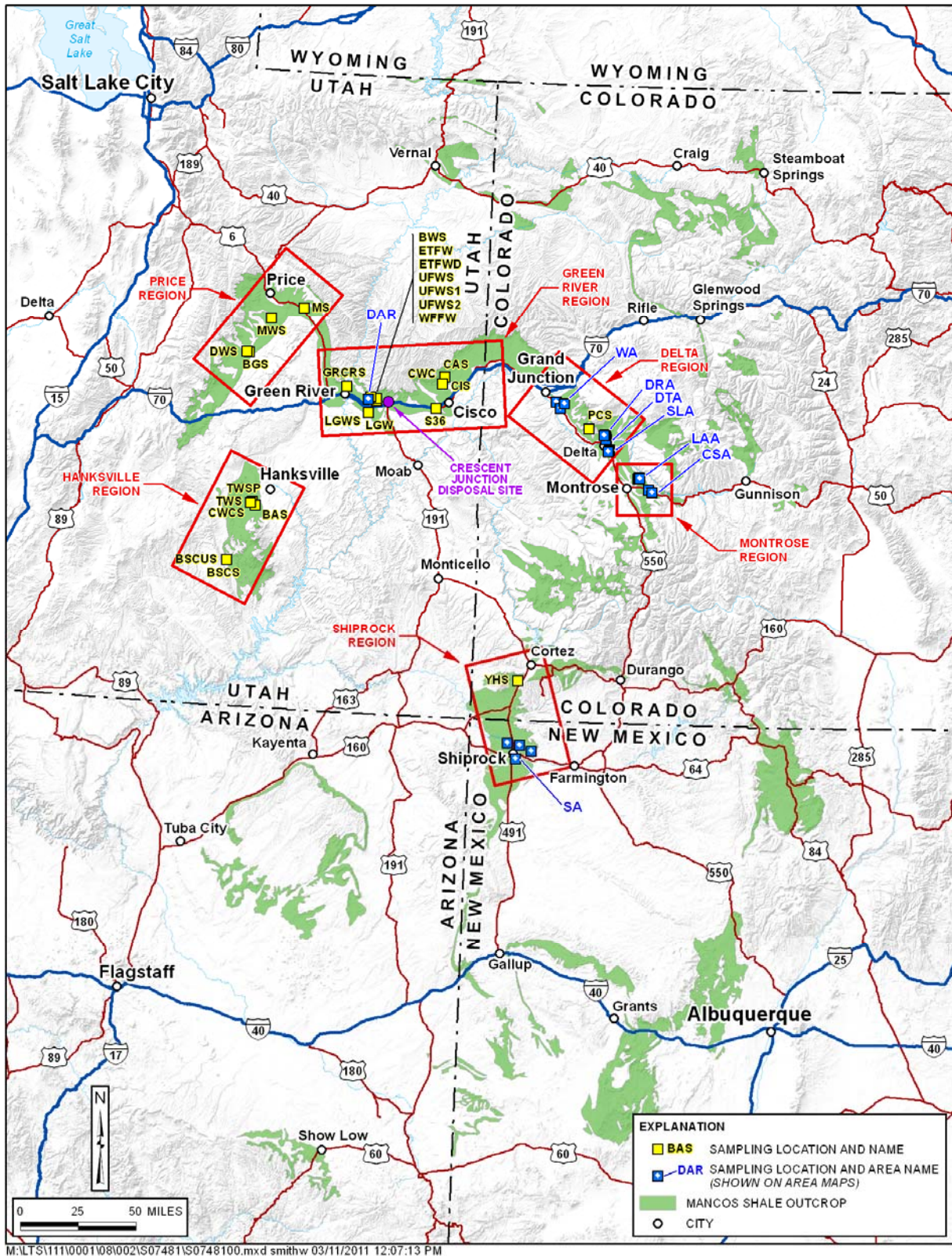
Figure 1. Locations of Sampling Regions and Mancos Shale Outcrops

CSA = Cerro Summit Area (Figure 10), DAR = Daly Reservoir Area (Figure 9), DRA = Delta Reservoir Area
(Figure 2), DTA = Devil's Thumb Golf Course Area (Figure 4), LAA = Loutsenhizer Arroyo Area (Figure 11),
SA = Shiprock Area (Figure 12), SLA = Sweitzer Lake Area (Figure 5), WA = Whitewater Area (Figure 6)

2.0   Geology of the Study Area

The Mancos Shale was deposited during the Late Cretaceous Epoch in the offshore and open-marine environment of the epicontinental Western Interior Seaway. The seaway corresponded to the Rocky Mountain foreland basin, an area of downwarping that developed as a result of active thrusting along the Sevier orogenic belt to the west (Johnson 2003). For about 13 to 15 million years, the slowly subsiding foreland basin accumulated sediment and ash-fall deposits from periodic uplift and volcanic activity in the Sevier highland to the west (Matthews et al. 2003).

The exposed formation reaches as much as 4,150 ft thick in west-central Colorado and east-central Utah (Fisher et al. 1960). Named by Cross and Purington (1899) for exposures in the valley around Mancos, Colorado, the Mancos Shale in that area is considerably thinner—only 2,238 ft, as measured in a section by Leckie et al. (1997).

The Mancos Shale represents the interplay of transgressive and regressive episodes of the seaway. Shale, mudstone, claystone, and limestone were deposited during transgressions, and sandstones were deposited during regressions. The lithologic variation around the depositional basin, reflecting the proximity to sediment sources in the Sevier highland, created a complicated nomenclature for the Mancos—Berman et al. (1980) referred to the nomenclature as "burdensome." Mancos Shale, as recognized in the Colorado Plateau and Southern Rocky Mountains, represents only part of the marine rocks formed in the western part of the seaway. Other formations represent these seaway deposits to the east and north. As thrusting progressed eastward in the Sevier orogenic belt with time, the west part of the seaway filled, and marine conditions shifted eastward where the Pierre Shale was deposited in eastern Colorado and in adjoining states to the east and north.

Mancos Shale nomenclature varied significantly across the Colorado Plateau in the six regions where samples were collected for this study. Figure 2 shows the various members of Mancos Shale for each of the sampled regions (Delta and Montrose Regions were combined because their Mancos Shale members are similar). Also shown in Figure 2 is a nomenclature column of Mancos-equivalent marine deposits for eastern Colorado where the Pierre Shale is present. In western Colorado, the upper part of the Mancos Shale is equivalent to the lower part of the Pierre Shale (Berman et al. 1980). For the Delta-Montrose and Shiprock Regions, much of the nomenclature is imported from the open-marine facies (and members) recognized in eastern Colorado.

Immediately underlying the Mancos Shale in the study area is the Dakota Sandstone, which was deposited during the initial transgression of the seaway. The maximum transgression of the seaway corresponding to its greatest depth is characterized by the deposition of fine-grained carbonates of the Bridge Creek, Fort Hays Limestone, and Greenhorn Limestone Members (Kauffman 1969). As the sea gradually regressed in cycles, the shoreline moved generally from the northwest to southeast across the study area. During the seaway regression, the Mancos typically intertongues with marginal-marine rocks in the overlying Mesaverde Group. Basal Mesaverde Group regressive coastal deposits in the study area include the Castlegate, Point Lookout, and Star Point Sandstones. The basal coastal deposit and equivalent to the basal Mesaverde in eastern Colorado overlying the Pierre Shale is the Fox Hills Sandstone.

Eastern Colorado Area (Generalized)			Delta and Montrose Colorado Regions		Shiprock New Mexico Region		Green River Utah Region		Price Utah Region		Hanksville Utah Region
Fox Hills Sandstone			Mesaverde Group	**Castlegate Sandstone**	Mesaverde Group	**Point Lookout Sandstone**	Mesaverde Group	**Sego Sandstone**	Mesaverde Group	**Blackhawk Formation**	**Mesaverde Formation**
Colorado Group	**Pierre Shale**	Hygiene Sandstone Member	Mancos Shale	Lujane Point Shale Unit	Mancos Shale	Cortez Member	Mancos Shale	**Buck Tongue of Mancos Shale**	Mancos Shale	**Star Point Sandstone**	Mancos Shale
		Sharon Springs Member		Sharon Springs Member				Mesaverde Group	**Castlegate Sandstone**			
	Niobrara Formation	Smoky Hill Member		Prairie Canyon Member		Smoky Hill Member		Upper Blue Gate Member		Upper Blue Gate Member	Masuk Member
		Fort Hays Limestone Member		Smoky Hill Member		Tocito Sandstone Lentil		Prairie Canyon Member		Emery Sandstone Member	Emery Sandstone Member
				Montezuma Valley Member		Juana Lopez Member		Lower Blue Gate Member		Lower Blue Gate Member	Blue Gate Member
	Benton Formation	Carlile Shale		Juana Lopez Member		Blue Hill Member		Juana Lopez Member		Ferron Sandstone Member	Ferron Sandstone Member
		Greenhorn Limestone		Blue Hill Member		Bridge Creek Member		Tununk Member		Tununk Member	Tununk Member
		Graneros Shale		Bridge Creek Member		Graneros Member					
				Graneros Member							
Dakota Sandstone			**Dakota Sandstone**		**Dakota Sandstone**		**Dakota Sandstone**		**Dakota Sandstone**		**Dakota Sandstone**

Figure 2. Mancos Shale Nomenclature for the Six Sampled Regions and Eastern Colorado Area

Mancos Shale generally consists of clayey to sandy to calcareous silt-shale with minor limestone, marlstone, bentonite, concretions, and sandstone beds (Noe et al. 2007a). These rocks represent muddy, shallow shelf deposits, and they typically form badland-style topography. A good example of this geomorphic expression is in the area of the South Branch of Loutsenhizer Arroyo in the Montrose, Colorado, Region (shown in the cover photo). Here, as in many other places of exposed Mancos, the shale is covered with a thin skin of residual or colluvial mud, as a result of in-place weathering (Noe et al. 2007a). Weathering commonly imparts a "popcorn" texture in calcareous shales of the thick Smoky Hill Member. Other characteristics of the Smoky Hill are the presence of *Inoceramus* shell fragments and its tendency to weather to a lighter gray or yellow-golden color. The overlying Prairie Canyon Member, is generally noncalcareous and organic-rich, and it contains very fine-grained, bioturbated, thin sandstone beds that weather out into small plates.

As used in this study, weathered Mancos Shale is defined as those portions of Mancos that have undergone significant chemical changes related to weathering processes, chiefly pyrite oxidation to iron hydroxide minerals and significant oxidation and loss of organic matter. This definition of weathering is consistent with that used by Berner (1987). These geochemical reactions are likely accompanied by mineralogical changes to the clay fraction, and manifest themselves in various ways including a change in the color of Mancos Shale from dark gray to yellowish gray and the production of a popcorn texture at the ground surface. Various terms have been used in the literature, but not well defined, for features that we presume to correlate with this definition of weathered Mancos Shale: Mancos Shale residuum (Wright and Butler 1993; Butler et al. 1994), shale residuum (Wright 1995, 1999), surficial Mancos Shale (Laronne 1977), weathered Mancos (Laronne and Shen 1982; Laronne 1977), weathered zone (Stillings et al. 2005), weathered shale (Wright 1995; Evangelou 1981), and partially weathered Mancos (Evangelou et al. 1984, 1985; Evangelou 1981). Similarly, our definition of unweathered Mancos Shale is probably mostly equivalent to Mancos Shale bedrock (Butler et al. 1994), competent Mancos (Laronne 1977), and less-weathered shale (Stillings et al. 2005). Mancos Shale hills are in most places capped by weathered shale that has a light-gray or yellow color. Another characteristic of weathered Mancos Shale is the presence of gypsum ($CaSO_4 \cdot 2H_2O$) and calcite ($CaCO_3$); the amounts of both decrease with increasing depth. However, weathering of Mancos Shale can apparently occur without any obvious change in appearance. In a study of the weathering of organic matter in the Mancos Shale, Leythaeuser (1973) found that core samples with a similar dark-gray appearance had significantly lower concentrations of organic carbon in the shallowest zones, likely due to weathering. In a study of black shale in Germany, Littke et al. (1991) also showed that organics can be weathered without a significant change in macroscopic appearance.

Thin bentonite beds have been identified in most members of the Mancos Shale. Thicknesses of the beds range from a fraction of an inch to as much as 5 ft and most commonly are 1 to 6 inches. Bentonite was first defined to be a highly colloidal, plastic clay found in Cretaceous rocks near Fort Benton, Wyoming (Knight 1898). Later definitions of bentonite limited it to clays composed mostly of montmorillonite produced by the alteration of volcanic ash. Approximately 400 to 450 distinct bentonite beds have been identified in the Western Interior Seaway deposits, and many of the bentonite beds extend for hundreds of miles across the depositional basin (Kauffman 1977). Radiometric dates of the bentonites correlate well with index fossils and provide a detailed geochronology for the seaway. Further definition of bentonite (in common usage, and in this report) classifies it as a rock derived from wind-transported volcanic ash, predominantly vitric in character, that fell into a body of water, and

then settled to form a discrete bed (Schultz et al. 1980). Glassy ash shards are altered most commonly to smectite, and phenocrysts in the ash are typically preserved. The rock is considered a bentonite if the ash-fall origin is recognizable. This definition was used by Schultz et al. (1980) for description of bentonite beds in the Pierre Shale, an eastern equivalent of the Mancos Shale. Numerous bentonite beds as much as 5 ft thick (but typically less than 1 ft thick) in the upper Pierre Shale just west of Denver, Colorado, are described by Noe et al. (2007b). Mineralogy of these bentonites indicates they are calcium bentonites and do not have as much swelling capacity as the very highly expansive sodium bentonites that occur in northern Wyoming.

During this study, bentonite beds were observed as light gray to white, thin layers in several exposures of Mancos Shale, particularly in the Montrose and Delta Regions. In the Delta Region, bentonite beds several inches thick were present at the Delta Reservoir seeps in the lower part of the Prairie Canyon Member. In the Montrose Region, bentonite beds were seen in the Prairie Canyon Member in areas investigated along a tributary to Loutsenhizer Arroyo. Also in the Montrose and Delta Regions, just above the Prairie Canyon Member, bentonite beds were observed in the Sharon Springs Member.

3.0   Site Descriptions

In November and December 2010, samples were collected from 69 sampling locations over a broad geographic area on the Colorado Plateau encompassing much of the Mancos Shale depositional basin (Figure 1). Latitude and longitude coordinates and geologic units for each sampling location are provided in Appendix A. For ease of discussion, these locations were grouped into six sampling regions named after the nearby towns of Delta, Green River, Hanksville, Montrose, Price, and Shiprock (Figure 1). Where there were clusters of sampling locations, the regions were subdivided into sampling areas. Some of the locations were in irrigated areas, whereas others were remote with little chance for anthropogenic impacts. Seeps were sampled at 51 of these locations and surface water at 18 locations. Seeps are surface expressions of groundwater with insignificant flow, whereas springs are the same but with sufficient flow to form a stream of water. These definitions were used in the location names (Appendix A), but for simplicity in the document, we use the terms "seep" and "spring" interchangeably.

Areas with known groundwater occurrences were identified using the USGS National Water Information Service (NWIS) Web Interface (USGS 2011a). Other areas likely to have groundwater seepage were identified using aerial photography in Google Earth and from data from DOE's National Uranium Resource Evaluation (NURE) program (USGS 2011b). Field reconnaissance investigations identified additional sampling locations.

Of the surface water locations, 12 were small streams and pools receiving water from the seeps or springs. At the other six surface locations, water bodies were identified as the source of water for the groundwater that surfaced at the seep sampling locations. These six surface locations are Whitewater Ditch No. 2 (WD2) that feeds Whitewater Ditch No.2 seep (WD2S); Bostwick Canal West Lateral (BCWL) that feeds the Loutsenhizer Area seeps; Sweitzer NE Garnet Canal (SNGC) that feeds the seeps northeast of Sweitzer Lake; Sweitzer Lake (SL) that feeds Buen Pastor Spring (BPS); Delta Reservoir (DR) that feeds Delta Reservoir Seep 1 (DRS1), Delta Reservoir Seep 3 (DRS3), and Delta Reservoir Dam Spring (DRDS); and Daly Reservoir (DAR) that feeds Daly Reservoir Spring 1 (DARS1) and Daly Reservoir Spring 2 (DARS2).

Many of the seep locations were conspicuous by the presence of extensive white efflorescent salt coatings on the ground surface. At a few locations, particularly those at the Sweitzer Lake Area and Dutchmans Wash Seep, the efflorescence was intense and formed several acres of crystalline salt crusts as much as one inch thick. Using samples collected from the West Salt Creek watershed near Grand Junction, Colorado, and the Miller Creek watershed near Price, Utah, Whittig et al. (1982) identified the mineral assemblage in efflorescence as gypsum ($CaSO_4 \cdot 2H_2O$), epsomite ($MgSO_4 \cdot 10H_2O$), hexahydrite ($MgSO_4 \cdot 6H_2O$), pentahydrite ($MgSO_4 \cdot 5H_2O$), starkeyite ($MgSO_4 \cdot 4H_2O$), kieserite ($MgSO_4 \cdot H_2O$), loewite ($Na_4Mg_2(SO_4)_4 \cdot 5H_2O$), bloedite ($Na_2Mg(SO_4)_2 \cdot 4H_2O$), mirabilite ($Na_2SO_4 \cdot 10H_2O$), and thenardite ($Na_2SO_4$). Bloedite, thenardite, and sideronatrite [$Na_2Fe(SO_4)_2(OH) \cdot 3H_2O$] were identified in efflorescent salts at DOE's Shiprock, New Mexico, disposal site (DOE 2000).

Shale beds were the source of the groundwater seeps, with the exception of nine locations. At BAS, BSCS, BSCUS, CWCS, TWS, and YHS the groundwater issued from sandstone beds in the Mancos Shale. At GRCRS, LGWS, and MS, groundwater issued from gravel alluvium. In the following discussion, we refer to these nine sites as "sandstone" seeps.

Each location is described individually and organized alphabetically by region.

3.1   Delta, Colorado, Region

3.1.1   Delta Reservoir Area and Devil's Thumb Area (Delta Reservoir Locations DR, DRDS, DRS1, DRS3 and Devil's Thumb Locations DTS1, DTS2, and DTS3)

Delta Reservoir (Figure 3) is located about 4 miles north of Delta, Colorado, and about 1 mile north of Devil's Thumb Golf Course. Sources for historical information about these areas include discussions with Mr. Andy Mitchell (City of Delta) and an unpublished report prepared by Golder Associates for Delta County (Golder Associates 2004). Delta Reservoir occupies 3.2 acres and is fed by a pipe from Doughspoon Reservoir high on the southwest side of Grand Mesa. Because Delta Reservoir is fed from the Grand Mesa, its water is pristine, as indicated by our sample collected on November 8, 2010, that had a low specific conductance of 114 µS/cm. Seeps DRS1 and DRS3 are located about 1,400 ft east of and hydraulically downgradient of Delta Reservoir. Seep DRS3 (Figure 3) emerges from the side of a steep hillside outcrop where two lines of tamarisks mark seepage (Figure 4). To reach seeps DRS1 and DRS3, the water must recharge into the Mancos Shale beneath Delta Reservoir and then travel along fractures and bedding planes. Several bentonite layers are present in the Mancos that appear to exert local control on the groundwater flow. The seeps sampled at DRS1 and DRS3 occur just above bentonite beds and had specific conductivity values of 27,250 and 22,840 µS/cm, respectively. Sampling location DRDS was established just downstream of the Delta Reservoir dam where water flowed down a small stream at more than a few gpm. The water emerging at DRDS would have had minimal residence time in the dam material, which appeared to be composed of alluvium and broken-up Mancos bedrock.

Figure 3. Delta Reservoir Area and Sampling Locations

Figure 4. View Northeast Toward Two Lines of Tamarisk That Mark Seepage along Two Separate Bentonite Beds. DRS3 is located just above the lower bentonite bed.

Devil's Thumb Golf Course is about 3 miles north of Delta and was constructed in 2000 (Figure 5). Delta Reservoir was used as the water supply for the City of Delta through 1990, after which the reservoir was drained and remained empty until 1998 when refilling was initiated to supply water for the planned Devil's Thumb Golf Course. Images from Google Earth confirm that the reservoir was dry in September 1993. Water was conveyed through pipes from Delta Reservoir to four unlined ponds on the Devil's Thumb Golf Course starting in August 2000. Initially, the course was irrigated with as much as 1 million gallons of water per day to establish the turf.

Figure 5. Devil's Thumb Golf Course Area and Sampling Locations

Shortly after the golf course opened, groundwater seeps started to appear in nearby areas. In November 2001, USGS personnel sampled a seep at location USGS Seep 2, also referred to in the NWIS database (USGS 2011a) as 384657108041901. This seep is 4,200 feet (ft) from the Devil's Thumb Golf Course pond and receives groundwater that has flowed through the Mancos Shale (Figure 5). Using the time period from the filling of the ponds in August 2000 to the first documented seepage at USGS Seep 2 in November 2001 and a flow distance of 4,200 ft, we estimated a minimum flow velocity through the shale of 8 ft per day. USGS Seep 2 was flowing at about 9 gallons per minute (gpm) at the time of the USGS sampling and had high concentrations of major ions, selenium, and uranium (Table 2). Concentration data for nitrate in this seep were not available in the NWIS database (USGS 2011a).

Table 2. Composition of Devil's Thumb USGS Seep 2 on November 28, 2001

Constituent	Concentration	Constituent	Concentration
Sp. Conductance	26,000 μS/cm	pH	7.9
Alkalinity	526 mg/L as CaCO$_3$	Selenium	18,700 μg/L
Calcium	435 mg/L	Sulfate	12,900 mg/L
Magnesium	1,220 mg/L	Chloride	1,240 mg/L
Sodium	5,730 mg/L	Arsenic	1,020 μg/L
Potassium	38.3 mg/L	Uranium	139 μg/L
Boron	634 μg/L	Nitrate	no value in NWIS

Source: USGS 2011a
μS/cm = microsiemens per centimeter

Largely because of the high selenium concentrations, efforts were undertaken by the City of Delta to minimize seepage from the golf course ponds. The four ponds were consolidated into a single, 2.9-acre pond prior to 2004. This larger pond (labeled "pond" on Figure 5) was lined with bentonite, and later, polyacrylic acid potassium (PAM) was applied to slow the recharge. On January 21, 2003, the seep was still flowing at a rate of about 14 gpm (USGS 2011a). A photograph taken in 2003 by Kenneth Leib (written communication) of USGS indicated that the seep had created a marsh area. Because neither the bentonite liner nor the PAM treatment was successful in eliminating recharge from the pond, in 2004 the pond was lined with plastic. Soon after the pond was lined with plastic, USGS Seep 2 dried up (Andy Mitchell, personal communication). It was dry at the time of our study and had apparently been dry for some time based on the difficulty we had in determining the location of the former marsh area. The rapid loss of the seepage at USGS Seep 2 following the pond lining confirmed that the golf course pond was the source of the seep water and that groundwater can move at high velocity through the Mancos.

3.1.2 Point Creek Seep (Location PCS)

Point Creek Seep (PCS) is an isolated seep flowing from shale in the Mancos Shale along the bank of Point Creek on the southwest flank of Grand Mesa about 9 miles northwest of Delta, Colorado (Figure 1). It was identified as location 385043108112901 in the NWIS database and was sampled by U.S. Bureau of Land Management personnel on April 18 and May 13, 1980, at which times it had specific conductivities of 7,380 and 7,480 μS/cm, respectively (USGS 2011a).

Several days prior to sample collection, we placed a sampling pipe in the seep by hand digging. At the time of sampling on November 8, 2010, the seep had a specific conductivity of 10,739 μS/cm. No obvious sources of surface water that might supply this seep were identified. The area is remote and there is no irrigation in the vicinity.

3.1.3 Sweitzer Lake Area (Locations BPS, SL, SNGC, SNS, SNS1, SNS2, SNS3, SRP, and US1)

Sweitzer Lake is located about 2 miles southeast of Delta, Colorado. The lake is fed from a diversion ditch off the Garnet Canal on the east side of the lake (Butler et al. 1991). Sweitzer Lake has long been known to have elevated concentrations of selenium. Butler et al. (1991) reported selenium concentrations ranging from 5 to 45 μg/L in the lake water.

Figure 6. Sampling Locations for Sweitzer Lake Area

We collected surface water samples from Sweitzer Lake at location SL and from the Garnet Canal at location SNGC. At the time of sampling on November 4, 2010, the water level in the Garnet Canal had dropped several feet from the week prior because it was near the end of the irrigation season. Samples were collected from locations SNS, SNS1, SNS2, and SNS3 on November 30, 2010, from hand-dug holes in a seepage area heavily encrusted with efflorescence along a tributary draining into Sweitzer Lake about 1,000 ft northeast of the lake (Figure 6). These seep samples had some of the highest concentrations of salts and trace metals of any samples collected for our study, with specific conductivity values as high as 68,114 µS/cm, and the water samples were deep yellow or red from dissolved organic carbon (DOC). Another seep (US1) located about 750 ft east of Sweitzer Lake and cited in Thomas (2009) was sampled from a hand-dug hole. A nearby pool of deep-red water (SRP) was also sampled. Buen Pastor Spring (BPS) is located about 800 ft south of Sweitzer Lake and was sampled from a sampling pipe placed about 2 ft into the ground.

3.1.4 Whitewater Area (Locations KCFS, WCTS, WCTSP1, WCTSP2, WD2, and WD2S)

The Whitewater Area is between Delta and Grand Junction, Colorado, about 6 miles southeast of Grand Junction (Figure 7). Efflorescence is common over several square miles in the Whitewater Area. Kannah Creek Flowline Spring (KCFS) was sampled in the nearly dry creek bed at the farthest upstream point where water starts seeping into the drainage. Efflorescence was abundant in the KCFS seepage area, and the specific conductivity was 26,250 µS/cm. Another seep (WD2S), located adjacent to U.S. Highway 50, had an unusually low pH of 4.15 and a specific conductivity of 14,285 µS/cm. Water supplying seep WD2S was sampled at location WD2 from Whitewater Ditch No. 2, which runs nearly parallel to U.S. Highway 50. As with location KCFS,

the vicinity at and near WD2S and WD2 had an extensive cover of efflorescence. A third seep (WCTS) was sampled in a tributary to Whitewater Creek. Specific conductivity of this seep was not measured, but samples from two nearby pools at locations WCTSP1 and WCTSP2 that were fed from the seep had high specific conductivity values of 47,655 and 67,474 µS/cm, respectively. This area is also characterized by widespread efflorescence.

Figure 7. Sampling Locations at the Whitewater Area

3.2   Green River, Utah, Region

3.2.1   Cisco Area (Locations CAS, CIS, CWC, and S36)

Location CAS is at Cato Springs about 42 miles east-northeast of Green River, Utah, and about 10 miles north of the unincorporated community of Cisco, Utah (Figure 1). The spring issued from a stream bank and was marked by red ferric oxyhydroxide deposits having a slimy appearance that might have been due to the presence of algae (Figure 8). This red coloration is distinctly different from the dissolved red coloration at some locations that is caused by DOC, such as at location HGS in the Montrose, Colorado, Region (Figure 9). The precipitates formed from reduced groundwater carrying ferrous iron at a concentration of 2.03 milligrams per liter (mg/L) that was exposed to atmospheric oxygen at the spring. The sample from CAS was collected from a hand-dug hole and had a relatively low specific conductivity of 2,184 µS/cm. A stream sample was collected at location CWC in Cottonwood Wash about 30 ft from location CAS.

Figure 8. Red Color Caused by Ferric Oxyhydroxide. Photo taken at Cato Springs, October 12, 2010.

Figure 9. Red Pool of Water Formed from Seep at Houston Gulch.
The red color is caused by dissolved organic carbon.

Seep location CIS was at Cisco Springs, about 3 miles southwest of Cato Springs. The seep is in a wash adjacent to outcrops of gray shale in the Mancos. Cattails are prominent in the immediate area of the sampling location and a prominent tamarisk stand was present about 100 ft upstream. The sample was collected from a pool in the stream bank and had a specific conductivity of 3,947 µS/cm.

Section 36 Seep (S36) is located about 200 ft south of Interstate 70 (I-70) and about 5 miles southwest of Cisco, Utah (Figure 1). The sample was collected from a hand-dug hole in the bank of a drainage that appeared to have been straightened during construction of I-70. Shale beds of the Mancos Shale underlie the area, and it was apparent that the seepage had originated in the Mancos. However, the sampling hole did not quite reach bedrock and was terminated in colluvium. Efflorescence coated much of the streambed. The sample, collected on November 11, 2010, had a specific conductivity of 24,522 µS/cm.

3.2.2 Daly Reservoir Area and Browns Wash Seep (Locations BWS, DAR, DARS1, and DARS2)

Daly Reservoir in Grand County, Utah, was built for range improvement in April 1983 (verbal communication from Becky Dolittle, Moab Field Office, U.S. Bureau of Land Management). It fills from an unnamed drainage that drains northwest to Browns Wash and has an area of 2.4 acres. Daly Reservoir was sampled from the dam at location DAR, and had a specific conductance of 1,720 µS/cm. Daly Reservoir Springs 1 and 2 (DARS1 and DARS2) were sampled at locations 230 and 360 ft from the reservoir, respectively (Figure 10). The springs were flowing from an embankment of gray shale of the Mancos into a small arroyo. Samples were collected from hand-dug holes in the bank of the arroyo. Efflorescence was abundant on the banks and in the bottom of the arroyo. Specific conductivity values in samples from seeps DARS1 and DARS2 were 9,187 and 15,377 µS/cm, respectively.

Sampling location Browns Wash Seep (BWS) is about 1.4 mile northeast of Daly Reservoir (Figure 1). Much of Browns Wash near BWS is eroded down to shale of the Mancos bedrock, but portions are covered by thin bars and lenses of alluvial gravel. Browns Wash Seep (BWS) was sampled from a sampling pipe emplaced about 1 ft deep in an alluvial lens. The sample had a specific conductivity of 10,798 µS/cm. Efflorescence in this area was minimal.

3.2.3 Floy Wash Area (Locations ETFW, ETFWD, UFWS, UFWS1, UFWS2, and WFFW)

West Fork Floy Wash (WFFW) is about 4 miles northeast of exit 175 on I-70 (Figure 1). The entire area is underlain by shale of the Mancos, and seepage appeared to be emanating from a series of locations along the wash. Specific conductivity was measured at six locations in pools along a 1,000 ft stretch of the wash; values ranged from 6,000 to 22,000 µS/cm. Pools with high specific conductivity had a yellow color. One sample from one pool (WFFW) was analyzed only for uranium, and it had a uranium concentration of 57.4 µg/L.

Figure 10. Sampling Locations at Daly Reservoir

Locations East Tributary Floy Wash (ETFW) and Upper Floy Wash Spring (UFWS) are about 1 mile south of location WFFW (Figure 1). Location ETFW was at the farthest upstream appearance of water in the wash, and although mostly concealed, it was probably formed from a seep. The pools that formed were red from precipitation of ferric iron, and cattails were abundant. Specific conductivity of the water at ETFW was 21,315 µS/cm, and specific conductivity in a pool about 50 ft downstream (location ETFWD) was 6,300 µS/cm. Samples were collected from a sampling pipe inserted about 2 ft into the ground at location UFWS, and the water had a specific conductivity of 6,514 µS/cm. Water in both of two hand-dug, 1 ft deep holes located 30 ft (UFWS1) and 50 ft (UFWS2) downstream had a specific conductivity of 2,236 µS/cm. Sediment in these holes was black and had an odor that indicated chemical reduction. Ferric iron coated portions of the stream and was likely derived from dissolved ferrous iron that had oxidized as it contacted the atmosphere at the seeps.

3.2.4   Green River Canal Return Seep (Location GRCRS)

This seep is referred to as SP-3 in Gerner et al. (2006) and is shown on Figure 1. USGS personnel collected samples from the seep between June and September 2004 to help determine salt loading from agricultural practices in the Green River, Utah, area (Gerner et al. 2006). Dissolved solids concentrations in the USGS samples ranged from 4,280 to 4,640 mg/L; our sample collected on November 11, 2010, had a specific conductivity of 3,847 µS/cm.

The seep is located on the bank of an irrigation return canal about 850 ft from its entry to the east side of the Green River. The sample was collected from a 2 ft deep hole that was dug by hand into the bank of the canal. Lithologic relationships are somewhat concealed, but the seep appears to result from water that had infiltrated from the canal to the Green River floodplain alluvium and then surfaced at or near the contact with the underlying Mancos Shale bedrock. Thus, the chemistry of this seep may be influenced by contact with both alluvium and Mancos Shale, and by irrigation.

3.2.5   Little Grand Wash (Locations LGW and LGWS)

The seep sample from site LGWS was collected from a sampling pipe inserted about 1.5 ft into the stream bank of Little Grand Wash (Figure 1). A stream sample was collected 2 ft from the seep in a pool composed mostly of seep water. The stream was partially frozen and was flowing at less than 1 gpm. The stream sample could have been affected by exclusion of some ions from the ice during freezing. Specific conductivity values measured on November 12, 2010, for the seep and wash samples were 1,637 and 1,326 µS/cm. respectively.

The seep appears to result from water that flowed through Little Grand Wash alluvium and then surfaced at or near the contact with the underlying Lower Blue Gate Member of Mancos Shale bedrock. Thus, the chemistry of the seep could be influenced by contact with both alluvium and Mancos Shale.

3.3   Hanksville, Utah, Region

3.3.1   Town Wash Spring (Locations TWS and TWSP)

Town Wash Spring location TWS is in the Henry Mountains Basin about 9 miles southwest of Hanksville, Utah, (Figure 1) and is listed in the NWIS database as location 381721110505401 (USGS 2011a). The sample from location TWS was collected from a 2 ft deep sampling pipe. At the time of our sampling on November 17, 2010, the specific conductivity was 10,018 µS/cm. A pool, sampled at location TWSP in Town Wash about 20 ft south of the TWS sampling pipe, had a specific conductivity of 5,630 µS/cm. Water emerging at the spring originated from flow through sandstone in the Ferron Sandstone Member of the Mancos at the contact with the underlying Tununk Member of the Mancos Shale.

3.3.2   Cottonwood Creek Spring (Location CWCS)

Cottonwood Creek Spring location CWCS is in the Henry Mountains Basin about 9 miles southwest of Hanksville, Utah, (Figure 1) and is listed in the NWIS database as location 381739110513801 (USGS 2011a). The sample from location CWCS was collected from a small pool that was fed from the seep. At the time of our sampling on November 17, 2010, the specific conductivity was 5,965 µS/cm. Water emerging at the spring originated from flow through sandstone in the Ferron Sandstone Member of the Mancos at the contact with the underlying Tununk Member of the Mancos Shale.

3.3.3 Bert Avery Spring (Location BAS)

Bert Avery Spring location BAS is in the Henry Mountains Basin about 9 miles southwest of Hanksville, Utah, (Figure 1) and is listed in the NWIS database as location 381603110491901 (USGS 2011a). The sample from location BAS was collected from a 2 ft deep sampling pipe placed at the base of a 30 ft thick sandstone cliff. At the time of our sampling on November 17, 2010, the specific conductivity was 418 µS/cm. Water emerging at the spring originated from flow through sandstone in the Ferron Sandstone Member of the Mancos at the contact with the underlying Tununk Member of the Mancos Shale.

3.3.4 Bitter Spring Creek (Locations BSCS and BSCUS)

Bitter Spring Creek Seep location BSCS (Figure 1) is southwest of the Henry Mountains in the Henry Mountains Basin about 400 ft east of the Capitol Reef National Park boundary. It is listed in the NWIS database as location 375458111011901 (USGS 2011a). The spring sample at location BSCS was collected from a sampling pipe near the base of a massive sandstone bed in the Emery Sandstone Member of the Mancos Shale. The spring water was depositing iron oxide on the rocks and streambed. Our sample, collected November 18, 2010, had a specific conductivity of 2,037 µS/cm. The upper spring sample at location BSCUS was collected from a shallow stream pool at the farthest upgradient location of seepage and had a specific conductivity of 1,079 µS/cm. This area is characterized by steep sandstone cliffs, and the intermittent stream has formed a series of falls up to 20 ft high. The groundwater flows through sandstone in the Emery Sandstone Member of the Mancos, and the springs emerge near the base of the Emery Sandstone at the contact with the underlying Blue Gate Member of the Mancos Shale.

3.4 Montrose, Colorado, Region

3.4.1 Cerro Summit Area (Locations CCS, HGS, HGSE, and HGRP)

Cedar Creek Seep location CCS is about 70 ft south of U.S. Highway 50 and about 2 miles northwest of Cerro Summit (Figure 11). The seep flows from the north side of a dirt road from the Highway 50 embankment, and efflorescence is apparent (Figure 11 inset). The groundwater sample was collected from a hand-dug hole in the highest-elevation portion of the seepage area. The water had a dark-yellow color and a specific conductivity of 16,409 µS/cm. The radon-222 concentration was 1,625 picocuries per liter (pCi/L), which was the highest value measured in our study. The source of the water feeding the seep was not determined.

Location HGS (Figure 11) in Houston Gulch is along Highway 50 about 1.7 miles northwest of location CCS and about 100 ft north of the highway. The sample was collected from a sampling pipe inserted about 1.5 ft into the seepage area. Groundwater issuing from the seep was red due to DOC and had a specific conductivity of 22,790 µS/cm. Sampling location HGSE was a hand-dug hole 30 ft southeast of HGS. The groundwater at location HGSE was also red and had a specific conductivity of 21,658 µS/cm. Red water flowed from the seepage area down a small stream (Figure 9). The stream at location HGRP had a specific conductivity of 45,645 µS/cm.
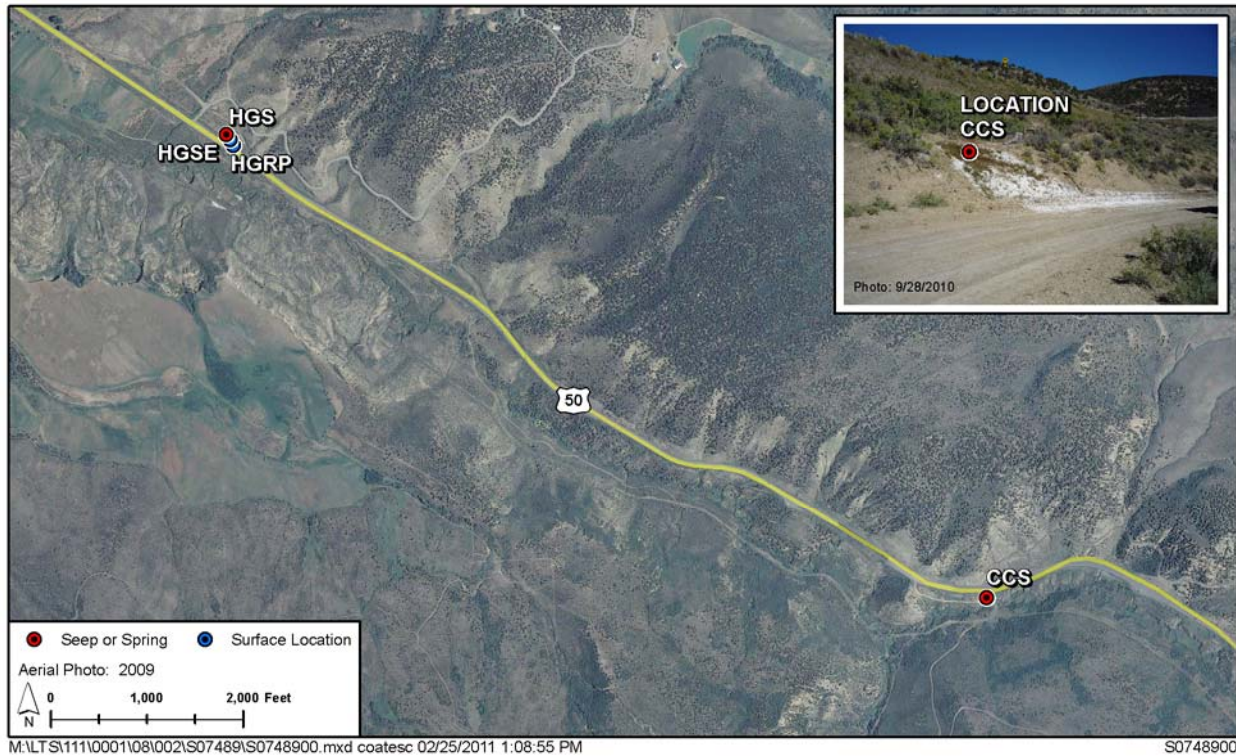
Figure 11. Sampling Locations at Cerro Summit Area. Inset is a September 28, 2010, photo of Cedar Creek Seep.

3.4.2 Loutsenhizer Arroyo Area (Locations BCWL, LOUT3, LOUT8, LOUT9, LOUT11, LOUT11W, LOUT12L, LOUT12U, LOUT13, LOUT14)

According to the USGS 1:24,000 topographic map of the Olathe quadrangle, the main portion of Loutsenhizer Arroyo runs northwest along the eastern side of the Uncompahgre River valley floor starting about 5 miles north of Montrose, Colorado. Our sampling was conducted in one of the upper reaches of Loutsenhizer Arroyo, which is unnamed on the USGS topographic maps but is referred to as South Branch of Louzenhizer [sic] Arroyo by Butler and Leib (2002). For ease of discussion, we will use the name Loutsenhizer Arroyo to refer to the South Branch and its tributaries in the area of our sampling (Figure 12). Bostwick Canal runs along the upper reach of Loutsenhizer Arroyo (Figure 12) and is likely the source for the seepage in the arroyo. Location BCWL, on the West Lateral of the Bostwick Canal with a similar water supply, had a specific conductivity of 197 µS/cm.
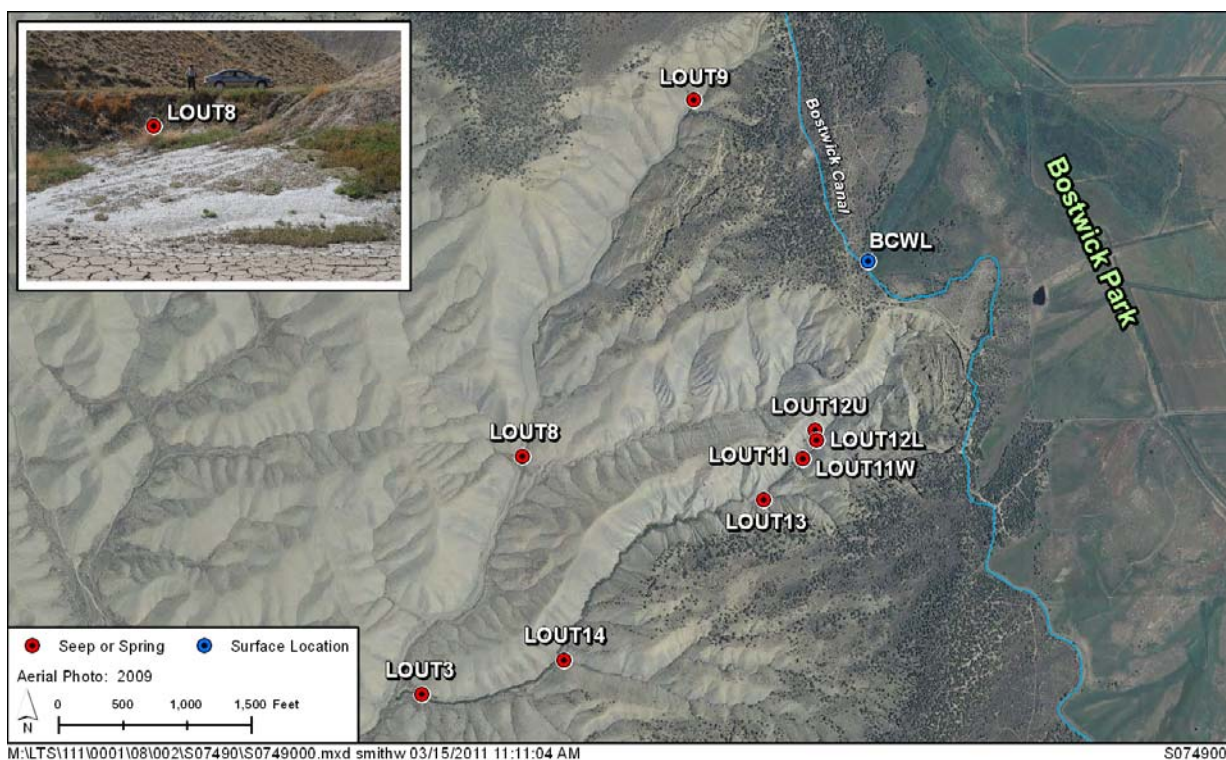
Figure 12. Sampling Locations at Loutsenhizer Arroyo Area and Location of the West Lateral of Bostwick Canal (labeled Bostwick Canal). Insert photo is LOUT8 seep looking southwest.

A spring with a high uranium concentration of 113.8 µg/L was discovered on September 26, 1977, during sampling for the NURE program in the Montrose 1º × 2º quadrangle (Broxton et al. 1979). Additional chemical data for this seep, from samples collected on May 15, 2000, are available in the NWIS database where it is listed as "Upper Seep, S. Branch Loutsenhizer Arroyo" with the index number 383307107464701 (USGS 2011a). On this date it had a specific conductivity of 10,600 µS/cm. The NWIS (USGS 2011a) database lists another seep in Loutsenhizer Arroyo as "Lower Seep, S. Branch Loutsenhizer Arroyo" with the index number 383242107470402 that has data for October 5, 2000, at which time the specific conductivity was 42,800 µS/cm. Our locations LOUT9 and LOUT8 are the same as the NWIS (USGS 2011a) locations Upper Seep and Lower Seep, respectively.

Efflorescence was common at the Lower seep, LOUT8 (Figure 12, inset), but efflorescence was minimal at LOUT9. Samples collected from locations LOUT9 and LOUT8 on November 4, 2010, had specific conductivity values of 8,844 and 22,130 µS/cm, respectively. Location LOUT11 was sampled from a shallow, hand-dug hole in a small tributary to Loutsenhizer Arroyo, and location LOUT11W was in the wash about 9 ft away. Samples of LOUT11 and LOUT11W had specific conductivity values of 11,600 and 315 µS/cm, respectively. Location LOUT12U was a seep dripping from a plant rootlet bedded in gray shale in a small ravine on the side of a steep Mancos hillside. Another seep was sampled at location LOUT12L near the bottom of the same ravine as LOUT12U, near where the ravine intersected the main arroyo. Specific conductivity values for samples at LOUT12U and LOUT12L were 5,190 and 6,220 µS/cm, respectively. Locations LOUT13 and LOUT14 were downstream from LOUT11 in the same tributary and were sampled to test chemical variability along the tributary.

Seep water measured in hand-dug holes at locations LOUT13 and LOUT14 had specific conductivity values of 5,880 and 17,700 µS/cm, respectively. Seep location LOUT3 was farther down the tributary and was sampled from a sampling pipe in a grassy area where seepage emerged from the Mancos Shale. Specific conductivity at this location was 15,330 µS/cm.

3.5   Price, Utah, Region

3.5.1   Mud Spring (Location MS)

At location MS, clear water was flowing up and out of an existing vertical PVC pipe, and the sample was collected by pumping water from the pipe. The spring is listed as Mud Spring on the USGS 1:24,000 map of the Sunnyside Junction quadrangle and is listed in the NWIS database as location 393103110315901 (USGS 2011a) (Figure 1). The site had plumbing that appeared to have been used to convey water from the spring to animal feeding areas, indicating that the spring had been flowing for some time. Specific conductivity measured on November 16, 2010, was 1,659 µS/cm. This spring appears to result from groundwater flowing through the alluvial fan extending outward (westward) from the mouth of Whitmore Canyon at the base of the Book Cliffs. Mud Spring is one of many springs in the area where groundwater emerges from the base of the alluvial fan material at the contact of the pediment surface on the underlying Mancos Shale.

3.5.2   Dutchmans Wash Seep and Blue Gate Spring (Locations DWS, BGS)

Dutchmans Wash Seep is located about 27 miles southwest of Price, Utah, on the western slope of the San Rafael Swell (Figure 1). The sampling location (DWS) was within a large, flat, open area with abundant efflorescence. Irrigated areas are nearby to the northwest, but it is unclear whether they supply water to this area. Specific conductivity of the seep water was 48,519 µS/cm on November 16, 2010.

Blue Gate Spring (BGS) is located about one mile east of location DWS and is listed in the NWIS database as site 391315110570301. The seep issues from the dark-gray shale of the Blue Gate Member and had a sulfurous odor. Ferric oxide deposits were visible along the seepage area. Specific conductivity of the seep water was 6,203 µS/cm on November 16, 2010.

3.5.3   Mathis Wash Seep (Location MWS)

Location MWS is about 11 miles south of Price, Utah, and is about 20 ft west of Upper Miller Creek Road (Figure 1). This location is within a large, irrigated area with abundant efflorescence. Specific conductivity of the seep water was high at 70,002 µS/cm on November 16, 2010. A 6-ft diameter pool of yellow-colored water on the opposite (east) side of Miller Creek Road had a specific conductivity of 53,800 µS/cm.

3.6   Shiprock, New Mexico, Region

3.6.1   Ditch 9 Spring (Location D9S)

Location D9S is about 375 ft west of Farm Road within a marshy area that extends about 75 ft along the base of a steep shale hill of Mancos bedrock (Figure 13). On December 2, 2010, the spring water had a specific conductivity of 4,045 µS/cm. Samples were collected from a hole hand dug about 2 ft into the weathered Mancos. Scattered areas of efflorescence are in the vicinity of the spring.
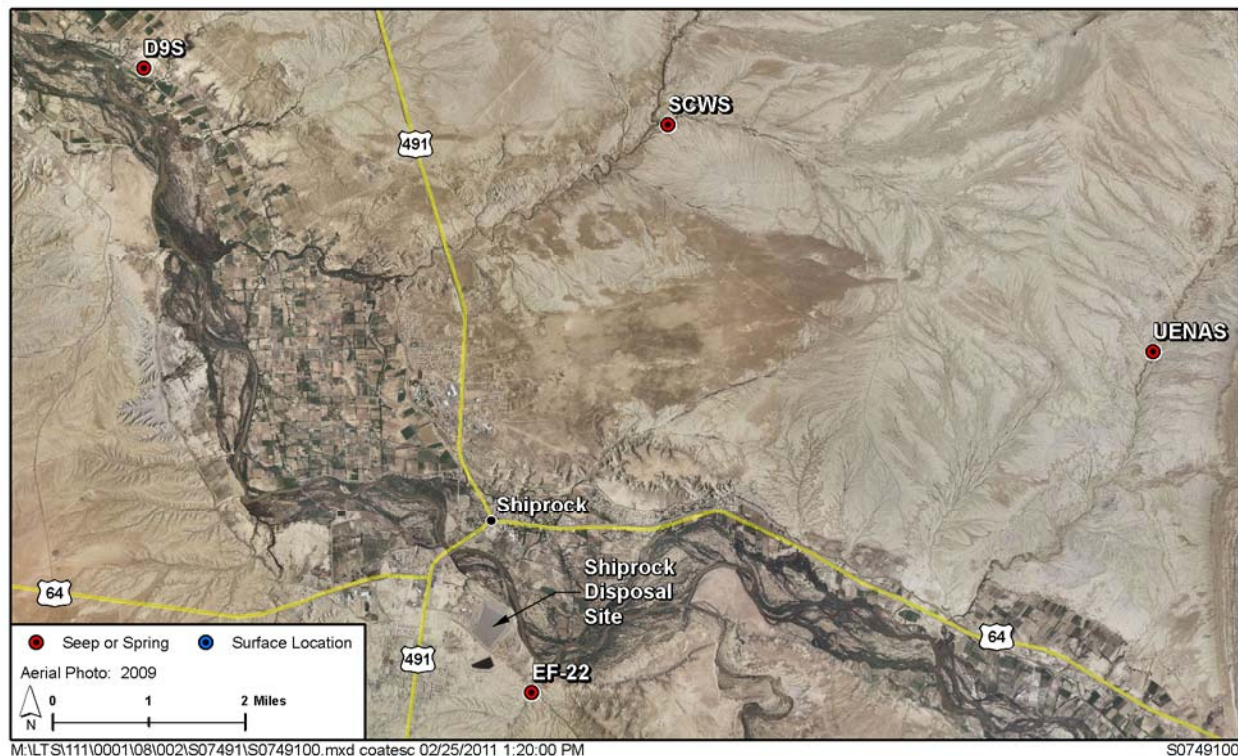
Figure 13. Sampling Locations in the Shiprock Area.

3.6.2   Many Devils Wash (Location EF-22)

Many Devils Wash is an arroyo that feeds into the San Juan River about 1.5 miles south of Shiprock, New Mexico. The wash is within about 0.5 mile of DOE's Shiprock uranium mill tailings disposal site, and DOE is currently remediating a portion of the wash by pumping groundwater and surface water to an evaporation pond (Figure 13). Groundwater with specific conductivity values ranging from about 20,000 to 35,000 µS/cm enters Many Devils Wash from seepage from a tributary called the East Fork (DOE 2000) at a relatively constant flow rate, estimated visually as 1 gpm. The seepage contains elevated concentrations of sulfate, nitrate, selenium, and uranium and is thought to originate as infiltration to groundwater derived from the uranium milling (DOE 2000). Because the suite of contaminants is similar to that observed as natural contamination from the Mancos Shale, it is reasonable to suggest that some or all of the contamination may be of a natural origin instead of related solely to the mill site.

Location EF-22 is in East Fork about 100 ft from its confluence with Many Devils Wash (Figure 13). A sample was collected at this location from a sampling pipe inserted to a depth of 2 ft. The area of East Fork about 50 ft downstream of EF-22 is saturated most of the time; thus, location EF-22 is near the surface emergence of the groundwater system. The area is often covered by efflorescence. This is the only site sampled during the study that is located relatively close (0.5 mile) to a known source of anthropogenic uranium contamination.

3.6.3 Salt Creek Wash Seep (Location SCWS)

Sampling location SCWS is about 4 miles northeast of Shiprock, New Mexico (Figure 13). The sample was collected from the first upstream appearance of water along Salt Creek Wash where the wash is bounded on both sides by shale outcrops of Mancos. The shale is weathered to a reddish orange color on the surface in places but still contains scattered black organic material. The sample was collected from a hole dug by hand to a depth of about 2 ft within the wash where the water was issuing from the shale. The water was saline with a specific conductivity of 48,639 μS/cm. Where the water pooled in the arroyo bed, it had a yellow to red color and a DOC concentration of 183 mg/L.

The source of the groundwater feeding SCWS was not identified; the site is in a remote area and there are no obvious nearby reservoirs, canals, or other standing bodies of water. Location SCWS is in the vicinity of the Salt Creek Dakota Oil Field and at least 47 test holes have been drilled within 1 mile of the sampling location, many of them hydraulically upgradient. Some of these test holes became oil wells that produce from a depth of about 1,100 ft in the Cretaceous Dakota Sandstone, just below the Mancos Shale (Jacobs and Fagrelius 1978). If any of these wells were incompletely sealed, groundwater could have migrated to the seeps from deeper horizons.

3.6.4 Upper Eagle Nest Arroyo Spring (Location UENAS)

Upper Eagle Nest Arroyo is about 7 miles northeast of Shiprock, New Mexico, and runs subparallel to and about 2 miles west of The Hogback, a monocline where rocks dip steeply eastward into the San Juan Basin. At sampling location UENAS (Figure 13), the arroyo has incised the Mancos Shale bedrock, which consists of siltstone and shale. The sample was collected in a hand-dug hole at a depth of about 1 ft into the arroyo bed and had a specific conductivity of 26,607 μS/cm. The sample was unusual in that it had a low color index of only 24 color units but having a high DOC value of 161 mg/L. No source of water was identified for the spring, because it is remote and far from irrigation, reservoirs, canals, and oil wells.

3.6.5 Yucca House Spring (Location YHS)

Yucca House Spring (YHS) is located about 30 miles north of Shiprock, New Mexico, and about 10 miles south of Cortez, Colorado, (Figure 1) and is within the boundary of Yucca House National Monument, one of the largest archeological sites in southwest Colorado (NPS 2011). Ancestral Puebloan people used water from the spring from A.D. 1150 to 1300 (NPS 2011).

The site is listed in the NWIS database as location 371500108410801 (USGS 2011a). At the time of our sampling on December 1, 2010, the specific conductivity was 1,442 μS/cm, and the spring was estimated to be flowing at 0.2 to 0.5 gpm. Wright (2006) reported specific conductivity

values ranging from 1,260 to 2,050 μS/cm for water sampled from Yucca House Spring during four sampling events from September 2002 to September 2003. During this time, Wright (2006) measured spring discharge at 0.45 to 0.90 gpm, and uranium concentrations ranged from 7.46 to 13.1 μg/L. Wright (2006) also measured a uranium concentration of 485 μg/L in a surface water sample collected from Navajo Wash 0.5 miles to the east.

Although partially concealed, the spring water appears to originate in the Mancos Shale from flow through sandy material in the Juana Lopez Member and emerge at the contact with the underlying Blue Hill Member, composed mainly of shale. During the irrigation season, groundwater may be supplemented by water from the Ute Mountain Ditch. Using infrared aerial photography to identify areas with high densities of phreatophytes, Wright (2006) suggested an area of alluvial and pediment cover located about 1 mile west of Yucca House Spring on the east slope of Sleeping Ute Mountain as the recharge area for the spring. Based on chemical signatures of area springs, Wright (2006) suggested that calcium-bicarbonate groundwater recharging the subsurface in the Ute Mountain area interacted with Mancos Shale to produce the calcium sulfate groundwater issuing from Yucca House Spring. He also suggested that irrigation water contributed to Yucca House Spring.

4.0   Methods

4.1   Sampling

We sampled groundwater seeps from the Mancos Shale over a large portion of its depositional basin (Figure 1). A single round of sampling was conducted during November and December 2010. This period was considered base flow conditions by Tuttle and Grauch (2009), a time when irrigation and runoff are at a minimum. This period of time is within the nonirrigation season that Butler et al. (1991) reported typically lasts from November through March. At all sampling locations, an effort was made to locate the farthest upgradient area of the seep in order to obtain groundwater at its first emergence from the formation. Flow from most seeps was less than 1 gpm.

Groundwater was collected either through a 1 to 3 ft long, vertical, 2-inch-diameter, slotted PVC casing (sampling pipe), or an open hole dug with a hand auger or shovel. The water was pumped from the "well" with a peristaltic pump. Field parameters (pH, specific conductivity, temperature, dissolved oxygen, and oxidation-reduction potential [ORP]) were measured either in a flow-through cell or by placing the sonde directly into the well. In some cases, groundwater flowed from the rock in a manner that a sample could be collected directly into a sampling container. This mode of sampling was used only if the sample could be obtained at the immediate point of groundwater emergence from the outcrop.

At a few of the seep locations, flowing groundwater could be identified mostly by wet or soggy ground conditions. At these sites, care was taken to ensure that groundwater was flowing, and was not simply stagnant water. Typically, the water was pumped from the sampling pipe or open hole until it reached a steady flow rate. At a few locations that had limited groundwater production, the "wells" were pumped down and left for some time (up to several hours) to refill before sampling. Not all analytes were measured at all locations. At some locations we only measured field parameters, and only uranium was analyzed at others.

In all cases, the seep and spring samples clearly represented flowing groundwater. The proximity of the seeps and springs to the ground surface suggested that alteration of the groundwater resulting from upward capillary flow and evaporation was possible in some samples. Evaporation effects were likely to be more dominant in areas covered by efflorescence, such as Sweitzer Lake and Dutchmans Wash. Because the areas with efflorescence had minimal or no plant growth, transpiration of groundwater at these locales was not considered significant. Measurements of radon-222 were made in an effort to help evaluate effects of evaporation.

Samples for chemical analyses were field filtered through 0.45 micrometer in-line filters using a low-flow peristaltic pump. Samples were collected in Nalgene bottles: 1 liter for uranium isotopes, 125 milliliters (mL) for anions, and 125 mL for cations and metals. An unfiltered sample was collected in a 50 mL plastic bottle for analysis of iron-related bacteria. Two samples were collected for radon-222 analyses in 40 mL glass vials with Teflon-lined septa. Samples for anions, radon-222, and bacteria analyses were not preserved but were placed on ice until analysis. All other samples were preserved with sufficient concentrated nitric acid to maintain the pH at less than 2.

4.2   Analysis

Field parameters (pH, ORP, specific conductivity, temperature, and dissolved oxygen) were measured on unfiltered water using a YSI Environmental (Yellow Springs, Ohio) 556 MPS meter and sonde. Measurement of pH employed a glass combination electrode, ORP a platinum electrode, conductivity a four-electrode cell, and dissolved oxygen a steady-state polarographic cell. Alkalinity was determined in the field on filtered samples by titration with sulfuric acid.

Most water analyses were conducted at the DOE Environmental Sciences Laboratory in Grand Junction, Colorado. Samples collected for analysis of arsenic, boron, selenium, uranium isotopes, and vanadium were sent to a commercial laboratory. Color analyses were performed on filtered samples using a Hach (Loveland, Colorado) DR/890 colorimeter, which measures light absorbance at 465 nanometers normalized to a platinum-cobalt standard. One color unit is equivalent to 1 mg/L platinum as chloroplatinate. Concentrations of anions (sulfate, chloride, and nitrate) were determined on a Dionex (Sunnyvale, California) Model ICS-1500 ion chromatograph, and cation (calcium, magnesium, sodium, iron, and potassium) concentrations were measured by flame atomic absorption spectrophotometry on a Perkin Elmer (Waltham, Massachusetts) AAnalyst 300. To minimize possible biodegradation of nitrate, samples were analyzed within 48 hours of collection. Radon-222 concentrations were measured within 48 hours of sample collection on a Beckman (Brea, California) LS6000IC liquid scintillation counter. Samples were rerun several days later to confirm, using decay-rate calculations, that radon-222 was the only significant alpha emitter. Care was taken throughout the sampling and preparation process to minimize exposure to the atmosphere prior to alpha counting. Uranium concentrations were determined by laser-induced kinetic phosphorescence analysis (KPA) using a Chemchek (Richland, Washington) KPA-11. Analysis of iron-related bacteria (bacteria that use iron in their metabolism and can be either iron oxidizing or iron reducing) was conducted on unfiltered samples by incubating the sample at room temperature for up to 9 days (Droycon 2004). Dissolved organic carbon concentrations were determined colorimetrically on filtered samples, after the samples were pretreated at pH less than 2 to remove inorganic carbon, and subsequently heated to a temperature of 105 °C in a Hach DRB 200 reactor.

Samples were analyzed for uranium-234, -235, and -238 by alpha spectrometry; for arsenic, selenium, and vanadium by inductively coupled plasma (ICP) mass spectrometry; and for boron by ICP emission at ALS Laboratory Group (Fort Collins, Colorado). Total uranium concentrations determined from the alpha spectrometry analyses were consistent with those determined by KPA. The results of the KPA analyses are used in this report for discussions of uranium where concentrations are provided in mass units.

4.3   Calculations

Though major ion analytical concentrations were reported in units of mass per liter of solution, geochemical modeling calculations (using the speciation code PHREEQC) required units of molality. Conversion of mass units to molality required corresponding measures of water densities, which were estimated from salinity values and temperature using the empirical equations in several published standard methods in Eaton et al. (1995). The calculation method is presented in Appendix B.

Values of pE used in geochemical modeling were estimated from ORP values per the following formula (Stumm and Morgan 1981):

$$pE = Eh/(2.3 \ RTF - 1)$$

where:
   $Eh = ORP - ORP_z + Eh_z$
   ORP_z = ORP of Zobell standard solution
   Eh_z = theoretical Eh of Zobell standard solution
   R = gas constant
   T = absolute temperature (K)
   F = the Faraday constant (96,490 C mol^{-1})
   C mol^{-1} = coulombs per mole

5.0   Results

Frequency distributions of concentrations in environmental samples collected for groundwater monitoring are often skewed toward low values, but logarithms of the concentrations are usually normally distributed (Gilbert 1987). Thus, the geometric mean is a useful statistic that is often used to describe distributions of environmental concentration data. Groundwater concentration data from our study, transformed to logarithmic base 10 values, were found to be nearly normally distributed. Thus, we use the geometric mean, which is equal to 10^{μ}, where μ is the mean of the logarithmic distribution, to describe the chemical distributions. In following report sections, the results of chemical analyses performed on samples of groundwater seeping from sandstone beds or alluvium (locations BAS, BSCS, BSCUS, CWCS, GRCRS, LGWS, MS, TWS, and YHS) are often distinguished from the results of analyses for all other seep locations, which are mostly associated with shale beds. The results from surface water samples (locations BCWL, DAR, DR, SL, SNGC, WD2) are also singled out, as are the results of groundwater collected from wells installed in deep shale.

We analyzed for constituents including arsenic, nitrate, selenium, sulfate, uranium, and vanadium that are often elevated in groundwater at uranium milling sites, to address the potential for contribution of contaminants from the Mancos Shale at uranium mill tailings disposal sites. We measured pH, oxidation-reduction potential and concentrations of major ions including calcium, carbonate (as alkalinity), chloride, magnesium, potassium, and sodium, for the purpose of tracking salt loads, assessing analytical accuracy using charge balance, to define water types, and to use in geochemical speciation modeling. Iron and dissolved oxygen were analyzed to help evaluate redox potentials. Dissolved organic carbon and color were measured to determine if the red or yellow colors observed in the Mancos Shale waters relate to an organic component. Uranium-234 and uranium-238 activities were analyzed because these isotopes have been used to help determine the sources and chemical evolution of dissolved uranium. Boron was analyzed because it is often enriched in marine black shales and may help to detect a Mancos Shale source. Radon-222 was analyzed mainly to help determine if the water had been altered by evaporation. Appendix C provides a complete listing of the chemical analytical results.

5.1   Arsenic

Of the 36 samples analyzed, only one sample of seep water had an arsenic concentration (12 µg/L) that exceeded the drinking water standard of 10 µg/L listed in 40 e-CFR 141. This sample was collected from location SNS in the Sweitzer Lake Area (Figure 6). Arsenic concentrations in more than 70 percent of the seep samples were less than values in surface water samples (Figure 14).
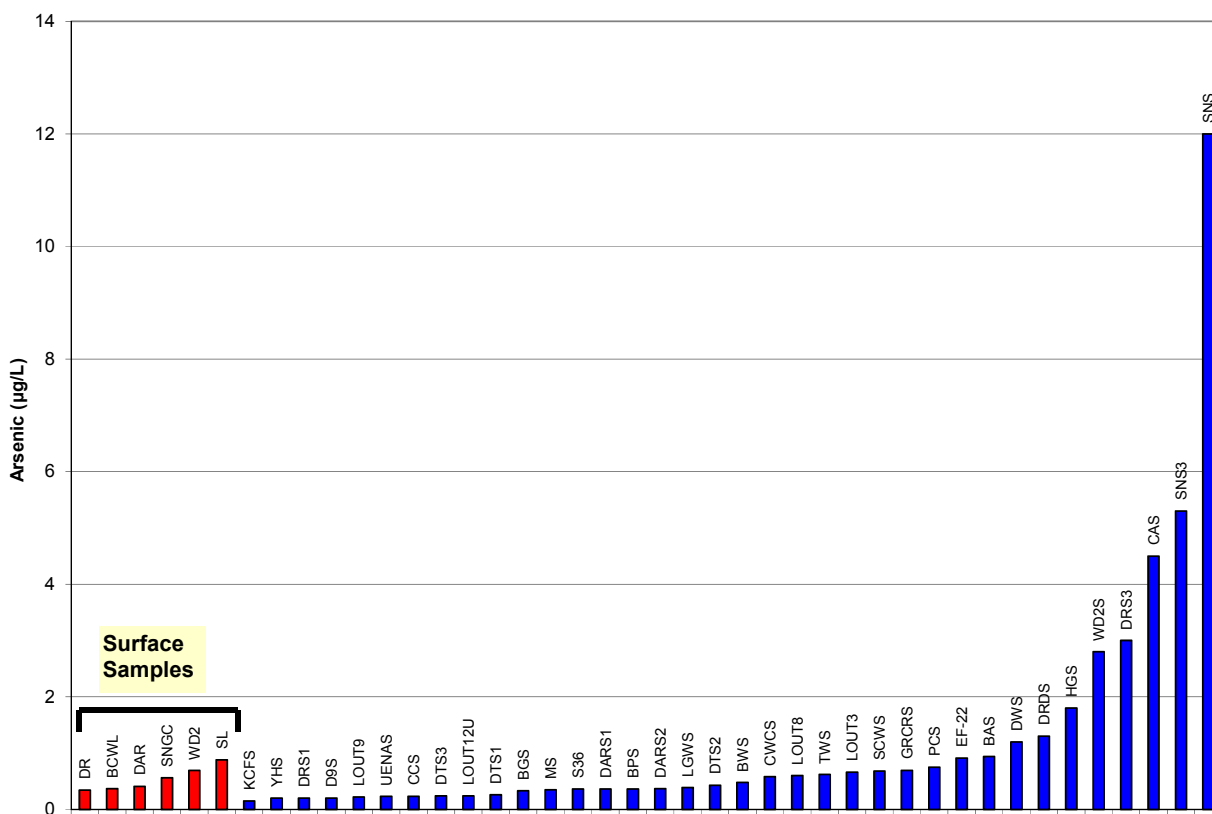
Figure 14. Arsenic Concentrations (µg/L) in Surface Water (Red) and Seep (Blue) Samples

5.2   Boron

Boron concentrations in the six surface water samples ranged from a low value of 3.1 µg/L in Bostwick Canal (BCWL) at the head of Loutsenhizer Arroyo to a high of 530 µg/L at Sweitzer NE Garnet Canal (SNGC). Boron concentrations in seep samples ranged from 16 to 3,200 µg/L with a geometric mean of 441 µg/L (Figure 15). Boron concentrations in seep samples were highest (concentrations of 2,000 and 3,200 µg/L) at two locations in the Sweitzer Lake seepage area. Seep samples with boron concentrations between 1,000 and 1,500 µg/L were collected at Loutsenhizer Arroyo (LOUT3, LOUT8, and LOUT9), Whitewater (WD2S), Point Creek (PCS), and Cedar Creek (CCS). Some of the sandstone seeps had low boron concentrations, including Bert Avery Seep (BAS), Little Grand Wash Seep (LGWS), and Yucca House Spring (YHS). The geometric mean boron concentration for the sandstone seeps was 110 µg/L, which was considerably less than the geometric mean of 692 µg/L for shale seeps.
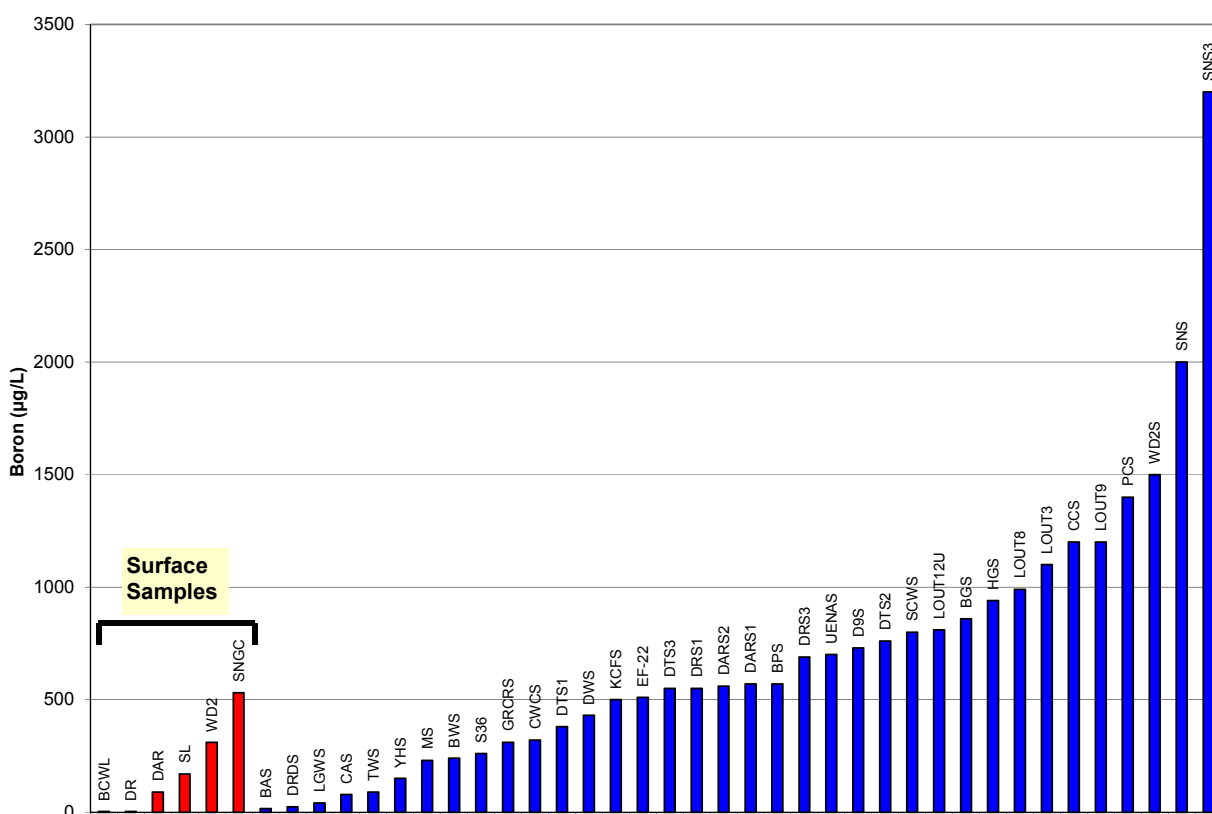
Figure 15. Boron Concentrations (µg/L) in Surface Water (Red) and Seep (Blue) Samples

5.3   Dissolved Organic Carbon (DOC)

DOC concentrations ranged from 2.9 to 265 mg/L in seep samples from the Mancos Shale (Figure 16). Samples from Whitewater Creek tributary (WCTS), Mathis Wash (MWS), and Sweitzer Lake (SNS) had DOC concentrations of more than 260 mg/L. Both locations, UENAS and SCWS, in areas north of Shiprock, New Mexico, had DOC values exceeding 150 mg/L. Samples from Loutsenhizer Arroyo (LOUT3 and LOUT8), Many Devils Wash (EF-22), Houston Gulch (HGS), and Dutchmans Wash (DWS) had DOC concentrations of more than 50 mg/L. DOC concentrations in samples collected at seeps DRS1 and DRS3 east of Delta Reservoir were 16 and 44 mg/L, respectively. At Daly Reservoir, seeps DARS1 and DARS2 had DOC concentrations of 17 and 41 mg/L, respectively. DOC concentrations in the six surface water samples ranged from 3.3 to 31 mg/L.
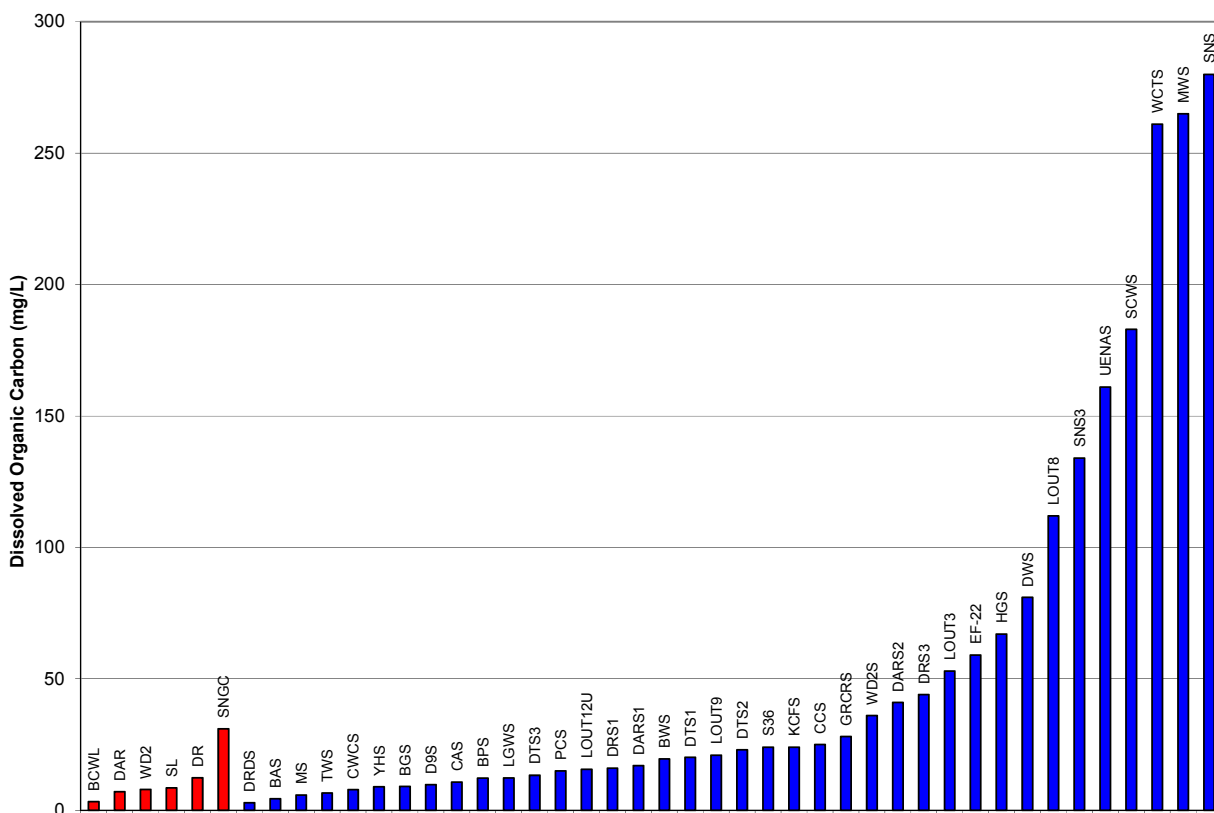
Figure 16. Dissolved Organic Carbon Concentrations (mg/L) in Surface Water (Red) and Seep (Blue) Samples

Much of the groundwater issuing from the Mancos Shale seeps was characterized by a distinctive yellow to deep red color (Figure 9). With the exception of samples from locations SCWS and UENAS in the Shiprock Region, color as measured by light absorbance correlated reasonably well with DOC concentration (Figure 17). Locations SCWS and UENAS showed high DOC concentrations but, for reasons unknown, did not exhibit a yellow or red color and had a low color value. Water color in the streams fed by the colored seepage varies depending on the thickness of the water column. The color is light yellow when the water thickness is less than a few inches, but in thicker pools of water it is deeper shades of yellow and amber, and in pools

more than 12 inches deep, the water has a deep-red color (e.g., Figure 9). Curtis and Schindler (1997) in a study of Canadian lakes demonstrated a correlation between DOC concentration and water color as measured by light absorption. Some authors have noted groundwater with similar coloration related to humic material in other environments. Foster (1950) describes yellow to dark-brown water, similar to the color of swamp water, in deep groundwater of the Gulf Coastal Plain in Mississippi that correlates with high concentrations of sodium bicarbonate stemming from interaction with subsurface humic material.
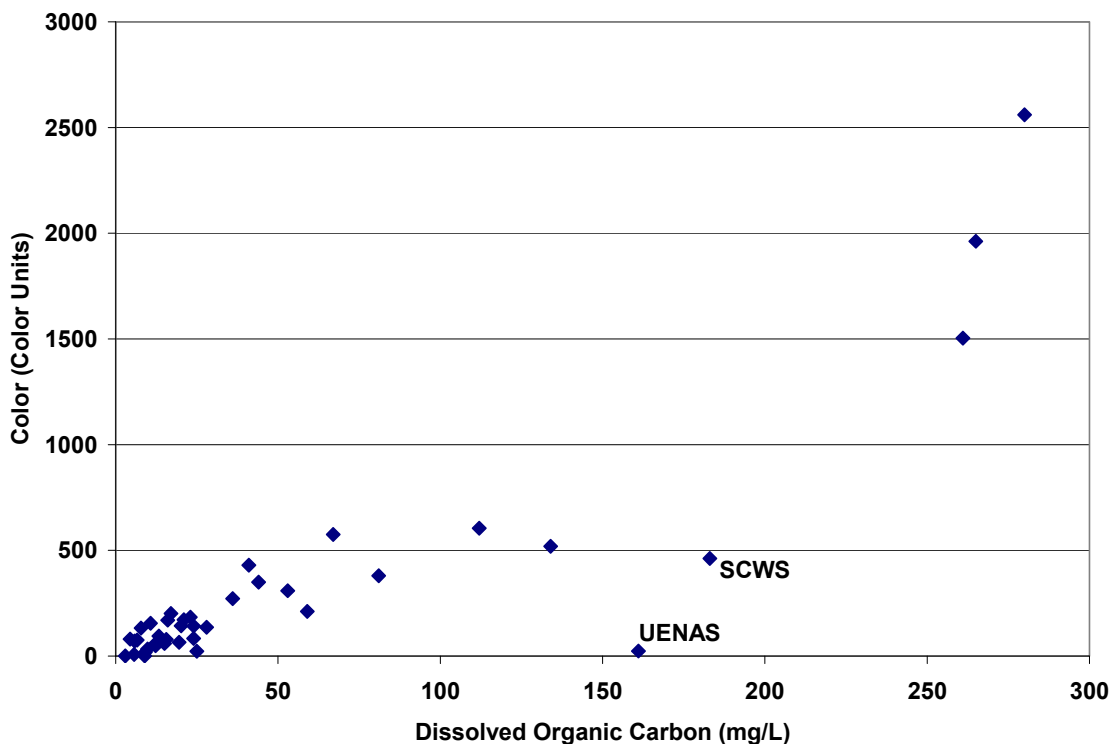
Figure 17. Correlation between DOC Concentration and Water Color in Mancos Shale Seeps

5.4 Major Ions and pH

Many seep samples were highly saline, as indicated by high specific conductivity values. Specific conductivity for the Mancos seeps ranged from 418 to 70,002 µS/cm with a geometric mean of 9,522 µS/cm (Figure 18). Nine seep samples had values exceeding 30,000 µS/cm, and 18 samples had values between 10,000 and 30,000 µS/cm. Specific conductivity values were more than 30,000 µS/cm in seeps associated with large expanses of efflorescence, including Dutchmans Wash (DWS), Many Devils Wash (EF-22), Mathis Wash (MWS), and Sweitzer Lake Area (SNS, SNS1, SNS2, SNS3, US1). Seeps with values of specific conductivity ranging from 15,000 to 30,000 µS/cm were found at Cerro Summit Area (CCS, HGS, HGSE), Daly Reservoir Area (DARS2), Delta Reservoir Area (DRS1, DRS3), Eagle Nest Arroyo (UENAS), Loutsenhizer Arroyo Area (LOUT8, LOUT14, LOUT3), Salt Creek Wash (SCWS), Section 36 Seep (S36), and Whitewater Area (KCFS). Efflorescence was common at most locations that had specific conductivity values more than about 15,000 µS/cm.

Some of the seeps had much lower values of specific conductivity and likely represent conditions other than groundwater issuing from shale. These include Bert Avery Spring (BAS) and Bitter

Spring Creek (BCSUS, BSCS); field observations indicate that these emanate from sandstone of the Ferron Sandstone and Emery Sandstone members of the Mancos Shale, respectively, rather than from shale. Stratigraphic projection suggests that Yucca House Spring (YHS) also issues from sandstone of the Ferron Member, but bedrock is not exposed at that location, and this determination is uncertain. Geometric means of specific conductivity in seeps issuing from shale and sandstone were 11,966 and 2,362 µS/cm, respectively. Six surface water samples, collected from sources of water that likely infiltrated into the Mancos Shale and fed some of the seeps had specific conductivity values ranging from 114 to 6,529 µS/cm (Figure 18).
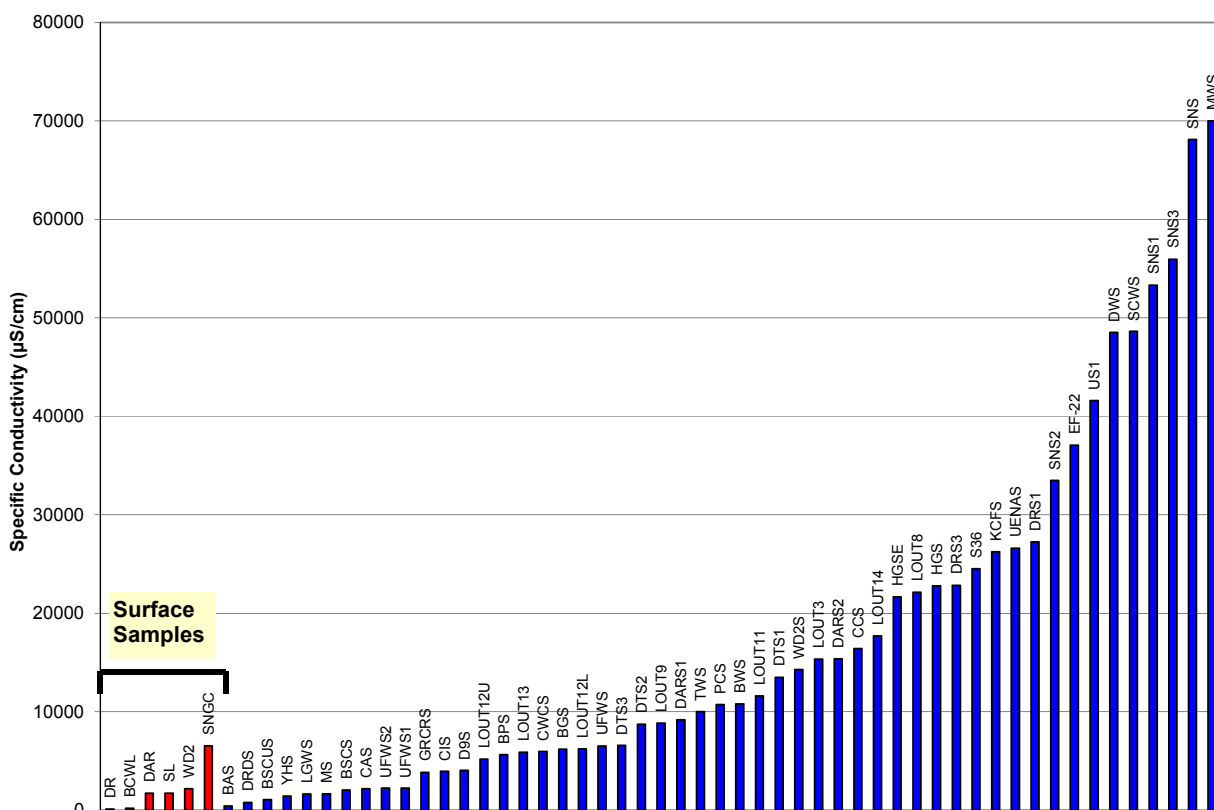
Figure 18. Specific Conductivity (µS/cm) in Surface Water (Red) and Seep (Blue) Samples

Values of pH in the seep samples ranged from 4.15 to 8.45 with a geometric mean of 7.32. Only four seep samples had pH values more than 8; three of these (SNS, SNS2, and US1) were collected in the seepage area at Sweitzer Lake, and the fourth was collected at Dutchmans Wash (DWS). More than half of the seep samples had pH values of less than 7.5. Thus, nearly all the seep samples were lower in pH than the surface water samples (Figure 19). Anomalously low pH values were measured at a tributary to Whitewater Creek, Colorado, where the seep sample (WCTS) had a pH of 4.15, and the surface water sample (WD2S) had a value of 6.57. The cause of these uncharacteristically low pH values is unknown. Surface water samples were typically higher in pH; five of the six surface water samples had a pH of more than 8 (Figure 19).

Concentrations of major cations (calcium, magnesium, sodium, potassium) and anions (carbonate, chloride, and sulfate) are often used to characterize water types and to help evaluate their origins and reactive history (Hem 1985). Groundwater from most seeps had a sodium

sulfate composition (Figure 20). Four samples had a significant (more than 30 percent) bicarbonate component, and about half of the samples contained more than 50 percent calcium plus magnesium. As the specific conductivity values of the seeps increased, so did the dominance of sulfate and sodium; however, magnesium was prevalent even in the high-salinity samples (Figure 21).
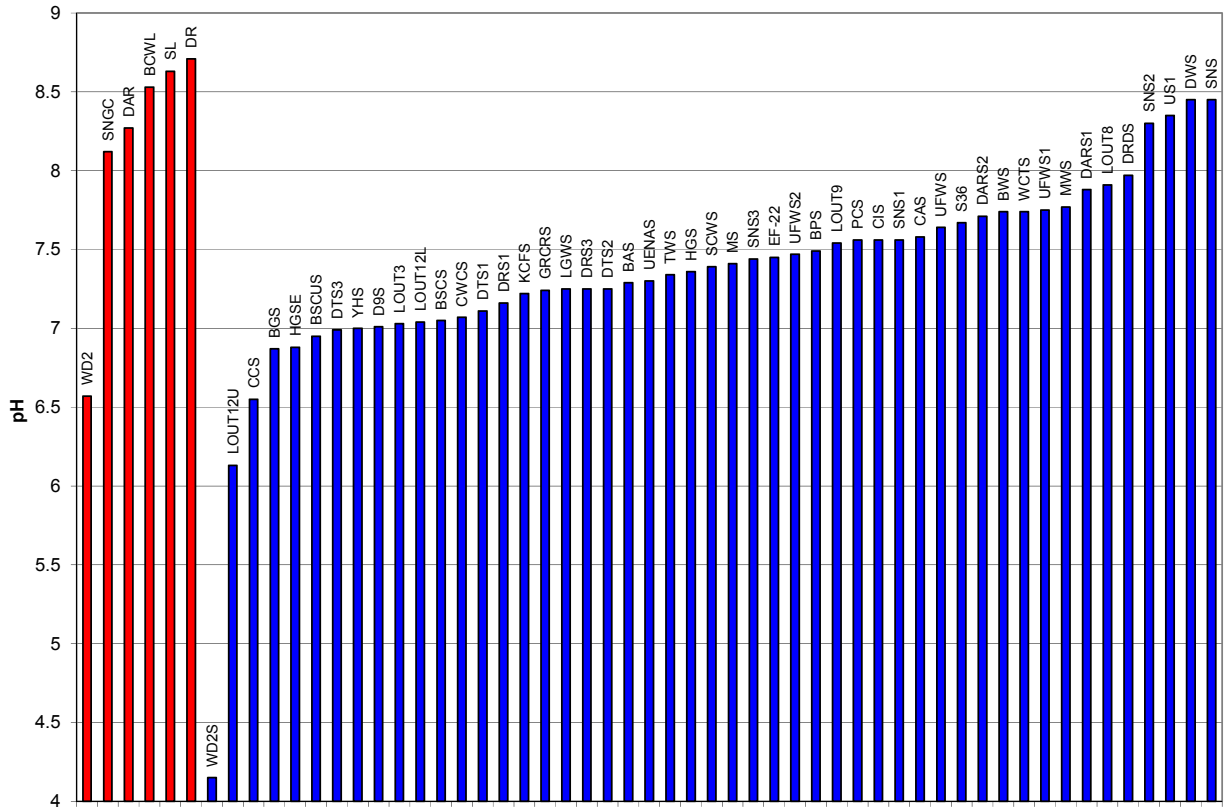
Figure 19. pH Values in Surface Water (Red) and Seep (Blue) Samples
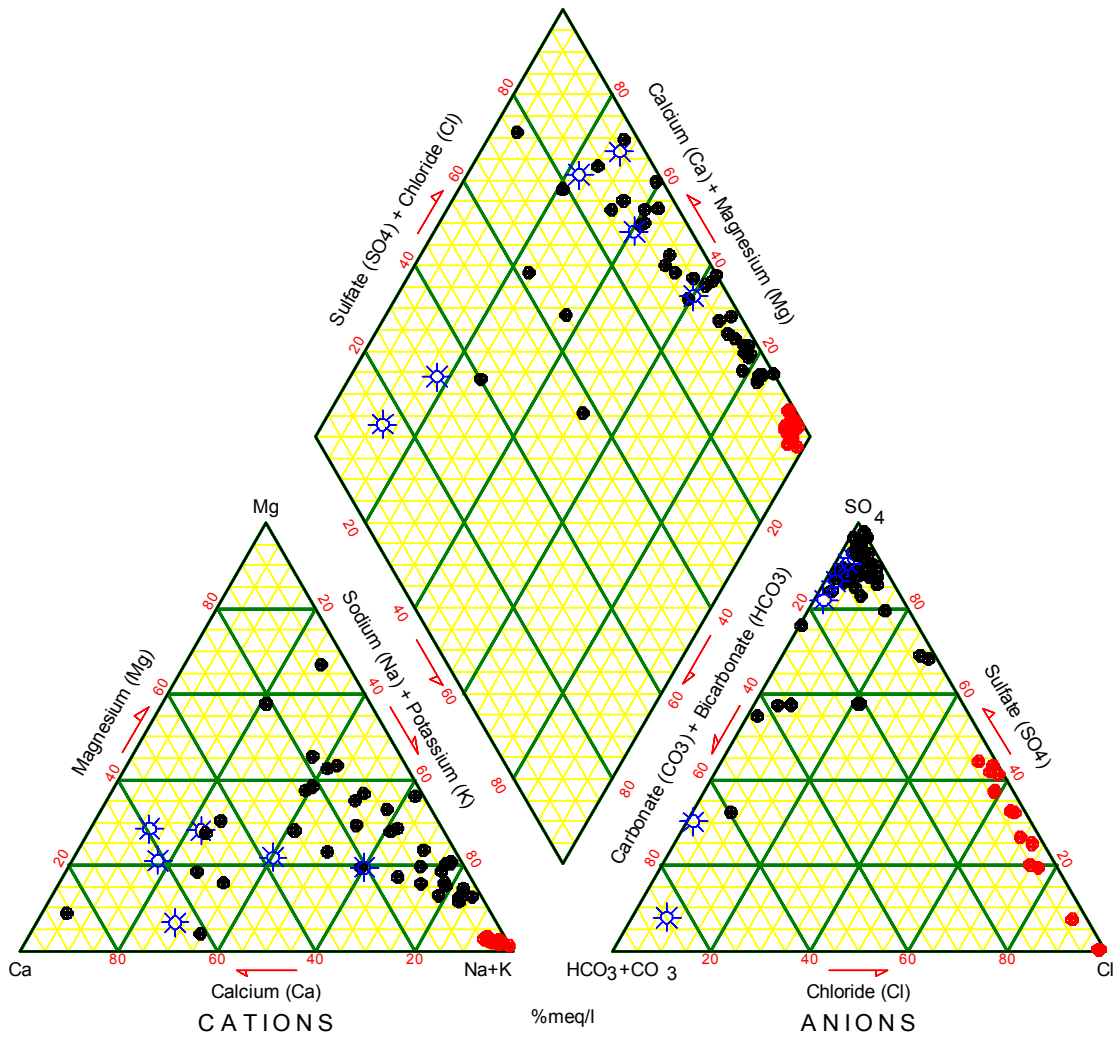
Figure 20. Piper Diagram Showing All Sampled Locations of Mancos Groundwater and Surface Water (black dots = seeps, blue stars = surface water, red dots = deep Mancos wells).
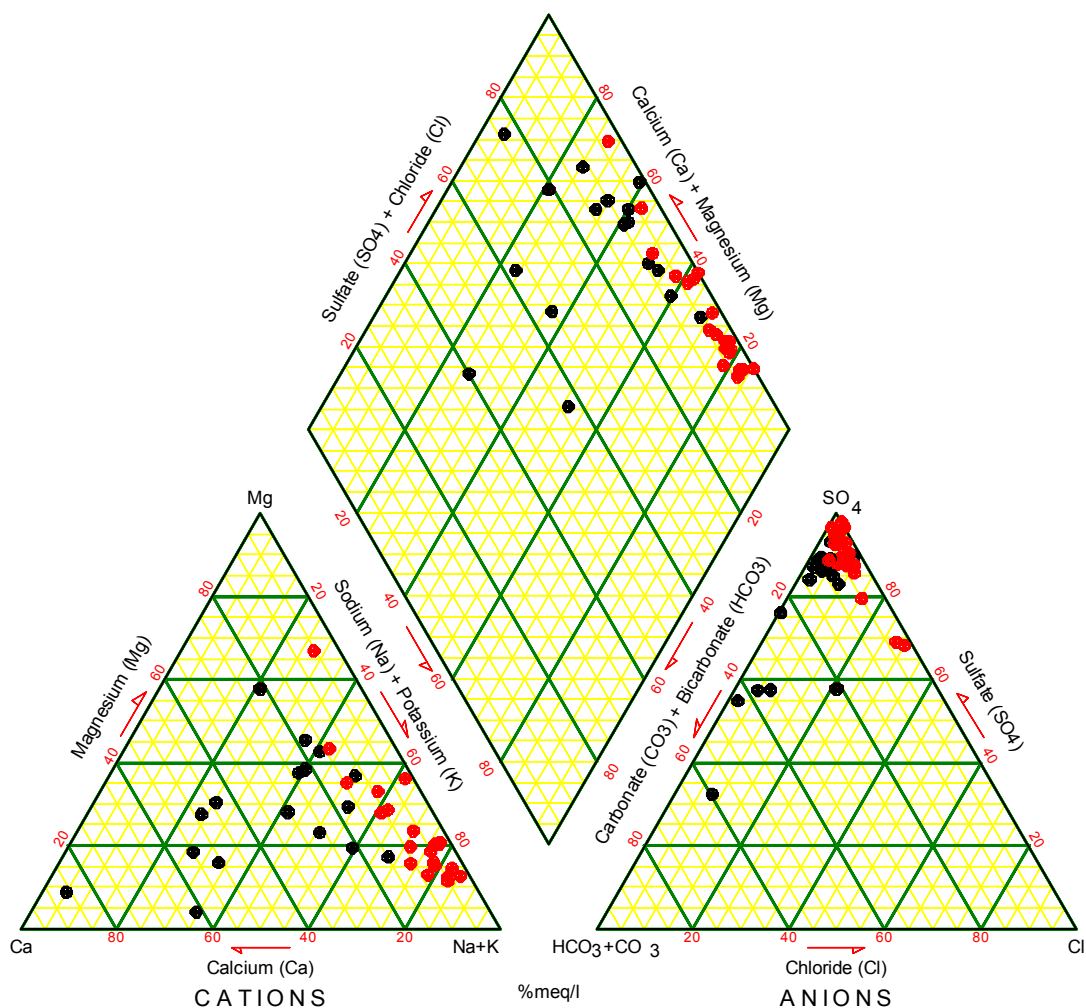
Figure 21. Piper Diagram of Seep Samples Showing Relationship of Seeps to Specific Conductivity. Red dots are samples with specific conductivity higher than 10,000 µS/cm. Black dots are samples with specific conductivity lower than 10,000 µS/cm.

Groundwater data from other studies were used to characterize deep (more than 90 ft below ground surface) horizons in the Mancos Shale. These include analyses of samples collected by DOE from wells used to characterize the geology of a uranium mill tailings disposal site at Crescent Junction, Utah, and from a former uranium mill site at Shiprock, New Mexico (DOE 2007). Groundwater data were also available from a deep Mancos Shale well at the Delta Landfill near the Devil's Thumb Golf Course in Delta County, Colorado, collected and analyzed by Golder Associates (2004). Mancos Shale groundwater samples from 16 deep wells examined for this study had specific conductivity values ranging from 17,030 to 66,120 µS/cm and pH values ranging from 6.84 to 8.2. The groundwater in the deep, unweathered Mancos Shale had a sodium chloride composition, in stark contrast to the sulfate-dominated water in shallow, weathered horizons (Figure 20). In a borehole at DOE's uranium mill tailings disposal site at Crescent Junction, Utah, groundwater flow through shale beds in the unweathered Mancos was confirmed using a downhole camera during which groundwater was observed flowing into the open borehole from fractures.

5.5   Nitrate (as NO₃)

Seeps at three sampling locations had nitrate concentrations of more than 3,000 mg/L, and samples from five additional locations had nitrate concentrations of more than 500 mg/L (Figure 22). Many values are higher than the drinking water standard of 44 mg/L (40 E-CFR 141). Two of the high-nitrate concentrations were from samples collected at locations SCWS and UENAS north of Shiprock, New Mexico, with nitrate concentrations of 1,074 and 3,614 mg/L, respectively. Samples collected from the Section 36 Seep (S36), Houston Gulch Seep (HGS), and Kannah Creek Flowline Spring (KCFS) had nitrate concentrations of more than 800 mg/L. Another area with high nitrate is Loutsenhizer Arroyo, where samples from four locations (LOUT8, LOUT3, LOUT9, and LOUT12U) exceeded 100 mg/L. The two seeps at Daly Reservoir had nitrate concentrations of 150 and 449 mg/L, and two seeps east of Delta Reservoir had concentrations of 76 and 535 mg/L. Two of the seeps near Devil's Thumb Golf Course had nitrate concentrations of 389 and 413 mg/L. Samples collected near the golf course may have some nitrate contributed from fertilizer. Five of the six surface water samples contained less than 3.7 mg/L of nitrate. The sixth sample was collected at the Sweitzer Lake Garnet Canal (SNGC) and had a nitrate concentration of 92 mg/L. Despite the higher concentration of nitrate in the Sweitzer Lake Garnet Canal, the seep samples from sites SNS3 and SNS at the Sweitzer Lake seepage area had relatively low nitrate concentrations of only 4.1 and 18 mg/L, respectively.
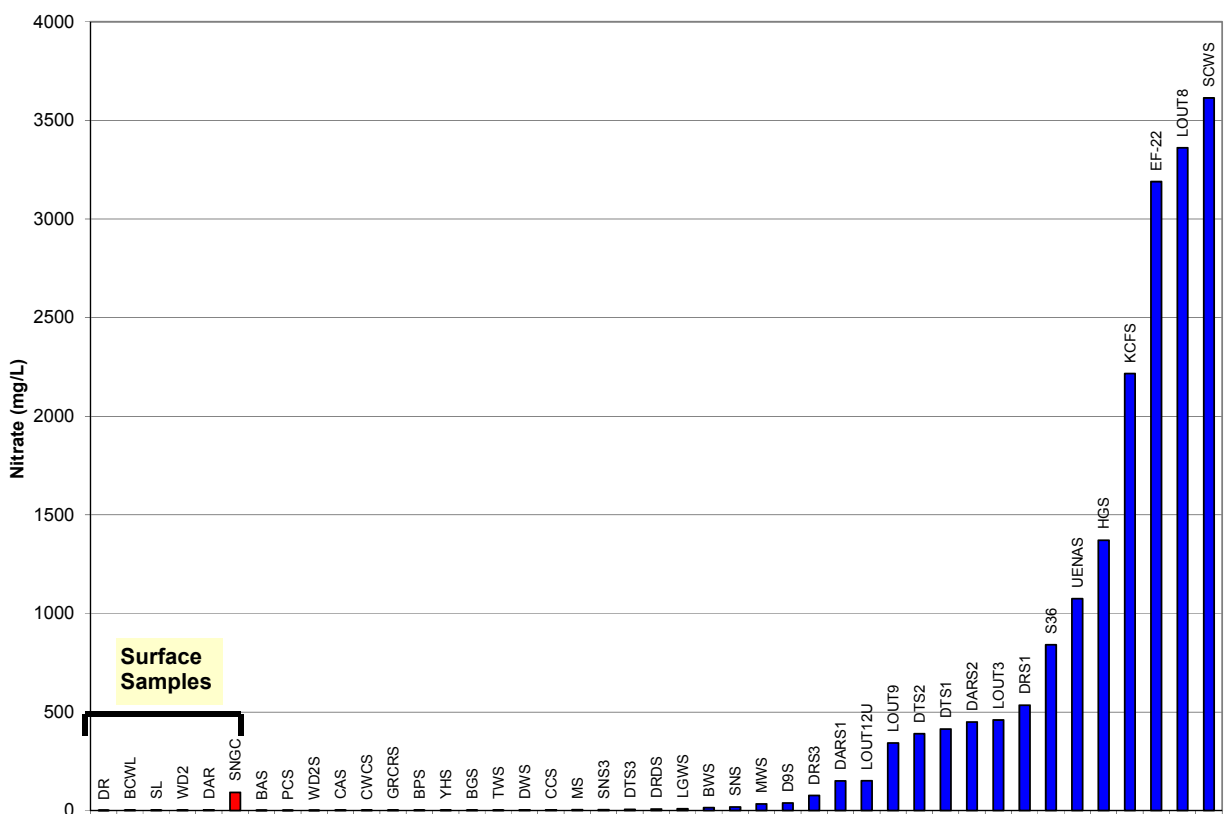
Figure 22. Nitrate Concentrations (mg/L) in Surface Water (Red) and Seep (Blue) Samples

5.6   Radon-222

Two samples were collected for radon-222 analysis at each sampling location, one early during the sampling and another near the end after most other samples had been collected. Generally, the sample collected later had a higher radon-222 value than the earlier one, suggesting that the early water sample had been affected by atmospheric exposure in the borehole, but that less-disturbed formation water was entering the borehole during purging and sampling. The higher of the two values is used for the discussion because the higher value is likely to be most representative of the radon-222 concentration in the formation water.

The highest radon-222 concentration in the six surface samples was 49.8 pCi/L, and all other concentrations were less than 12.6 pCi/L (Figure 23). These low values confirm that radon-222 is released to the atmosphere from standing bodies of water. Seep samples ranged from less than 1 to 1,625 pCi/L. The data show a plateau at about 425 pCi/L and another at about 800 pCi/L (Figure 23), and these values may be indicative of average values for the Mancos Shale. The plateau at 425 pCi/L included three sites in the Loutsenhizer Arroyo Area, and it seems reasonable that this value may represent in situ concentrations for the Mancos Shale in that area. However, the concentration of radon-222 in the groundwater varies from site to site, and data can only be used as a qualitative indicator of atmospheric exposure. The three seep samples (DWS, LGWS, and BGS) with the lowest radon-222 values were collected from water that had flowed along the surface a short distance, and there was opportunity for radon to be lost to the atmosphere.
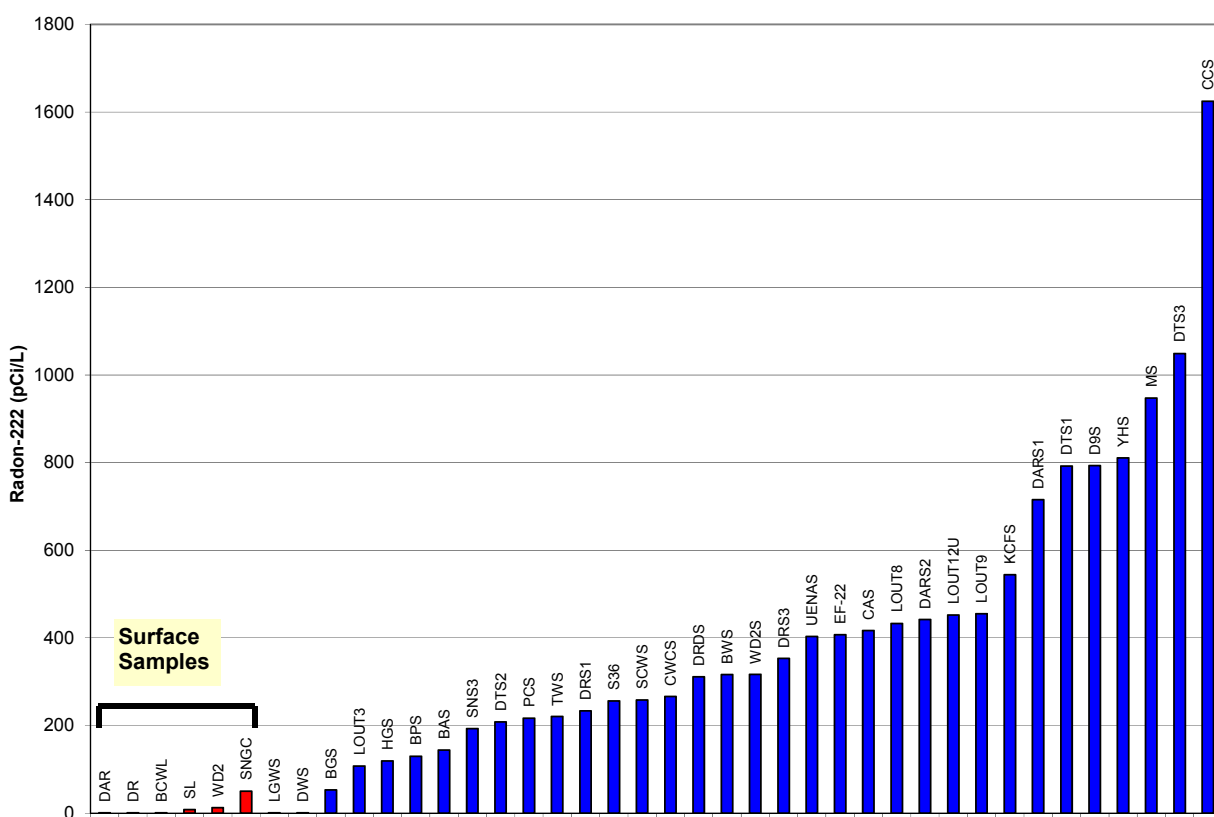
Figure 23. Radon-222 Concentrations (pCi/L) in Surface Water (Red) and Seep (Blue) Samples

5.7   Selenium

Selenium concentrations in seep samples ranged from 0.14 to 4,700 μg/L with a geometric mean of 51.5 μg/L. Many values are higher than the drinking water standard of 50 μg/L (40 E-CFR 141). Four of the sites (LOUT3, LOUT8, LOUT9, and LOUT12U) in Loutsenhizer Arroyo had selenium concentrations of more than 700 μg/L, and the LOUT8 sample had the highest value of 4,700 μg/L (Figure 24). Selenium concentrations of more than 1,000 μg/L occurred in seeps at Section 36 (S36) near Cisco, at EF-22 and SCWS near Shiprock, and at KCFS near Grand Junction. Samples of seeps from two sites at Sweitzer Lake were sampled for selenium; one (SNS) had a high value of 3,500 μg/L, whereas the concentration in the other (SNS3) was only 13 μg/L. The two seeps at Daly Reservoir had selenium concentrations of 110 and 400 μg/L, whereas concentrations in those at Delta Reservoir were 100 and 950 μg/L. All of the seeps associated with sandstone were relatively low in dissolved selenium (a geometric mean of 3.0 μg/L) compared to seeps associated with shale, which had a geometric mean of 124.2 μg/L. Seeps at sites that were elevated in other contaminants but were low in selenium include Point Creek, Dutchmans Wash, and Cedar Creek. Five of the six surface samples had low selenium concentrations (less than 15 μg/L), but the Garnet Canal sample at Sweitzer Lake had 110 μg/L selenium, probably derived from irrigation return flow.
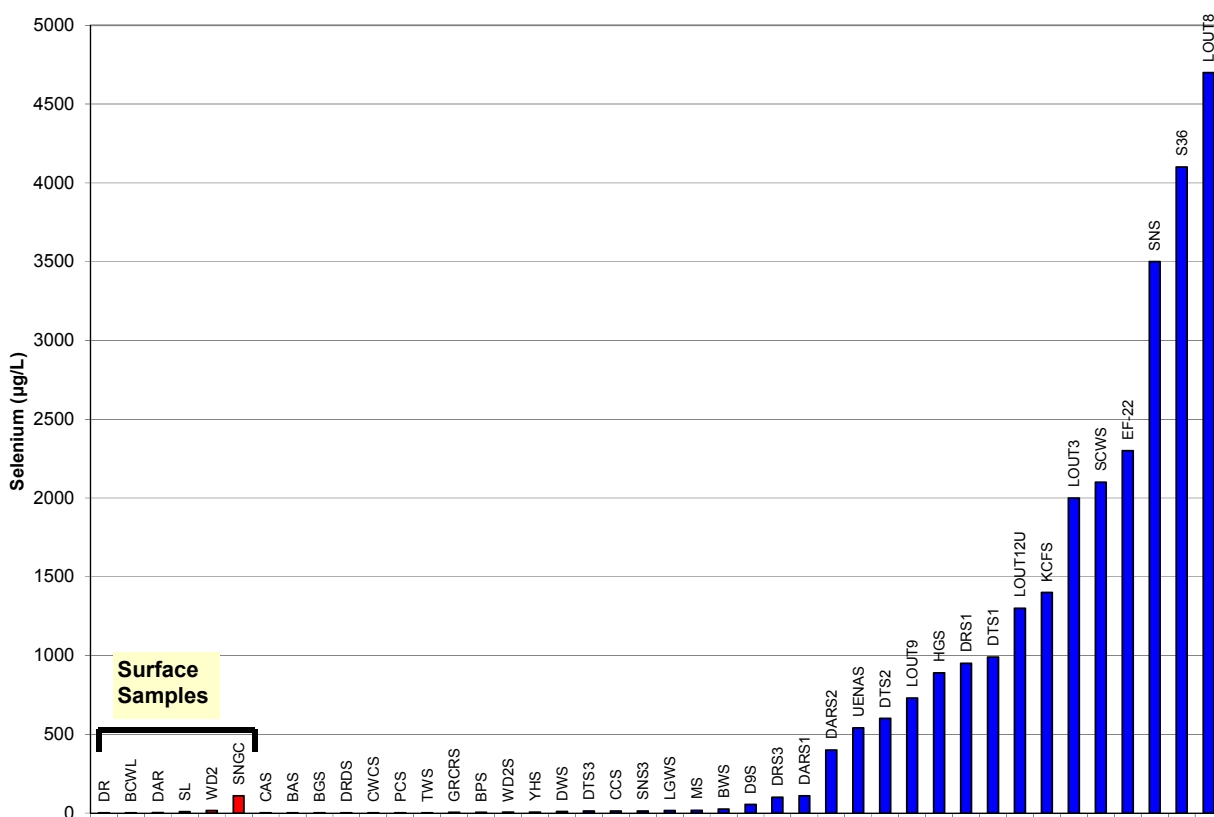
Figure 24. Selenium Concentrations (μg/L) in Surface Water (Red) and Seep (Blue) Samples

5.8　Uranium

Uranium concentrations in groundwater samples collected for this study ranged from 0.2 to 1,922 µg/L and had a geometric mean of 49.7 µg/L (Figure 25). Many values are higher than the drinking water standard of 30 µg/L (40 E-CFR 141). Five samples (SNS, SNS1, SNS2, SNS3, and US1) with uranium concentrations more than 200 µg/L were collected from the seepage east and northeast of Sweitzer Lake. Seepage formed a marsh area covered by thick efflorescence. Thus, although care was taken to ensure that groundwater flowed to each shallow (2 ft deep) sampling hole, upward capillary flow and evaporation may have concentrated dissolved constituents in these samples. Other samples with uranium concentrations more than 200 µg/L were collected at seeps near Whitewater, Colorado (WCTS); Mathis Wash (MWS) and Dutchmans Wash (DWS) near Price, Utah; Houston Gulch (HGS) near Montrose, Colorado; and Point Creek (PCS) near Delta, Colorado. All of these seeps except Point Creek are in or near irrigated areas and are likely fed from irrigation canal water. Point Creek is in a remote area, and no source of water for this seep was apparent during our reconnaissance. Samples from locations near Shiprock (EF-22 and SCWS), Loutsenhizer Arroyo (LOUT3, LOUT8, LOUT9), Delta Reservoir and Devil's Thumb Golf Course Area (DRS3 and DTS1), and Section 36 (S36) had uranium concentrations between 100 and 200 µg/L, which are all well above the mean value of 8.1 µg/L for the Four Corners states (USGS 2011b). Uranium concentrations in seep samples collected from shale beds were higher than those from seeps that discharged from sandstone. The geometric mean of uranium in shale bed seeps was 83.4 µg/L, and the geometric mean for sandstone seeps was 7.3 µg/L. Uranium in samples from the deep, unweathered Mancos Shale had a geometric mean of 7.4 µg/L (Table 3).
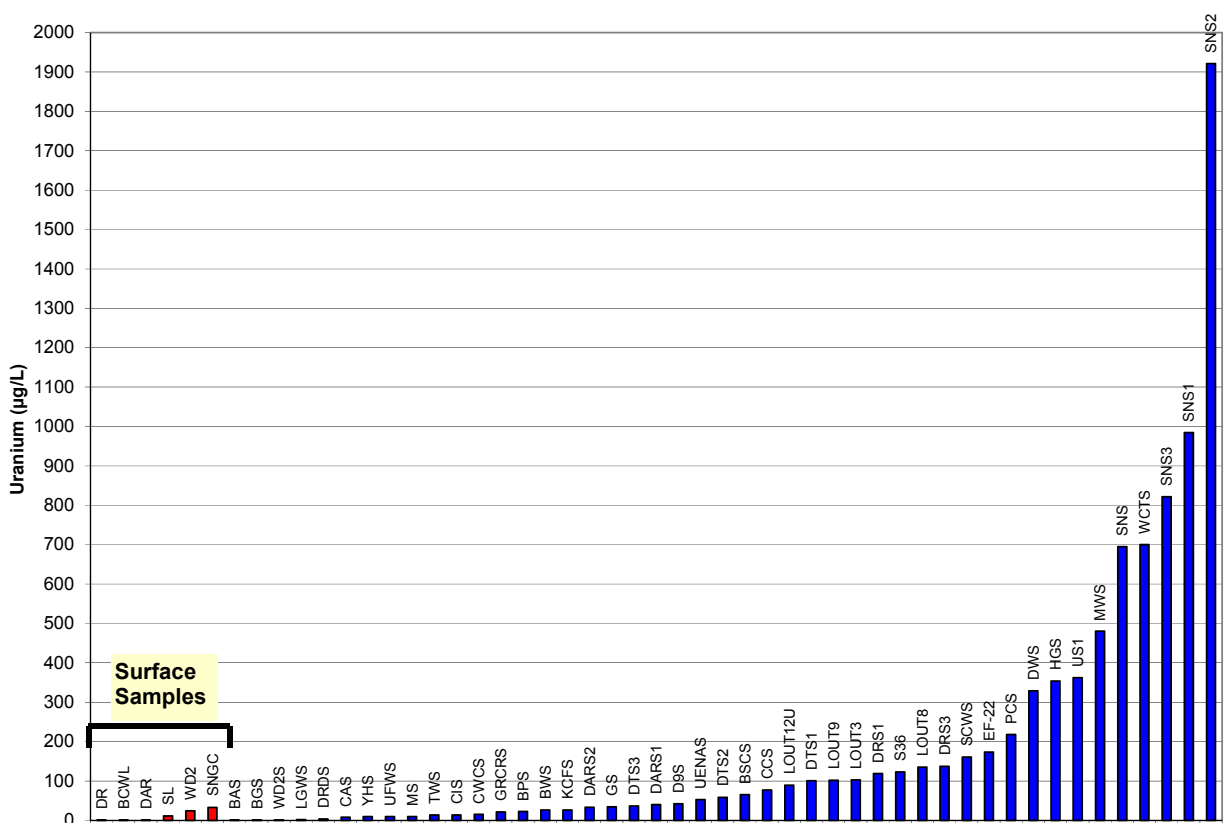
Figure 25. Uranium Concentrations (µg/L) in Surface Water (Red) and Seep (Blue) Samples

Table 3. Uranium Concentration (µg/L) Statistics for Samples from this Study

	Count	Minimum	Maximum	Geometric Mean
All Seeps	45	0.2	1922	49.7
Shale Seeps	38	1.0	1922	83.4
Sandstone Seeps	8	0.2	76.7	7.3
Deep Wells	15	0.23	270	7.4
Surface Water	6	0.20	32.8	2.9

5.9 Uranium Isotopes

Uranium-234 and -238 isotopes were analyzed on all samples that had sufficient sample volume and sufficient uranium concentrations (generally, more than about 0.5 µg/L). Uranium concentrations in samples BGS, WD2S, BAS, and DR were too low to get quantifiable uranium isotopic results with the counting times used. Uranium activity ratios (ARs) of uranium-234 to uranium-238 ranged from 1.22 to 4.08, and uranium concentrations ranged from 1.5 to 822 µg/L (Table 4). AR values ranged from 1.50 to 3.06 at the five surface water sites, and uranium concentrations ranged from 0.40 to 32.8 µg/L.

Table 4. Ranges and Geometric Means of Uranium Concentration (µg/L) and AR for the 38 Samples with Quantifiable Uranium Isotopic Results

	No. of Samples	Range of U Concentration	Geometric Mean U	Range AR Values	Geometric Mean AR
Seeps	33	1.5–822	53.6	1.22–4.08	2.05
Surface Sites	5	0.40–32.8	4.9	1.50–3.06	1.90

Uranium isotopic analyses are often used to help interpret the chemical evolution of groundwater systems (Osmond and Cowart 1976). Because our samples were collected from widely separated areas on the Colorado Plateau and are not from a single aquifer system, it was not possible to interpret groundwater evolution with these data. However, the results can be used to better understand the variation in uranium isotopic signatures in groundwater that interacts with the Mancos Shale. Figure 26 shows the AR values plotted against uranium concentration and displays relative specific conductance values (symbol size) and water-type designation (symbol color). All samples of both seeps and surface water had uranium-234 activities greater than the secular equilibrium values. There was little difference between AR values for seeps from shale and those from sandstone; the geometric means were 2.06 and 1.95, respectively. There were no obvious correlations between AR values and lithology, stratigraphic position, uranium concentration, or groundwater chemistry. A seep sample from the Whitewater Area (KCFS) had the highest AR of 4.08. More than half of the seep samples had AR values greater than 2.0, including samples from the Green River Region (CAS, LGWS, and S36), Hanksville Region (TWS), Delta Area (DRS1, DRS3, DTS1, DTS2, DTS3, Price Region (DWS), Shiprock Region (D9S, EF-22, SCWS, UENAS, and YHS), and Buen Pastor Spring at Sweitzer Lake (Figure 26). AR values of the surface samples were all more than 1.50, and the sample from Daly Reservoir (DAR) had the highest surface water AR value of 3.06. The four samples from Loutsenhizer Arroyo had consistent AR values ranging from 1.71 to 1.87. AR was measured on February 15, 2001, on a single sample from the deep, unweathered Mancos Shale at Shiprock, and this result is plotted on Figure 26 for comparison.
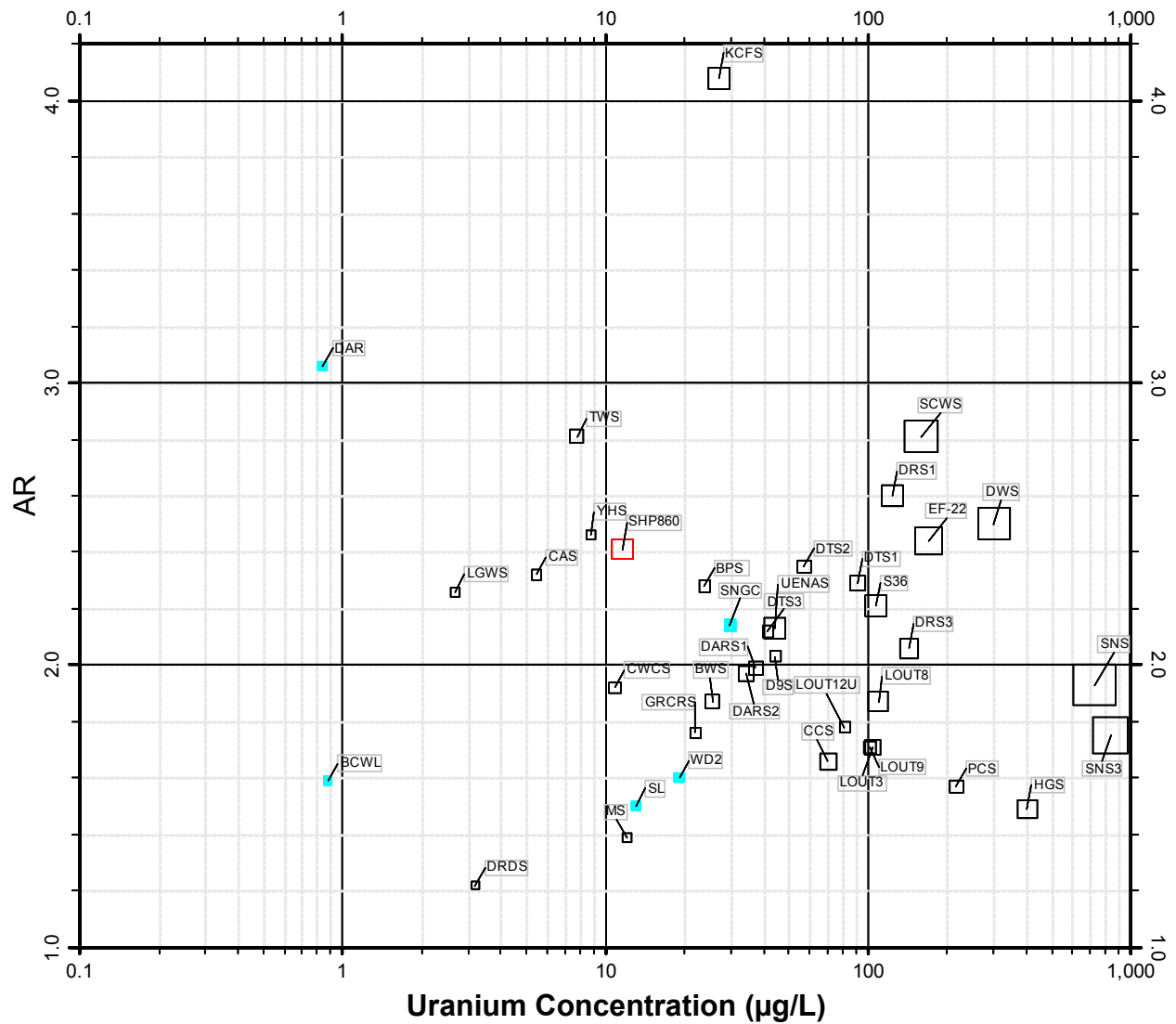
Figure 26. Binary Plot of AR Versus Uranium Concentration for all Samples Analyzed in the Study. Size of square represents relative specific conductivity value. Red, black, and turquoise symbols represent deep well, groundwater, and surface water samples, respectively.

5.10 Vanadium

Vanadium concentrations were low in all samples. The highest value of 19 µg/L was measured in sample SNS from Sweitzer Lake. All other samples had vanadium concentrations less than 3.8 µg/L (Figure 27).
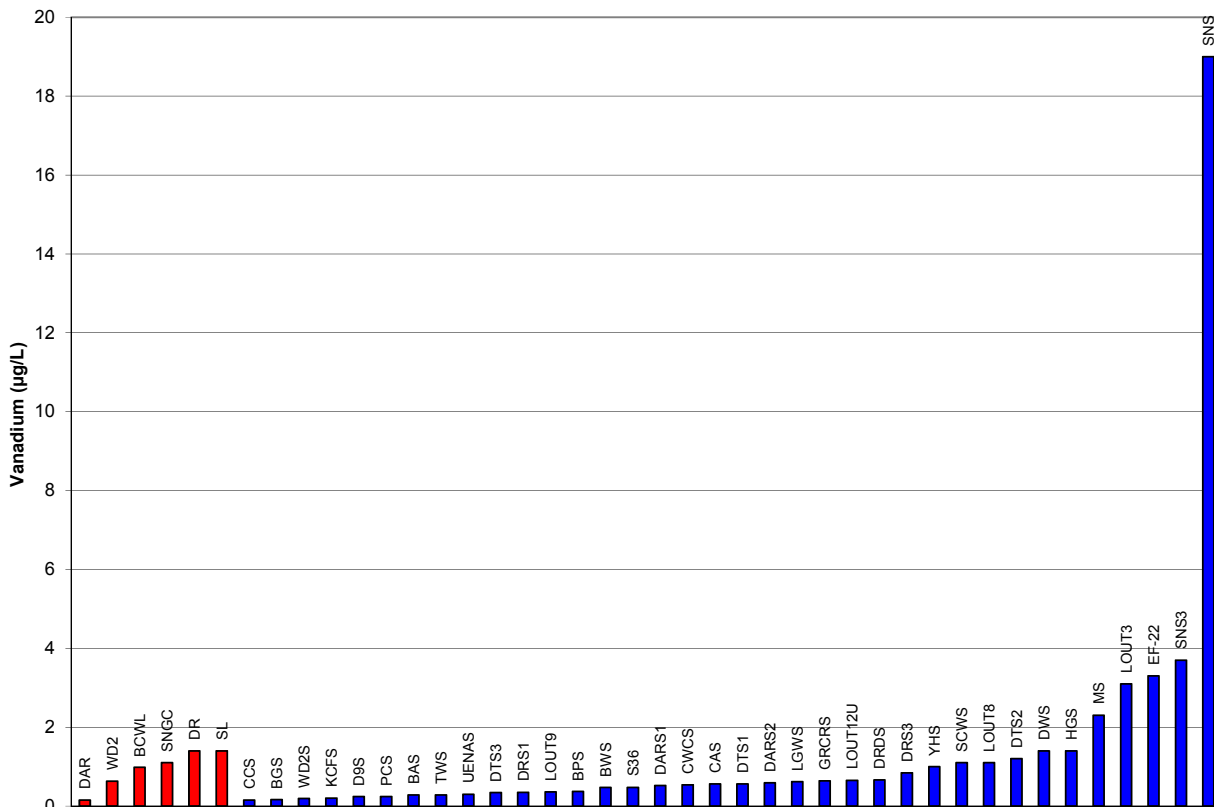
Figure 27. Vanadium Concentrations (µg/L) in Surface Water (Red) and Seep (Blue) Samples

6.0   Discussion

Naturally contaminated seeps develop in areas where water contacts shale of the Mancos Shale and the topography is favorable. The seeps often have specific conductivity values exceeding 15,000 µS/cm, indicating that they have high salinity. Butler et al. (1994) also reported values of high specific conductivity from the weathered Mancos Shale for eight groundwater sampling locations in the Uncompahgre and Grand Valley project areas, where specific conductivity values ranged from 3,650 to 13,900 µS/cm. Groundwater in the weathered Mancos Shale has a sodium sulfate composition, whereas groundwater in the unweathered Mancos Shale has a sodium chloride composition.

Concentrations of nitrate, selenium, and uranium in groundwater from shale beds of Mancos are usually higher than the Safe Drinking Water Act (40 e-CFR 141) drinking water standard, often by a factor of 10. Thus, evaluations of contaminant plumes in Mancos Shale terrain should consider the possible contribution of natural contamination. Because of the wide geographic

separation of the sampling locations and the association with various geologic units of the Mancos Shale, we conclude that natural contamination from Mancos Shale is ubiquitous and is not confined to specific areas or specific geologic members. Contaminant concentrations are higher in groundwater flowing through shale than in groundwater flowing through sandstone, as indicated by the geometric means in Table 5.

Table 5. Geometric Means of Mancos Groundwater Concentrations for Shale and Sandstone Aquifers

Analysis	Shale	Sandstone
Uranium (µg/L)	83.4	7.3
Selenium (µg/L)	124.2	3.0
Nitrate (mg/L)	68.2	2.2
Boron (µg/L)	692.1	110.4
Specific Conductivity (µS/cm)	14,086	2,108

Although care was taken to ensure that all of the groundwater samples were collected from active seepage areas, some of the sampling sites were obscured by alluvium or soil, and some could have been affected by fertilizer chemicals. For the following discussion, six key areas were selected that were either isolated from irrigated areas or the source of recharge water was known and was accessible for sampling. These areas are Daly Reservoir, Delta Reservoir, Loutsenhizer Arroyo, Point Creek Seep, Salt Creek Wash, and Upper Eagle Nest Arroyo. The chemistry of samples collected from the seeps at these key areas is a direct result of interaction with the host rock. Because bedrock and seeps are well exposed at these six areas, the exact point where the seeps emerge from dark-gray shale bedrock could be observed, and samples were collected at that point. The construction and water level history of Delta Reservoir (Figure 3) are well known, and the water infiltrating the Mancos Shale is pristine, having been derived from high on the Grand Mesa. Once this water enters the groundwater, it flows through Mancos Shale to the seeps at locations DRS1 and DRS3, located about 1,400 ft from the reservoir. Thus, any constituents dissolved in the seep water must have been derived from chemical transfer from the Mancos Shale to the groundwater.

A similar situation exists at Daly Reservoir (Figure 10) with sampling sites DARS1 and DARS2 located 230 and 360 ft from the reservoir, respectively; however, the infiltrating water is not as pristine, having been derived from ephemeral surface flows in this arid region. Because the composition of the water in Daly Reservoir is known from analysis, the constituents derived from Mancos Shale can be determined by difference. At Loutsenhizer Arroyo (and its tributaries), groundwater emerging as seeps likely is from the upland West Lateral of the Bostwick Canal located about 800 ft (LOUT9) to 4,700 ft (LOUT3) hydraulically upgradient (Figure 12). Bostwick Canal conveys pristine water from the north side of the San Juan Mountains to irrigate agricultural fields in Bostwick Park (Figure 12). Infiltration from the irrigated fields supplies some of the groundwater in Loutsenhizer Arroyo, but infiltration from applied irrigation water is probably minimal compared to the seepage contribution from the canal itself. Bostwick Canal receives irrigation return and thus is not pristine; however, because the composition of the canal water is known from chemical analysis, again the constituent contributions from Mancos Shale can be determined by comparison. The sources of water at Point Creek Seep, Salt Creek Wash, and Upper Eagle Nest Arroyo are unknown; however, there are no obvious anthropogenic water sources in these remote areas.

Because the geologic and hydrologic relationships at these areas are well known, data from them are emphasized in the following discussion of the origin of the seep chemistry. Table 6 shows the composition of natural contaminants in the seeps from the six areas. In all these key areas, concentrations of nitrate, selenium, sulfate, and uranium are elevated, indicating a natural contamination source in the Mancos Shale.

Table 6. Concentrations of Groundwater Constituents in Six Key Areas

Area	Location	Specific Cond. (µS/cm)	SO$_4$ (mg/L)	NO$_3$ (mg/L)	U (µg/L)	Se (µg/L)
Daly Reservoir	DARS1	9,187	5,729	150	39.7	110
Daly Reservoir	DARS2	15,377	9,865	449	33.2	400
Delta Reservoir	DRS1	27,250	18,497	534	119.1	950
Delta Reservoir	DRS3	22,840	15,087	76	137.2	100
Point Creek	PCS	10,739	7,282	<0.5	217.6	1.5
Salt Creek Wash	SCWS	48,639	23,800	3,614	160.3	2,100
Upper Eagle Nest Arroyo	UENAS	26,607	12,839	1,074	53	540
Loutsenhizer Arroyo	LOUT3	15,330	8,820	459	102.6	2,000
Loutsenhizer Arroyo	LOUT8	22,130	14,942	3,361	135.2	4,700
Loutsenhizer Arroyo	LOUT9	8,844	5,696	342	101.6	730
	Standard[a]	na	na	44	30	10

[a] Safe Drinking Water Act standard (40 e-CFR 141)
na = not applicable

6.1   Geochemistry and Mineralogy of Marine Black Shale and Mancos Shale

To understand the origin and evolution of groundwater chemistry, it is important to know the mineralogy and chemical exchange capacity of the Mancos Shale with which the groundwater interacts. This section is a summary of the literature containing data on the solid-phase composition and groundwater chemistry of the Mancos Shale, leading to development of a conceptual model for the chemical evolution of the Mancos Shale groundwater. Finally, we numerically simulate processes comprising the conceptual model using a numerical reaction progress modeling approach.

Clay minerals, sulfide minerals, organic matter, carbonate minerals, and sulfate minerals are likely to have an effect on Mancos Shale groundwater chemistry. It is also important to know the solid-phase residences of the chemical constituents. Mass transfer processes likely to be important in controlling groundwater chemistry include ion exchange, mineral dissolution and precipitation, adsorption, and desorption. Table 7 shows a generalized composite of the mineralogical and chemical composition of shale beds in the Mancos Shale based on information presented in the following sections. This generalized composite is used later to help understand the interactions of Mancos Shale with groundwater.

The geochemical and mineralogical contents of the Mancos Shale and some major black shale formations, as discussed herein, were derived from multiple information sources. As part of DOE's siting evaluation for the Crescent Junction uranium mill tailings disposal site, we logged and analyzed core samples collected from 10 borings of the Prairie Canyon and Lower Blue Gate Members of the Mancos Shale (DOE 2007). All 10 borings were cored continuously to a depth of 300 ft below ground surface. Core was logged, and selected samples were analyzed for

chemistry and mineralogy. Tuttle et al. (2007) excavated trenches in the Mancos Shale and associated soils in three areas: (1) Elephant Skin Wash located near the upper reach of Loutsenhizer Arroyo about 1.5 miles due west of our location LOUT9, (2) Candy Lane located about 10 miles due north of Montrose, Colorado, and (3) Hanksville, Utah[1]. Butler et al. (1994) analyzed four samples of weathered Mancos Shale, two samples of unweathered Mancos Shale, and two samples of ash beds (bentonite beds) from the Uncompahgre Valley and Grand Valley areas in Colorado[2]. Results from these three studies are presented in this report section along with other literature data from additional sources.

Table 7. Generalized Mineralogical and Chemical Composite of Unweathered Shale in Mancos Shale

Mineralogy	
Carbonate Content	20%
Cation Exchange Capacity	20 meq/100 g
Clay Minerals	mixed-layer illite/smectite, illite, kaolinite
Gypsum Content	present
Minerals Present	calcite, dolomite, feldspar, gypsum, halite, nahcolite, pyrite, quartz, sylvite
Nahcolite, Halite	trace
Pyrite Content	1%
Surface Area	10 m^2/g
Chemistry	
Arsenic	15 mg/kg
Boron	50 mg/kg
Organic Carbon	1% C
Selenium	2 mg/kg
Uranium	3.7 mg/kg
Vanadium	100 mg/kg

meq/100 g = milliequivalents per 100 grams
m^2/g = square meters per gram

6.1.1   Arsenic Content

The average arsenic concentration in 21 samples of shale and marlstone of the Pierre Shale analyzed by Tourtelot (1962) was 14 mg/kg; one additional sample that was particularly rich in organic matter had an anomalously high arsenic content of 41 mg/kg. Schultz et al. (1980) determined the arithmetic mean arsenic concentration of more than 200 shale and siltstone samples of the Pierre Shale to be 14 mg/kg with a standard deviation of 35 mg/kg.

Butler et al. (1994) reported arsenic contents of 2 unweathered shale samples of 10 and 22 mg/kg, ash beds of 20 and 25 mg/kg of arsenic, and 4 samples of weathered shale of 10 mg/kg or less. Tuttle et al. (2007) reported arithmetic means for arsenic concentrations on 72 samples from Elephant Skin Wash, 94 samples from Candy Lane, and 16 samples from Hanksville as 5.82, 11.93, and 4.63 mg/kg, respectively.

---

[1] The exact location near Hanksville was not provided. Chemical digestion methods for the core and soil samples were not provided, but we assume the results represent total digestions.
[2] The chemical digestion methods are uncertain, but we presume that the results represent a total digestion, including resistate grains.

6.1.2 Boron Content

Harder (1970) provided mean boron concentrations of 100 mg/kg for clay and shale, 35 mg/kg for sandstone, 27 mg/kg for limestone, and 28 mg/kg for dolomite. Boron occupies tetrahedral sites in mica, and the concentration of boron in illite had been used as an index of paleosalinity, although this concept has not received widespread acceptance (Harder 1970). Boron concentrations in 67 samples of shale and marlstone of the Pierre Shale measured by Tourtelot (1962) ranged from 15 to 150 mg/kg with most values near 30 mg/kg. Schultz et al. (1980) determined the arithmetic mean boron concentration of more than 200 shale and siltstone samples of the Pierre Shale to be 99 mg/kg with a standard deviation of 49 mg/kg. Schultz et al. (1980) found that high boron concentrations were present in both marine and nonmarine shale of the Pierre Shale, and thus, they were not a good indicator of salinity. They also found that boron concentrations did not correlate with organic carbon concentrations.

6.1.3 Carbonate and Sulfate Content

In a detailed study of drill core from the lower 855 feet of Mancos Shale in the Disappointment Syncline near Slick Rock, Colorado, Shawe (1968) analyzed concentrations of calcite from nine vertically separated samples. Calcite concentrations were as high as 40 percent and averaged about 20 percent throughout the core except in the Lower Carlile Shale[3], where it was nearly absent. It is not clear from Shawe's paper whether calcite content is presented as weight or volume percent, but weight percent is most likely based on the analytical method (carbon dioxide release following acid treatment) used. Shawe (1968) did not mention the presence of gypsum in the core.

Evangelou (1981) analyzed carbonate content of weathered and unweathered Mancos Shale at four locations in the West Salt Creek area of the Grand Valley, western Colorado. At each location, three or four samples were analyzed, and results are in weight percent. At three of the locations the arithmetic mean carbonate concentrations in the weathered and unweathered strata were 14.92 and 16.24 percent, respectively. At the fourth area, which was at the base of the Book Cliffs, the carbonate concentrations were lower, with arithmetic means of only 2.58 and 3.07 percent for weathered and unweathered shale, respectively, and dolomite was the only carbonate mineral present. Both calcite and dolomite were present at the other three sampling locations, and gypsum was present at all four locations in the weathered samples.

Evangelou et al. (1985) used column tests to investigate dissolution and desorption rates of carbonate minerals characteristic of weathered Mancos Shale in samples collected from Salt Creek Wash near Grand Junction, Colorado. They concluded that Mancos Shale is an important source of calcium and magnesium loading to surface waters. In column tests, they showed an early release of calcium that exceeded the solubility of calcite. They attributed the calcium release to dissolution of gypsum, but over time, the calcium release rate stabilized, and after a few hours calcium was in equilibrium with calcite. Magnesium release rate was variable but generally increased with time, and dolomite dissolution was thought to be an important source of the magnesium. Evangelou et al. (1985) also speculated that calcite coatings on dolomite may explain the variable magnesium release rates.

---

[3] The lower part of the Carlile Shale referred to by Shawe (1968) corresponds to the Graneros, Bridge Creek, and Blue Hill Members of the Mancos Shale, as shown in Figure 13.

Core examination from the Crescent Junction, Utah, uranium mill tailings disposal site indicated that carbonate, mostly in the form of calcite, was present throughout both the weathered and unweathered Mancos Shale but was more concentrated in the weathered zone. Gypsum was common in the upper 50 ft of core but was nearly absent in the deeper unweathered Mancos.

Many authors (e.g., Laronne and Schumm 1982, Whittig et al. 1983, Whittig et al. 1986, Wright 2006) mention the widespread occurrence of gypsum in the Mancos but few data are available with which to quantify its abundance or distribution. Gypsum often occupies fractures and is more abundant in weathered Mancos.

6.1.4   Clay Mineralogy and Cation Exchange Capacity

In a comprehensive study of Mancos Shale clay mineralogy, Nadeau and Reynolds (1981) analyzed 580 samples of shale and bentonite collected at 154 sites throughout the Mancos Shale depositional basin. Samples were analyzed using X-ray powder diffraction on specimens treated (oriented, glycolated, and heated) so as to distinguish clay mineral types (e.g., illite versus smectite), approximate interlayering percentages, and ordering (ordered versus random). They found that the main clay in the shale was mixed layered illite/smectite with 20 to 60 percent illite layers. They suggested that burial metamorphism resulted in increased ordering as smectite layers converted to illite. Uncharacteristic of burial metamorphism was the retention of bentonite beds containing nearly pure smectite. Nadeau and Reynolds (1981) describe a correlation of carbonate content with these bentonites and speculate that the clay alteration was impeded by the presence of carbonate. Kaolinite was found to be a common accessory clay mineral in both bentonite and shale samples, discrete illite was a common accessory in the shale, but chlorite was rarely observed. In a study of clay mineralogy of the Pierre Shale in the northern Great Plains, Schultz (1964) found primarily randomly interstratified illite/smectite containing 20 to 60 percent illite layers, and pure smectitic bentonites.

In a detailed study of a drill core from the lower 855 ft of the Mancos Shale in the Disappointment Syncline near Slick Rock, Colorado, Shawe (1968) logged 24 thin layers of greenish-gray bentonitic shale, particularly in strata equivalent to the Greenhorn Limestone, Carlile Shale, and the lower Niobrara Formation[4]. Pyrite and swelling clays were more abundant in the bentonite-bearing beds. Shawe (1968) stated that the bentonite was likely volcanic ash-fall material. His measured sections of Mancos Shale contained claystone and mudstone beds (some were pyritic) but no bentonite beds, although bentonite was listed occasionally as a component of the claystone beds. Shawe (1968) also described petroliferous odor in some of the mudstone beds, carbonized plant fragments, and numerous observations of carbonates. He described limestone occurring as thin beds in the Mancos Shale, often only a fraction of an inch thick, and the limestone sometimes contained pyrite and/or organic matter.

As part of another DOE project, we measured cation exchange capacity on 20 core samples collected from the Crescent Junction uranium mill tailings disposal site and found a range of 0.54 to 36.29 meq/100 g, with an arithmetic mean of 11.23 meq/100 g. The clay fraction was dominated by mixed-layer (mostly illite-smectite) clays, illite, and kaolinite, with illite layers dominating the mixed-layer clays. Particle surface area was determined by multipoint Brunauer, Emmett, Teller (BET) analysis on 10 samples collected at a depth of 40 ft. The surface area of

---

[4] These stratigraphic units are equivalent to the Graneros up through the Smoky Hill Members, as shown in Figure 13.

the 1 to 2 mm fractions of these samples ranged from 8.81 to 13.22 m^2/g with an arithmetic mean value of 11.02 m^2/g. Evangelou (1981) determined that the cation exchange capacity of weathered Mancos Shale samples ranged from 13.14 to 25.15 meq/100 g and provided a single value for unweathered Mancos of 13.02 meq/100 g.

6.1.5 Nitrogen Content

Holloway and Smith (2005) determined nitrogen concentrations of 0.10 to 0.13 percent (as N) on four shale samples of Mancos from the Grand Valley in the Grand Junction, Colorado, area. They found that 58 to 74 percent of the nitrogen was organic, and the rest may have been in ammonium associated with clay minerals and nitrate salts.

6.1.6 Organic Matter

The organic content of geologic materials including marine shale can be classified as sapropelic and humic matter (Vine et al. 1958). Sapropelic material is derived from hydrogen-rich organic matter such as algae, waxes, resins, and spores, whereas humic material is derived from more oxygen-rich plant remains such as lignin and cellulose. Petroleum is a product of sapropelic material, whereas peat, lignite, and coal are products of humic-rich material. Humic acid is soluble in weakly alkaline aqueous solution but forms a gel or precipitate at pH values less than about 4. Dissolved humic acid can impart a yellow or amber color to water similar to the color we observed in the Mancos Shale seeps. Diagenesis of humic acid results in an insoluble compound that can be redissolved under oxidized conditions such as occur during weathering (Vine et al. 1958; Swanson 1961).

Kakouros et al. (2006) determined organic carbon concentrations of 0.44 and 1.34 percent in one sample each from weathered and unweathered shale, respectively, in core samples of the Mancos Shale near Jensen, Utah. Leythaeuser (1973) measured mean organic carbon concentrations of 1.08 percent (11 samples) and 1.58 percent (6 samples) on relatively uniform shallow (21 ft) cores from a highly calcareous core and a noncalcareous core, respectively, in the Tununk Member of the Mancos Shale in Emery County, Utah. Butler et al. (1994) analyzed four samples of weathered Mancos Shale, two samples of unweathered Mancos Shale, and two samples of ash beds (bentonite beds) from the Mancos Shale in the Uncompahgre Valley and Grand Valley, Colorado, areas. The organic carbon contents of the two unweathered shale samples were 1.36 and 1.55 percent, the ash beds had 0.12 and 0.39 percent, and organic carbon in the weathered shale ranged from 0.44 to 0.64 percent with an arithmetic mean of 0.54 percent. Palsey et al. (1989, 1991) measured organic carbon concentrations ranging from 0.49 to 5.29 percent in core and outcrop samples of marine shale from the Mancos Shale just above and below the Tocito Sandstone in the San Juan Basin near Shiprock, New Mexico. Tourtelot (1962) observed that bentonites appeared as lighter-colored beds upon weathering because they are derived from volcanic ash and contain no organic matter. Holloway and Smith (2005) determined organic carbon concentrations of 2.00 to 2.53 percent on four shale samples of Mancos from the Grand Valley in the Grand Junction, Colorado, area. They found that 68 to 83 percent of the carbon in these samples was organic.

Organic carbon concentrations ranged from 0.6 to 7.4 percent in 18 samples of shale and marlstone of the Pierre Shale analyzed by Tourtelot (1962); another 40 samples had organic carbon concentrations less than 0.5 percent. Samples containing organic carbon of more than

1 percent had a distinctively dark color (Tourtelot 1962). Schultz et al. (1980) analyzed more than 200 shale and siltstone samples of the Pierre Shale and determined the arithmetic mean organic carbon concentration to be 0.94 percent with a standard deviation of 1.8 percent. Clayton and Swetland (1978) analyzed 15 samples of unweathered core samples from the Pierre Shale in Boulder County, Colorado, and found a tight range of 0.78 to 0.97 percent.

We found that samples of cores from the Crescent Junction disposal site commonly contained visible organic matter that was present mostly in the deeper unweathered horizons. Organic matter was often found in contact with pyrite and was typically disseminated as black, fine particles coating fracture planes or bedding surfaces.

6.1.7 Pyrite and Accessory Minerals

Although there are many references to the presence of pyrite in shale of the Mancos Shale, few data are available to quantify its abundance. In a detailed study of a drill core from the lower 855 ft of the Mancos Shale in the Disappointment Syncline near Slick Rock Colorado, Shawe (1968) used petrographic methods to determine concentrations of pyrite. The core contained pyrite concentrations up to 10 percent. Based on the methods used, we presume that the pyrite concentrations are in volume percent; however, the authors did not specify whether they are based on weight or volume. The highest pyrite concentrations were in the lower Niobrara Formation, the upper Carlile Shale, and the Greenhorn Limestone[5].

By analogy with typical sapropelic marine environments of today, Shawe (1976) indicated that hydrogen sulfide would be abundant at the bottom of the Mancos sea, but suggests that sulfur might also be derived from volcanic ash. Shawe (1976) observed compaction of bedding around pyrite crystals, indicating that the pyrite had formed earlier than the compaction and was likely formed syngenetically. Shawe (1976) also observed a lack of black opaque minerals such as magnetite and ilmenite in the Mancos Shale that he ascribed to dissolution by pore waters. Using petrographic data from uranium-bearing geologic formations, Adams et al. (1974) demonstrated the alteration of black opaque minerals to titanium oxide minerals by reducing solutions, and even suggested that magnetic susceptibility could be used to detect the loss of magnetite to reveal reducing provinces favorable for formation of uranium ores.

Samples from the Crescent Junction, Utah, cores commonly contained visible pyrite as shallow as 14 ft. Pyrite was noted in both weathered and unweathered Mancos and often was associated with organic matter. Pyrite was often framboidal but also occurred as coatings on fracture planes and as fossil shell replacements. Limonite staining was common in the core descriptions and likely reflected an oxidized product of former pyrite.

Fifty Mancos Shale core samples collected from 40 to 300 ft depths at the Crescent Junction disposal site were also analyzed for water soluble fraction (DOE 2007). Based on chemistry of the water soluble fractions, we deduced that the water soluble mineral suite was dominated by nahcolite, with major amounts of Ca-Na exchange and gypsum. Halite, sylvite, and dolomite occurred in lesser amounts, and calcite was present. X-ray diffraction analysis of 10 samples indicated that the shale was composed dominantly of quartz, with lesser amounts of dolomite and calcite, small amounts of feldspar, and traces of gypsum.

---

[5]These stratigraphic units are equivalent, respectively, to the Smoky Hill, Juana Lopez, and Bridge Creek-Graneros Members, as shown in Figure 13.

6.1.8 Selenium Content

Kakouros et al. (2006) analyzed two core samples of Mancos Shale (one each of weathered and unweathered material) collected near Jensen, Utah. They found selenium concentrations in the weathered and unweathered shale samples of 3.0 and 1.9 mg/kg, respectively. Using selective extraction methods, they surmised that most of this selenium resided in the organic fraction.

The average selenium concentration in 21 samples of shale and marlstone of the Pierre Shale analyzed by Tourtelot (1962) was 2 mg/kg. One anomalously high value of 50 mg/kg occurred in a sample that was particularly rich in organic content. Schultz et al. (1980) determined an arithmetic mean selenium concentration for more than 200 shale and siltstone samples of the Pierre Shale to be 3.7 mg/kg with a standard deviation of 15 mg/kg.

Butler et al. (1994) analyzed four samples of weathered Mancos Shale, two samples of unweathered Mancos Shale, and two samples of ash beds (bentonite beds) from the Uncompahgre Valley and Grand Valley, Colorado, areas. The selenium contents of the two unweathered shale samples were 0.8 and 1.6 mg/kg; one sample from the ash beds had less than 0.1 mg/kg selenium, and the other had 3.9 mg/kg. Selenium in the weathered shale ranged from 0.8 to 1.6 mg/kg with an arithmetic mean of 1.1 mg/kg. Tuttle et al. (2007) derived arithmetic means of selenium concentrations for 72 samples from Elephant Skin Wash and 94 samples from Candy Lane in Colorado, and 16 samples from the Hanksville, Utah, area of 2.73, 2.94, and 1.09 mg/kg, respectively.

Thomas et al. (1998) analyzed selenium concentrations in stream bottom sediment and soils in a study of irrigation drainage to the San Juan River in New Mexico. They reported that the arithmetic mean and median selenium contents were 4.6 and 2.2 mg/kg for areas of Cretaceous bedrock, whereas in areas of non-Cretaceous bedrock the arithmetic mean and median contents were only 0.6 and 0.15 mg/kg.

6.1.9 Uranium Content

Because anomalously high uranium concentrations were known to exist in some black shale, an extensive campaign was undertaken in the 1940s and 1950s in the United States to test black shale for uranium content to determine its capacity as a uranium resource (Swanson 1961). Swanson states that, during this period, an estimated 8,000 samples were collected and analyzed from more than 200 geologic formations containing marine black shale. Some black shale formations such as the Chattanooga Shale in the southeast United States and phosphatic black shale in Kansas and Oklahoma have anomalously high uranium concentrations of up to 100 mg/kg (Swanson 1961); however, black shale has yet to be mined for uranium.

The Mancos Shale is composed dominantly of dark-gray shale beds and has been described as containing beds of black shale (Wright 2006). Black shale deposits are extensive in the United States and worldwide and are usually dark gray (N3) or grayish black (N2) with common dark hues of brown (5YR 2/1) and olive (5Y 3/2–2/1) (Swanson 1961). After an extensive review of black shale and modern mud deposits, Swanson (1961) included the requirement of having more than 2 percent organic carbon as part of the definition of black shale. Mancos Shale typically contains less than this and therefore would not be considered black shale by Swanson's definition.

McKelvey et al. (1955) compiled data worldwide on uranium in marine black shale. They described several uraniferous marine black shale formations, including the Upper Cambrian Alum Shale of Sweden, the Devonian and Mississippian Chattanooga shale of Tennessee, and shale in the Pennsylvanian Hartville Formation in Wyoming that contain from 50 to 200 mg/kg uranium. However, they stated that not all black shale is high in uranium. In a study of 287 samples of Paleozoic and Mesozoic black shale, Quinby-Hunt et al. (1989) determined a mean and mode for uranium of 15.2 and 3 mg/kg, respectively. Black shale high in uranium was often found to (1) contain high concentrations of sapropelic relative to humic material, (2) be rich in sulfide minerals and distillable hydrocarbons, (3) be low in fossil content except for plankton and nekton, (4) contain higher than average concentrations of phosphate, and (5) have low carbonate concentrations, although interbeds may have carbonate (McKelvey et al. 1955). The observation by McKelvey et al. (1955) that uranium is associated with sapropelic material seems to contrast with those of others (notably Vine et al. 1958; Swanson 1961) that maintain uranium in marine black shale is associated with humic material. The highest uranium concentrations in the Alum Shale are in lenses of dark bitumen. McKelvey et al. (1955) state that it was widely accepted at that time that the uranium was syngenetic, and seawater was the source of the uranium. It was also thought that reducing conditions were a prerequisite for transfer of uranium from seawater to black shale. A syngenetic origin explains the widespread, relatively even distribution of uranium in shale formations and the lack of deposition along faults and joints. Syngenesis was favored by Swanson (1961) and is still the most widely accepted mode of origin for the occurrence of uranium in marine black shale.

Adams and Weaver (1958) provided data on the concentration of uranium in shale samples collected worldwide, using data from their own analyses and literature compilations. They reported the following arithmetic mean and median values from distributions having reasonably normal distributions: 3.2 and 2.7 mg/kg from 52 samples of gray and green shale, 4.1 and 4.1 mg/kg from 15 composite samples representing 4,795 shale samples from the Russian Platform, and 5.0 and 4.5 mg/kg from 69 samples of bentonite. They also reported that uranium concentrations ranged from 1.4 to 69 mg/kg in 17 samples of black shale with a highly skewed distribution. They concluded that a value of 3.7 mg/kg is appropriate for average shale. The analytical method used by Adams and Weaver (1958) assumes secular equilibrium.

The uranium content of the marine Mancos Shale is low compared to that of many other black shale deposits (Shawe 1976). Shawe (1976) explains that the low uranium content may result from low uranium concentration in the seawater, rapid accumulation of sediment, or loss of uranium during compaction. He rejected the first two ideas: evidence from Swanson (1961) suggested that seawater had not been anomalously low in uranium, and deposition likely took place in the seaway in a subsiding basin for more than 20 million years. Thus, the loss of uranium was favored to explain the low concentration.

Using 102 shale samples collected from the Mancos Shale over much of the same outcrop area as used in the current study, Pliler and Adams (1962) determined arithmetic mean and median uranium concentrations of 3.7 and 3.2 mg/kg, respectively. They found that the Mancos Shale is remarkably uniform in uranium concentration, as evidenced by 19 samples collected at 6 ft intervals at a site located 14 miles west of Shiprock, New Mexico, that had an average uranium concentration of 2.9 mg/kg with a standard deviation of 0.3 mg/kg. They also found little variation among nine samples collected from the same stratigraphic layer (middle Mancos Shale of Spieker and Reeside [1925]) but widely separated along a 50-mile-long traverse southwest of

Price, Utah. Unfortunately, Pliler and Adams (1962) did not provide details of the digestion method used to prepare samples for the chemical analyses or the preparation method used for gamma spectrometry. Because the uranium concentrations in a suite of their samples analyzed using both chemical and gamma spectrometric analyses were similar, we assume that a digestion method capable of complete dissolution of the rock material was used, and as such, the concentrations are those of the total rock, including both easily leachable uranium and that residing in resistate grains.

Butler et al. (1994) analyzed four samples of weathered Mancos Shale, two samples of unweathered Mancos Shale, and two samples of ash beds (bentonite beds) from the Mancos Shale in the Uncompahgre Valley and Grand Valley areas in Colorado. The uranium concentrations were 7.4 and 11.2 mg/kg in the two unweathered shale samples, 8.4 and 13.9 mg/kg in the two ash bed samples, and ranged from 4.1 to 5.4 mg/kg in the four weathered shale samples. The average uranium concentration in 22 samples of shale and marlstone of the Pierre Shale analyzed by Tourtelot (1962) was less than 10 mg/kg. Schultz et al. (1980) determined the arithmetic mean uranium concentration of more than 200 shale and siltstone samples of the Pierre Shale to be 5.8 mg/kg with a standard deviation of 5.2 mg/kg. Tuttle et al. (2007) determined arithmetic means of uranium concentrations on 72 samples from Elephant Skin Wash, 95 samples from Candy Lane, and 16 samples from the Hanksville area as 4.79, 5.71, and 4.65 mg/kg, respectively.

In summary, it appears that shale in the Mancos Shale has a mean uranium concentration of about 3.7 mg/kg, which is similar to mean shale concentrations worldwide. We are not aware of any uranium isotopic analytical results for Mancos Shale rock samples.

6.1.10   Vanadium Content

Butler et al. (1994) analyzed four samples of weathered Mancos Shale, two samples of unweathered Mancos Shale, and two samples of ash beds (bentonite beds) from the Mancos in the Uncompahgre Valley and Grand Valley areas in Colorado. The vanadium concentrations were 13 and 50 mg/kg in the two unweathered shale samples, 4 and 40 mg/kg in the ash bed samples, and ranged from 130 to 180 mg/kg in the four weathered shale samples. Tuttle et al. (2007) determined arithmetic means of vanadium concentrations on 72 samples from Elephant Skin Wash, 95 samples from Candy Lane, and 16 samples from the Hanksville area as 142, 192, and 80 mg/kg, respectively.

6.2   Geochemistry of Groundwater in Mancos Shale

6.2.1   Arsenic

Wright (1995) reported that arsenic concentrations were not high in samples from approximately 50 wells and streams located within Colorado irrigation projects in Mancos Shale terrain. Arsenic concentrations in three of four groundwater samples in weathered Mancos Shale reported by Butler et al. (1994) for the Uncompahgre and Grand Valley, Colorado, areas were less than the detection limit of 1 μg/L, and the concentration in the fourth sample was 2 μg/L. Arsenic concentrations from eight samples of Sweitzer Lake water collected in 1987 and 1988 ranged from less than 1 to 2 μg/L, and concentrations were less than 1 μg/L in four samples of water from the Garnet Canal diversion ditch at Sweitzer Lake (Butler et al. 1991).

The arsenic concentration in Mancos Shale is about 15 mg/kg, which is higher than some other trace elements, including uranium (about 3.7 mg/kg; Table 7). Despite these higher, solid-phase concentrations, arsenic concentrations were less than 2 μg/L in all but five of our groundwater samples. Thus, arsenic must be more tightly bound to the solid phase, perhaps as an organic complex. Because it is not easily released to the groundwater, and only one sample had an arsenic concentration that exceeded the drinking water standard, arsenic is not considered a natural contaminant in the Mancos Shale. Sampling site SNS at Sweitzer Lake was anomalous with an arsenic concentration of 12 μg/L, a result that suggests that this sample was affected by evaporation.

6.2.2   Boron

Boron concentrations were measured in groundwater samples collected during this study, not because it is considered a contaminant, but because boron is known to have high concentrations in marine shale and might be an indicator that groundwater has interacted with Mancos Shale. Deverel and Millard (1988) found that boron concentrations in shallow groundwater of the western San Joaquin Valley, California, correlated with salinity. Butler et al. (1994) reported concentrations of boron from the weathered Mancos Shale for eight groundwater sampling locations in the Uncompahgre and Grand Valley areas; the boron results from representative samples ranged from 220 to 1,200 μg/L and had an arithmetic mean of 648 μg/L. Boron concentrations from eight samples of Sweitzer Lake water collected in 1987 and 1988 ranged from 200 to 390 μg/L, and concentrations in four samples of water from the Garnet Canal diversion ditch at Sweitzer Lake ranged from 180 to 800 μg/L (Butler et al. 1991).

Figure 28 shows a histogram of boron concentrations in water samples (most of which are groundwater samples) collected at 14 DOE remediation sites in the Four Corners states. The boron concentrations range from 2 to 75,000 μg/L but are highly skewed to the lower values; the geometric mean is 163 μg/L. The geometric mean of seep samples collected for this study was 441 μg/L (Section 5.2), and the geometric mean concentration in shale of 692 μg/L is distinctly higher than the geometric mean of 110 μg/L from sandstone. These results coupled with literature data suggest that a boron concentration of more than approximately 500 μg/L is an indication of Mancos Shale interaction.
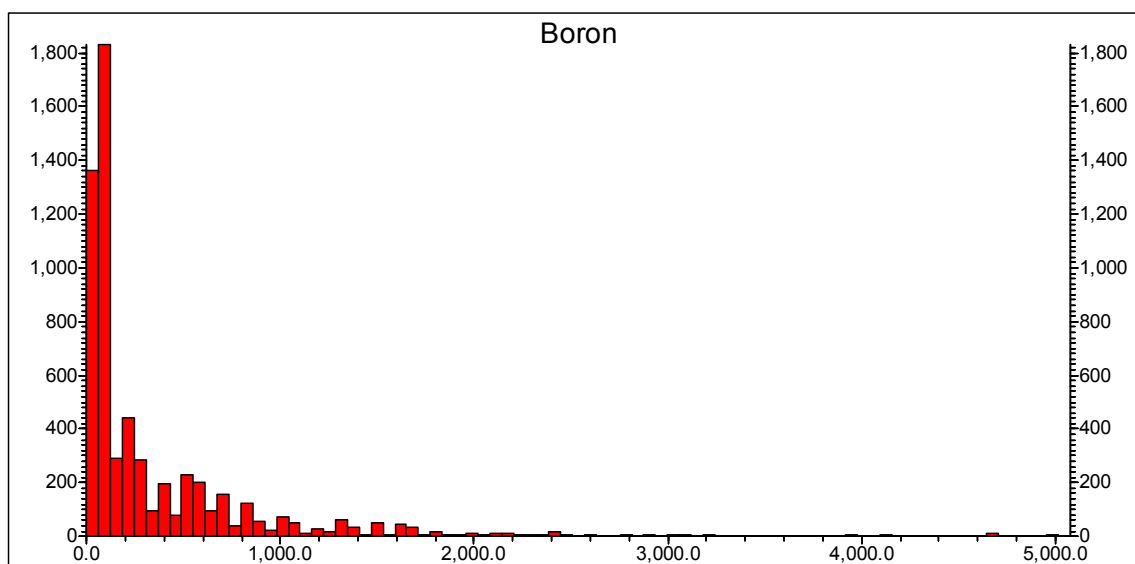
*Figure 28. Histogram of Boron Concentrations (µg/L) in Water Samples
Collected at DOE Sites in the Four Corners States. Sampling locations are Ambrosia Lake and Shiprock,
New Mexico; Durango, Grand Junction, Gunnison, Maybell, Naturita, Rifle, and Slick Rock, Colorado;
Mexican Hat, Moab, and Monticello, Utah; and Monument Valley and Tuba City, Arizona.*

6.2.3   Dissolved Organic Carbon (DOC)

Natural fresh surface waters typically contain a few milligrams per liter of DOC but can be as high as 50 mg/L in swamps or bogs; DOC in ocean water ranges from about 0.5 to 1.2 mg/L (Stumm and Morgan 1981). In a summary of literature data, Reuter and Perdue (1977) found that most naturally occurring DOC is highly oxidized and similar in composition to soil humic substances, with an origin likely from meteoric water leaching of land-based, plant-derived humus. They report that a DOC concentration of more than 10 mg/L is sufficient to complex and mobilize trace metals, and that DOC concentrations of more than about 20 mg/L impart a distinctive yellow color to the water. Groundwater is generally low in DOC, with concentrations ranging from about 0.1 to 1.3 mg/L (Reuter and Perdue 1977).

DOC has rarely been measured in groundwater associated with Mancos Shale. Leythaeuser (1973) reports that solid-phase total organic carbon was reduced by up to 25 percent in the weathered (10 ft thick) portion of Mancos Shale (Tununk Member, Emery County, Utah), indicating that organic matter is lost from solid kerogen in the shallow weathering zone. In contrast, Clayton and Swetland (1978) analyzed weathered and unweathered core samples of the Pierre Shale in Boulder County, Colorado, and found that there was no loss of organic carbon in the weathered samples. In a study of the Crow Creek Member of Pierre Shale, Tourtelot (1962) indicated that organic carbon had been removed during weathering. Clayton and Swetland (1978) observed that up to 60 percent of the organic carbon was lost from black shale during weathering of the Permian Phosphoria Formation in northeastern Utah.

In situ generation of DOC has been described without the need for near-surface weathering processes. In situ generation of DOC was demonstrated in a study of the Gorleben aquifer in Germany by Buckau et al. (2000), who found that DOC concentrations exceeding 200 mg/L were produced by microbially mediated oxidation of sedimentary organic carbon during sulfate

reduction. The recharged DOC was composed mainly of fulvic acid, whereas the in situ–produced DOC had a large component of humic acid. Aravena and Wassenaar (1993) deduced that much of the DOC in glacial sediments in southern Ontario, Canada, is derived by in situ generation.

Swanson (1961) states that the dark brown to black structureless material found in black shale may be humate that precipitated from aqueous humic acid. Humate is soluble in slightly alkaline solution but forms a gel upon acidification. During shale diagenesis, the humic material loses its solubility but becomes soluble again if oxidized (Swanson 1961). Thus, oxidation during Mancos Shale weathering may cause dissolution of organic carbon and produce the high concentrations of DOC we observe.

Holloway and Smith (2005) treated a Mancos Shale sample containing 2.40 percent organic carbon with deionized water for 2 weeks and found that 86 mg of DOC was released per kg of shale, or 0.5 percent of the available organic carbon.

High groundwater concentrations of DOC, up to 265 mg/L as measured in our samples, occur from natural processes in the Mancos Shale. High DOC concentrations imparted yellow to red colors to the groundwater, evidenced by a positive correlation between DOC concentrations and color as measured by light absorbance (Figure 17). We suggest that weathering of humic organic carbon in the Mancos Shale is the source for the DOC observed in the groundwater samples. The presence of the red coloration imparted by the DOC is easily seen in arroyos and is an indicator of natural contamination.

6.2.4   Major Ions

In a study of the contribution of Mancos Shale to salt loading in West Salt Creek, near Grand Junction, Colorado, Evangelou (1981) determined that the salts were derived by dissolving carbonate minerals from the Mancos caused by lowered pH values from biological oxidation of pyrite. Gypsum and magnesium sulfate solid phases were precipitated by the same reactions, and additional ions were dissolved from dolomite, feldspar, and mica. Sodium and magnesium were contributed during cation exchange with unweathered Mancos clays.

Many of the groundwater seeps sampled in this study had high salinities, with specific conductivity values exceeding 20,000 µS/cm at many locations. Cation composition in the Mancos Shale seeps was dominated by sodium and sulfate, and pH values were typically less than 7.5. The major-ion chemistry in the seeps was generally consistent with the major-ion chemical model put forth by Evangelou (1981). Conceptually, oxidation of pyrite and organic matter contribute sulfate, bicarbonate, and protons to the groundwater. Lowering of pH affects carbonate mineral dissolution, adding calcium and, to a lesser extent, magnesium to the groundwater. Sodium is transferred to groundwater as calcium exchanges with sodium on cation exchange sites. Gypsum and other secondary minerals precipitate or dissolve according to constraints of solubility equilibrium.

6.2.5   Nitrate (as NO₃)

Pottorff et al. (2005) sampled surface water and groundwater associated with selenium contamination near the Devil's Thumb Golf Course, Delta, Colorado. They found a positive

relationship between selenium and nitrate, which they attributed to oxidation of selenium by nitrate, the source of nitrate being fertilizer applied to the golf course. They reported nitrate concentrations of more than 1,000 mg/L. Wright (1995, 1999) presented data on nitrate (plus nitrite), selenium, and uranium concentrations from about 50 wells and streams selected from samples of Colorado irrigation projects in Mancos Shale terrain. He found that nitrate correlated positively with both selenium and uranium; however, the correlation coefficient for selenium was only 0.50, and although the correlation coefficient for uranium was not provided, the graph showed considerable scatter. Using these correlations, the results of selenium release experiments in batch tests of Mancos Shale treated with variable concentrations of nitrate, and oxidation thermodynamics, Wright (1995, 1999) reasoned that nitrate may play a role in oxidative release of selenium and uranium from the Mancos Shale.

Most of the literature references to high nitrate concentration in the Mancos Shale suggest that fertilizer is the main source of the nitrate. In contrast, Holloway and Smith (2005) found that nitrate could be released naturally from the Mancos Shale. They treated a Mancos Shale sample containing 0.13 percent nitrogen with water for two weeks and found that 2.22 mg of inorganic nitrogen was released per kilogram of shale, or 0.2 percent of the available nitrogen. Our findings also indicate that nitrate can be leached directly from the Mancos Shale at high concentrations without a contribution from fertilizers. Seeps that are unrelated to irrigation and not likely to be significantly affected by evaporation include those at Eagle Nest Arroyo, Salt Creek Wash, Daly Reservoir, and Delta Reservoir; these had nitrate concentrations that ranged from 380 to more than 3,500 mg/L. A possible source for the nitrate is biogenic degradation of humic material during sediment deposition or early burial diagenesis. The nitrate remained associated with the organic matter until released by weathering processes.

6.2.6   Radon

Radon-222 measurements were made to evaluate the extent to which groundwater may have been evaporated by exposure to the atmosphere. Radon is a noble gas and is present in measurable concentrations in most groundwaters. Radon-222 has a half-life of only 3.8 days and is not transported far in groundwater. It is constantly produced in aquifers from the decay of its parent radium-226. Numerous studies of radon-222 in groundwater aquifers indicate that its aqueous concentration is tied to aquifer lithology (Michel 1990). Although large variations exist, radon-222 concentrations in limestone aquifers are typically low, ranging from about from 15 to 90 pCi/L. Radon-222 concentrations in unconsolidated sand aquifers typically range from about 200 to 700 pCi/L, and values from 2,000 to 20,000 pCi/L are common in metamorphic and igneous aquifers. We were unable to locate data regarding radon-222 concentrations in groundwater in shale.

Because it is a gas, radon-222 partitions rapidly into the vapor phase and may indicate whether a sample has been exposed to the atmosphere, either in situ or as a result of sampling. Radon-222 loss can occur without evaporation, so it is a one-sided test—if radon-222 is present in concentrations similar to those in unevaporated formation water, the sample has not been subject to evaporation; however, radon-222 loss could occur without significant evaporation. Unfortunately, few radon-222 concentration data are available for the Mancos Shale, so the concentration expected for formation water must be estimated. Because of these uncertainties, radon-222 data were only used in conjunction with other observations as a qualitative assessment of evaporation effects.

Our results were inconclusive as to whether radon-222 measurements were a useful indicator for atmospheric exposure. All of the surface water samples had low radon-222 signatures, confirming that exposure to the atmosphere depleted radon. Sweitzer Lake sample SNS3 had a relatively low radon-222 signature, consistent with its anomalously high concentrations of other dissolved constituents that might indicate evaporation. The use of radon-222 may have an additional problem if used to indicate evaporation coupled to capillary transport. If groundwater is moving to the ground surface via capillary processes, then it is still in contact with sediment, and the extent of radon emanation from that sediment is unknown. Others have found the water isotopic couple, oxygen-18 and deuterium, to be a useful indicator of evaporation in groundwaters in Mancos Shale terrain (Butler et al. 1996; Golder Associates 2004; Tuttle and Grauch 2009), although Golder Associates (2004) caution that the water isotopes may also be affected by interaction with the Mancos Shale. Perhaps the use of water isotopes in conjunction with radon-222 analyses would provide a more rigorous test of evaporation effects.

6.2.7 Selenium

Nolan and Clark (1997) presented data from more than 600 surface water samples collected in 14 states in the western United States and showed positive correlations of selenium with the presence of Cretaceous sediments, salinity, and irrigated areas. They found median selenium concentrations of 14 µg/L for areas underlain by Cretaceous sediments and less than 1 µg/L for areas underlain by non-Cretaceous sediments. Deverel and Millard (1988) found that selenium concentrations in shallow groundwater of the western San Joaquin Valley, California, correlated with salinity.

Butler et al. (1994) determined aqueous selenium species concentrations for two samples of groundwater collected from weathered Mancos Shale, one each from the Uncompahgre Valley and Grand Valley areas in Colorado. Both samples contained more than 97 percent of the oxidized species $Se^{VI}O_4^{2-}$, the remainder being the reduced species $Se^{IV}O_3^{2-}$, suggesting transport of selenium in the oxidized state. Wright and Butler (1993) reported selenium concentrations in groundwater from weathered Mancos Shale in irrigated areas of the Grand Valley and Uncompahgre Valley that ranged from less than 1 to 65 µg/L, but they found higher concentrations, up to 1,300 µg/L, in alluvial groundwater overlying Mancos Shale. Wright and Butler (1993) found that the selenium concentrations in groundwater were somewhat higher during the irrigation season than during the nonirrigated season and found that selenium in weathered Mancos Shale groundwater is negatively correlated with salinity. On the basis of these relationships, they proposed that selenium mobility is controlled predominantly by processes of uptake via reductive precipitation of pyrite and ion exchange on clays. Butler et al. (1996) using a similar database proposed a similar model for selenium migration.

Selenium concentrations in 14 seep samples collected during this study exceeded 500 μg/L, confirming observations by previous researchers that Mancos Shale is a source of elevated selenium concentrations in groundwater. Most of the higher concentrations were in samples that had high concentrations of other constituents, including uranium, DOC, nitrate, and total salinity; although the relative abundances of these constituents varied. The high groundwater concentrations of selenium are not reflected in the solid-phase concentrations. The generalized estimate in this study of solid-phase selenium concentration in the Mancos Shale was 2 mg/kg (Table 7), which was less than each of the solid-phase concentrations of uranium, boron, or arsenic.

Selenium concentrations in groundwater resulting from contact with gray shale beds in the Mancos Shale often exceed 500 μg/L. We propose that selenium is introduced into the Mancos Shale groundwater in a manner consistent with many previous studies. Selenium was adsorbed to humic organic matter and substituted for sulfur in pyrite from seawater during deposition of the Mancos Shale in the Late Cretaceous Western Interior Seaway. Selenium in these solid hosts was in its reduced selenite form. Concentration and redistribution likely occurred during burial diagenesis. As the Mancos Shale was uplifted and became weathered, selenium was oxidized to its more mobile selenate form. Wherever groundwater finds a migration pathway through the Mancos Shale, selenium transfers to the aqueous phase and migrates to the seeps.

6.2.8   Uranium

Data from the NURE program (USGS 2011b) were used to form a basis for comparison with the uranium concentrations encountered in our study. Figure 29 shows a histogram of uranium concentrations in 23,659 groundwater samples collected in the Four Corners states of Arizona, Colorado, New Mexico, and Utah. The NURE samples were obtained from seeps, springs, and wells and represent a wide range of geologic units. The frequency distribution for this set of uranium data is highly skewed with many more observations made at the low end of the concentration distribution; correspondingly, the arithmetic mean and median uranium concentrations were 8.67 and 2.63 μg/L, respectively (Table 8). Several high values skew the distribution but, because the statistics are based on such a large population there was little change to the mean and median values, even when some of the highest uranium concentrations were omitted. If all the uranium concentrations more than 1,000 μg/L uranium are omitted (five values), the mean decreases slightly to 8.13 μg /L, and the median remains the same at 2.63 μg/L (Table 8). Based on this data set, we adopt a value of 8.1 μg/L as a reasonable estimate of the mean.
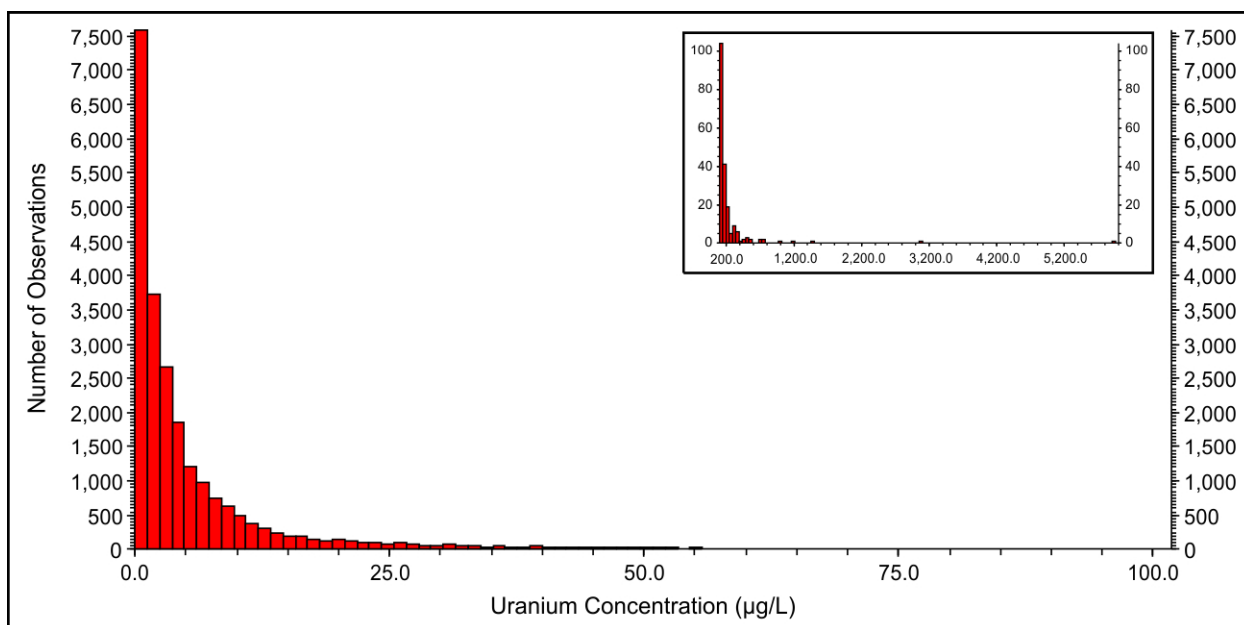
Figure 29. Histogram of Uranium Concentrations (µg/L) in 23,659 Groundwater Samples Collected in the Four Corners States of Arizona, Colorado, New Mexico, and Utah. Inset shows samples with more than 100 µg/L uranium.

Figure 30 provides a map-based representation of all the groundwater uranium concentration data from the Four Corners states, and Figure 31 shows locations that have groundwater uranium concentrations greater than 100 µg/L. There is a dense area of the higher values in an area in northeast Colorado (area A, Figure 31). This area is in the transition from the Rocky Mountains region to the Great Plains region and is characterized geologically by the transition to flat-lying Cretaceous and Tertiary marine and transitional shale-dominated beds, including large areas of strata that are equivalent to the Mancos Shale. Similarly, an area in the transition zone in southeast Colorado has a high density of locations with elevated uranium concentrations with Mancos equivalent strata (area B, Figure 31). Shannon (1979) reported on NURE results of samples collected from the Lamar 1º × 2º quadrangle that is located in eastern Colorado and includes the higher uranium concentrations in area B in southeast Colorado and a portion of the Arkansas River valley (Figure 31). He noted that of all the quadrangles investigated for the NURE program (which includes much of the United States), the Lamar quadrangle had one of the highest mean uranium concentrations in groundwater samples collected from wells. He further noted a correlation of the higher anomalies with units of Upper Cretaceous rocks that are stratigraphically equivalent to the Mancos Shale. Zielinski et al. (1995) reported high uranium concentrations in surface water and groundwater in the Arkansas River valley where the Arkansas River emerges from the Rocky Mountains to the Great Plains, near Cañon City, Colorado (Figure 31). They found concentrations of uranium exceeding 100 µg/L resulting from water contacting marine shale, including Mancos Shale-equivalent strata.
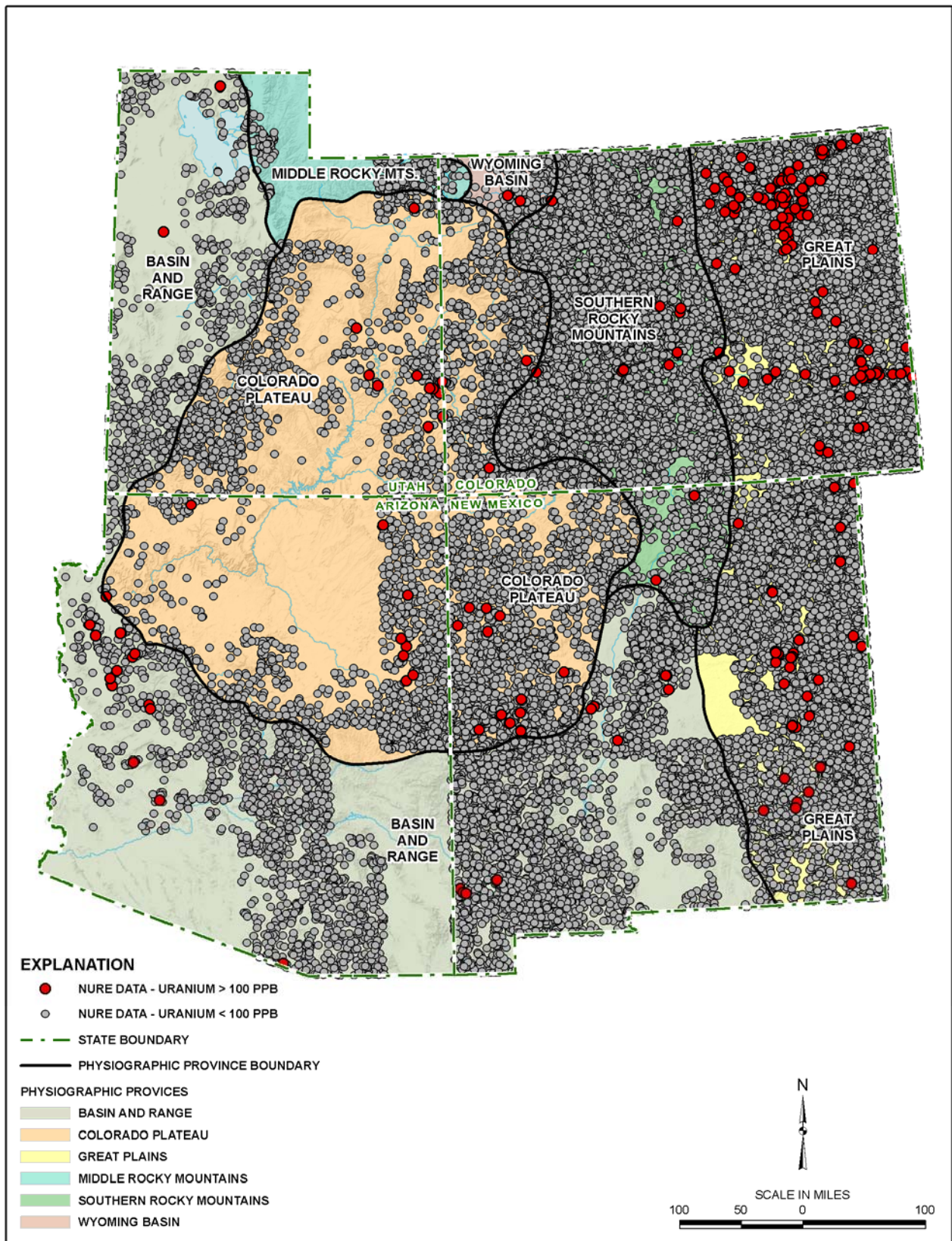
Figure 30. Uranium Distribution in Groundwater in the Four Corners States. Data from the NURE database from samples collected 1976 through 1979.
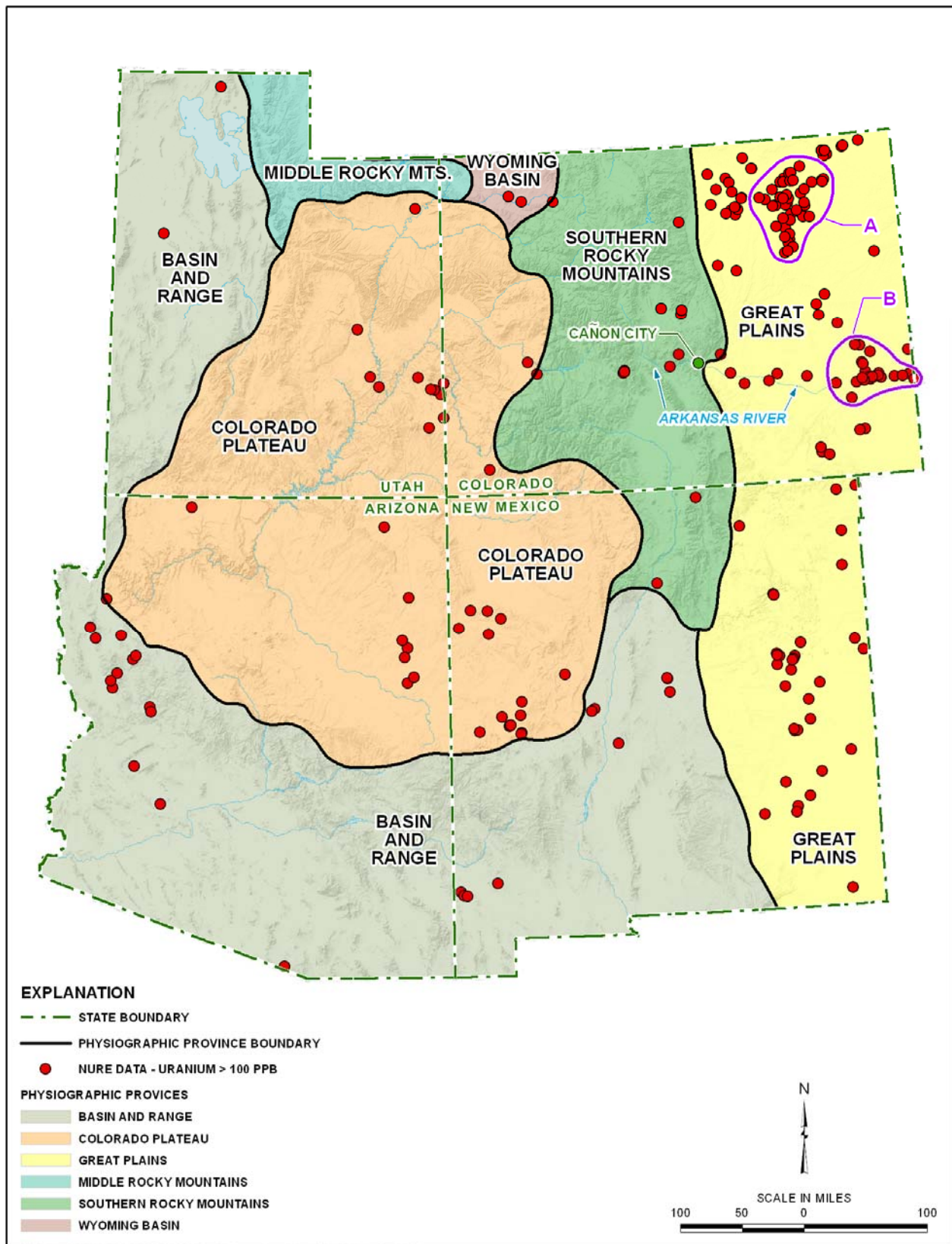
Figure 31. Groundwater Samples in the Four Corners States with Uranium Concentration more than 100 µg/L. Data from the NURE database from samples collected 1976 through 1979. Areas A and B are discussed in the text.

In many other locations scattered among the Four Corners states that exhibit elevated uranium concentrations (Figure 31), an association with Mancos Shale equivalent strata appears to exist. Note that we did not conduct a critical analysis of the NURE data for the purpose of correlating Mancos Shale with groundwater contamination. Were such an investigation performed, it is likely that some of the high uranium concentrations, particularly solitary high values in outlying areas, would be attributed to anthropogenic activities. Nonetheless, the information presented in this section (e.g. Table 8) suggests that a thorough assessment of the NURE data would enhance an analysis of natural contamination in the Mancos Shale.

Table 8. NURE Statistics of Groundwater Uranium Concentration (µg/L)
Data for Arizona, Colorado, New Mexico, and Utah Collected from 1976 to 1979.
First row represents all reported data. Second row is based on all data except for the five values that exceed 1,000 µg/L.

	Count	Min.	Max.	Mean[a]	Median	Std Dev
All Values	23,659	0.002	5934	8.67	2.63	51
Minus Highest Five Values	23,654	0.002	748	8.13	2.63	23

[a] Arithmetic mean

In addition to presenting uranium concentration data from seven wells and one spring located in weathered Mancos Shale in the Uncompahgre Valley and Grand Valley areas in Colorado, Butler et al. (1994) presented data from seven wells completed in alluvium overlying weathered Mancos Shale in the same area. Their uranium concentrations for the alluvium ranged from 9 to 72 µg/L and an arithmetic mean of 37 µg/L, as compared to a range of 8 to 75 µg/L with an arithmetic mean of 27 µg/L for the weathered Mancos Shale. A well log obtained from the U.S. Bureau of Reclamation in Grand Junction indicated that one well was screened from alluvium to about 80 ft into the Mancos Shale. Butler et al. (1994) reported that a sample from this well had a uranium concentration of 450 µg/L, which is much higher than two previous values (9.4 and 3.8 µg/L) from the same well. We speculate that this may be an analytical error. Wright (1995) presents uranium concentration data ranging from about 2 to 60 µg/L in 50 water samples collected from wells and streams in western Colorado irrigation projects in Mancos Shale terrain. Some of the data used by Wright (1995) may be the same as those presented in Butler et al. (1994). Uranium concentrations from eight samples of Sweitzer Lake water collected in 1987 and 1988 ranged from 12 to 29 µg/L, and in four samples of water from the Garnet Canal diversion ditch at Sweitzer Lake ranged from 14 to 64 µg/L (Butler et al. 1991).

Uranium concentrations in samples collected from Mancos Shale seeps for this study were relatively high, ranging from 0.2 to 1,922 µg/L. Seeps issuing from shale beds had much higher concentrations (a geometric mean of 83.4 µg/L) than those emanating from sandstone beds (a geometric mean of 7.3 µg/L; see Table 5). Samples from seeps that were apparently unrelated to anthropogenic activity had elevated uranium levels. Uranium concentrations in groundwater contacting gray shale beds in the Mancos Shale often exceed 100 µg/L from natural processes. Uranium is thought to have adsorbed to organic matter from sea water and was reduced to the uranous state at the bottom of the Late Cretaceous sea. Some concentration and redistribution may have occurred during burial diagenesis. As the Mancos Shale was uplifted and weathered, uranium was available for transfer to groundwater in its uranyl state.

6.2.9 Uranium Isotopes

Uranium-234 and -238 both undergo alpha decay with half-lives of 4.468×10^9 and 2.48×10^5 years, respectively (Faure 1977). A closed system requires nearly one million years to achieve secular equilibrium, a condition in which the decay rates of uranium-234 and uranium-238 are equal. Most uranium ores discovered in the Four Corners region are older than this and have achieved secular equilibrium. Individual silicate mineral grains, even those deposited in sediments, are likely to be in secular equilibrium at least in the inner portion that has not been subjected to leaching. There are two principal ways uranium can be transferred to groundwater from solid phases: (1) chemical dissolution, and (2) alpha recoil and associated leaching. Only the second causes fractionation of uranium-234 from uranium-238 (Petit et al. 1985).

Research that began in 1953 in Russia and became widespread in the United States by the mid-1960s recognized that the activity of uranium-234 was higher than the activity of uranium-238 in many groundwaters (Osmond and Cowart 1976; Faure 1977). Uranium-238 decays to thorium-234 by the energetic release of an alpha particle which causes the thorium atom to recoil directly into nearby pore fluid or to become lodged in the mineral crystal lattice (Kigoshi 1971). With a half-life of only 24.1 days, thorium-234 decays rapidly to uranium-234 in a portion of the crystalline lattice that was disrupted by the alpha recoil process. Alpha recoil is also thought to produce oxidation at the site of the newly born uranium-234 atom (Rosholt et al. 1963; Petit et al. 1985; Suksi et al. 2006). When coupled with the lattice disruptions, the oxidized uranium-234 atoms become more amenable to release into the pore fluids than uranium-238. Although there have been several variations on the details of the alpha recoil process and its effect on preferential release of uranium-234, it is well accepted that alpha recoil is the only mechanism that causes fractionation of uranium-234 from uranium-238. Having a single fractionation mechanism can make the interpretation of uranium isotopic signatures more straightforward than interpretations for many of the lighter environmental isotopes (e.g., ^{18}O, ^{2}H, ^{32}S, ^{15}N) that fractionate under a wider range of conditions. Also, fractionations of uranium isotopes are typically larger than those of other environmental isotopes; differences in the percentage range are common, compared to parts-per-thousand differences for many of the other environmental isotopes (Osmond and Cowart 1976). Interpretation of uranium isotopes is further simplified because fractionation is independent of the chemistry of the aqueous phase. Despite these benefits, the use of uranium isotopes still suffers from an incomplete knowledge of the exact fate of thorium-234 and its daughter uranium-234 following alpha decay.

Based on literature surrounding the occurrence of uranium in dark marine shale, we assume that much of the uranium in the Mancos Shale resides in organic matter. Research on preferential release of uranium-234 due to alpha recoil has been universally directed to uranium bound in silicate or carbonate minerals, and we were unable to locate similar research on uranium bound to organic matter. Kigoshi (1971) assumes that the recoil length for thorium-234 is inversely proportional to the density of the material and estimates a 900-angstrom (Å) recoil length for pelagic sediment from experimentally determined recoil lengths of 550 Å for zircon. Presumably, low-density humic matter would have longer recoil lengths, and thus, fractionation due to direct thorium-234 recoil from organic matter would exceed those based on a silica framework. The AR of uranium-234 to uranium-238 has been used in various groundwater studies to help determine the origin of the uranium. The AR is near unity if both isotopes are in secular equilibrium. As alpha recoil processes cause preferential transfer of uranium-234 from

Natural Contamination from the Mancos Shale   U.S. Department of Energy
Doc. No. S07480   April 2011
Page 62

the solid to the aqueous phase, the AR increases. AR values up to 2 are common in groundwater, but values up to 9 or more have been reported (Osmond and Cowart 1976; Suksi et al. 2006).

Zielinski et al. (1997) used AR values to help determine the source of uranium in a groundwater uranium plume emanating from a uranium mill site near Cañon City, Colorado. The AR values in the mill effluent were near 1.0 because the uranium ores were in secular equilibrium, and the milling process was sufficiently aggressive to cause essentially congruent mineral dissolution, thus maintaining the isotopic signature. In contrast, Zielinski et al. (1997) reported that AR values in background areas unaffected by the mill-generated plume were between 1.3 and 1.5. The AR values in the groundwater plume correlated well with uranium and molybdenum (another mill contaminant) concentrations, further indicating that AR values could be used to delineate the plume.

Weathering and oxidation processes are often cited to interpret some of the observed AR patterns in nature. Hussain and Krishnaswami (1980) state that intense weathering (presumably caused by congruent mineral dissolution) could result in high uranium concentrations and AR values near 1.0; whereas less-intense weathering (incongruent mineral dissolution) would selectively remove uranium-234 from the oxidized sites created by alpha recoil. Using theoretical modeling of the alpha recoil process, Suksi et al. (2006) concluded that direct alpha recoil to the groundwater is minimal and that uranium-234 fractionation is largely due to preferential oxidation. From this they reasoned that fractionation of uranium-234 only occurs from a reduced substrate. Cowart and Osmond (1977) observed low uranium concentrations with high AR values in groundwater within the reducing zone of uranium ore bodies. They reasoned that oxidized groundwater, high in uranium and with AR near 1.0, transports the uranium to the reduced zone where uranium mineral precipitation caused a sharp decrease in uranium concentration and an increase in AR values due to alpha recoil. In contrast, Maher et al. (2006) matched data from leaching of fine-grained sediment separates with an alpha recoil model based on grain geometry, suggesting that direct alpha recoil loss dominated, and preferential leaching is insignificant in a sediment with slowly dissolving silicates.

All of our uranium isotope data from Mancos Shale seeps show that AR values were more than 1.0 and most exceeded 2.0, indicating that uranium-234 activity regularly exceeds uranium-238 activity in Mancos groundwater throughout its depositional basin. A conceptual model for the groundwater AR values should explain several observations: (1) all samples have excess uranium-234, and many have twice the activity of uranium-234 as uranium-238, (2) these high AR values of near 2.0 are present over wide geographic areas, (3) samples collected from separate locations but within the same local area often have similar AR values, (4) many samples have elevated uranium concentrations, often exceeding 100 μg/L, and (5) groundwater contacting Mancos Shale for as little as one year is sufficient to produce AR values more than 2.0. The last of these observations is based on evidence that USGS Seep 2 near Devil's Thumb Golf Course originated less than a year after the filling of a pond that was the source of the seep water. Uranium isotopic data were not available from this seep, but nearby seeps DTS1, DTS2, and DTS3, which likely formed at the same time, had AR values greater than 2.0.

The apparently short groundwater residence time in the case of USGS Seep 2 seems to refute the possibility that direct recoil of thorium-234 atoms into pore fluids from host organic matter is responsible for the larger AR values that we see in Mancos Shale groundwater. Instead, we suggest that during uplift and erosion of Mancos Shale, perhaps over the last thousand years or

so, alpha recoil of thorium-234 into pore fluids was followed by rapid sorption of the recoiled atom to surfaces of oxidized organic matter or minerals formed by the weathering process. The rock matrix at this time was relatively dry. By the time the shale beds were uplifted to within about 50 ft of the surface, uranium-234 preferentially occupied sorption sites on secondary minerals. Once groundwater was able to find pathways through the weathered shale beds, uranium enriched in uranium-234 was desorbed into the groundwater and subsequently transported to the seep locations. This hypothesis remains conjectural until more research can be conducted on the solid-phase AR values, and similar AR values can be produced from controlled laboratory tests. This hypothesis has similarities with the work of Rosholt et al. (1963) who found high variability of uranium isotopic signatures in 28 sandstone uranium ores from the United States; and they found that these ratios did not correlate with the oxidation states of the samples. Rosholt et al. (1963) suggested that uranium-234 was preferentially leached from ores, and then uranium from these fluids reprecipitated to form secondary ores with high uranium-234.

Petit et al. (1985) provided a succinct review and evaluation of the various mechanisms thought to be responsible for the excess of uranium-234 commonly found in groundwater. Importantly, they demonstrated that dissolution of uranium-bearing minerals produces a dilution of the uranium isotopic signature by adding a significant amount of uranium-238 to the groundwater. Their analysis indicated that production of excess uranium-234 by alpha recoil processes to increase the AR value from 1.0 to as little as 1.2 required unrealistically low rates of mineral dissolution. They also suggested that in a situation where water is present in a rock only intermittently, the alpha recoil products are implanted in adjacent grains to be released later when groundwater resaturated the system. The dilution by uranium-238 in the Mancos Shale seep samples investigated in this study would be extreme if mineral dissolution (or desorption) involved uranium that was at secular equilibrium in the shale. Using this reasoning, it is possible that recent groundwater in Mancos Shale released uranium from minerals containing excess uranium-234 that had previously been concentrated on secondary minerals and organic matter over long time periods.

6.2.10 Vanadium

There are few data available to assess vanadium concentrations in Mancos Shale groundwater. Vanadium concentrations from eight samples of Sweitzer Lake water collected in 1987 and 1988 ranged from less than 1 to 7 μg/L, and concentrations in four samples of water from the Garnet Canal diversion ditch (Figure 6) at Sweitzer Lake ranged from less than 1 to 14 μg/L (Butler et al. 1991). Deverel and Millard (1988) found that vanadium concentrations in shallow groundwater of the western San Joaquin Valley, California, correlated with salinity.

Despite its much higher concentration (about 100 mg/kg) than uranium or selenium in the Mancos Shale, vanadium has low concentrations in groundwater. In the seep samples, all but one sample had less than 2 μg/L of vanadium. Sample SNS from Sweitzer Lake was the only exception with a concentration of 19 μg/L, suggesting that this sample was affected by evaporation. We suggest that vanadium is tied up with a more hydrophobic fraction of the shale, perhaps sapropelic-based kerogen, that is not released easily upon contact with an aqueous phase. The affinity of vanadium for petroleum is well documented (Erickson et al. 1954; Hyden 1956).

There is no drinking water standard for vanadium; however, New Mexico has a livestock drinking water standard of 100 µg/L (Thomas et al. 1998). Because all of the groundwater vanadium concentrations measured in the seeps were much below this value, we conclude that vanadium is not a natural contaminant in the Mancos Shale.

6.3   Conceptual Model of Seep Chemistry

Clay and silt particles were deposited as mud at the bottom of the broad shallow Western Interior Seaway during the Late Cretaceous Epoch. Later lithification of these mud deposits became the shale of the Mancos Shale. Calcium carbonate precipitation in the shallow sea resulted in sporadic but substantial beds of limestone. Chemically reducing conditions caused by microbial degradation of organic compounds at the sea bottom caused formation of pyrite. Uranium from seawater was incorporated into organic matter by adsorption and reductive precipitation. Uranium concentrations in seawater may have been increased by devitrification of volcanic ash that periodically fell into the sea. Uranium isotopic signatures reflected those in seawater, which currently has a fairly constant AR of about 1.15 (Faure 1977). Selenium substituted for sulfur in pyrite, and some was adsorbed to organic matter. Nitrate production accompanied biodegradation, and nitrate was concentrated with organic matter. Pore water chemistry reflected the high sodium chloride composition of sea water. Chemical reduction continued during shallow burial, accompanied by minor redistribution of selenium, uranium, and other natural contaminants. Boron, which occurred in seawater at concentrations that were relatively high, was adsorbed by settling mud but was subsequently incorporated in phyllosilicate tetrahedral sites during diagenesis. Calcium carbonate was also redistributed, resulting in calcareous cementation. During burial diagenesis, the original clay and silt deposited during the Late Cretaceous was compacted to about a third to a tenth of its original water-saturated volume by the time it was buried to 10,000 ft in Tertiary time (Shawe 1976). By this time, a large proportion of smectite layers in illite-smectite clay minerals had been transformed to illite, and the Mancos Shale had become lithified. For reasons yet to be determined, nearly pure smectite in bentonite beds went unaltered. Pore fluids were dominated by sodium chloride, and cation exchange sites were occupied by sodium.

During the Neogene, the Mancos Shale was uplifted and became exposed over large areas of the Colorado Plateau, and erosion was coupled to uplift such that the Mancos Shale continually supplied unweathered shale and natural contaminants to the weathering horizon. Chloride minerals are highly soluble, and some chloride was lost from the system before the beds reached the weathering horizon. Oxidation of pyrite and organic matter in the weathering horizon caused formation of gypsum, lowering of pH, and dissolution of some organic matter. The contrast between the sodium-chloride chemistry of the deep, unweathered Mancos Shale groundwater and the sodium-sulfate composition of the shallow, weathered Mancos Shale is caused by the contribution of sulfate by oxidation of pyrite in the weathering horizon. Lowering of pH was buffered by dissolution of calcite, which was abundant in the Mancos Shale. The transfer of calcium from carbonate minerals to the aqueous phase made it available to exchange with sodium on cation exchange sites and to combine with sulfate to form gypsum. Sodium dominated the ion exchange sites as indicated by high sodium concentrations in both weathered and unweathered Mancos Shale. Although shales of the Mancos Shale are mostly dry, they contain an abundance of soluble matter that can be released whenever water is applied. The main elements of major ion chemistry as proposed by this conceptual model were simulated using a numerical model, as discussed in the next section.

6.4   Reaction Progress Model of Seep Chemistry

Groundwater can flow at high rates through the Mancos Shale, as demonstrated at the Devil's Thumb Golf Course, where groundwater flow rates of 8 ft per day were observed. It is likely that flow in the shallow Mancos Shale follows fractures, bedding planes, and other structural or weathered features and is not likely to be accurately portrayed using traditional models invoking porous media flow. Because of the uncertainty of the flow system, we elected not to model flow; rather, we used a reaction progress model to simulate the main chemical features of the shallow groundwater system. Reaction progress modeling is well suited to simulating mass transfer of chemicals between Mancos Shale and groundwater. This type of modeling uses a set of irreversible reactions to produce changes to a chemical system, with all other chemical reactions evolving in local equilibrium. An excellent example of the usefulness of reaction progress modeling is provided by Helgeson (1979), who modeled the progressive evolution of hydrothermal vein minerals driven by irreversible feldspar hydrolysis.

We conceptualize a system in which relatively clean water infiltrates into the Mancos Shale and migrates along fractures, bedding planes, and bentonite layers to seeps or springs. Seeps commonly occur along the strike of the Mancos Shale beds, indicating that bedding planes, and in some cases bentonite beds, exert a major control on groundwater flow. At most sites, the flow regime is relatively shallow and mostly within the weathered Mancos Shale. Based on the core data from the Crescent Junction site and reports of Mancos chemistry and mineralogy from the literature, we assume that the Mancos contains gypsum, calcite, pyrite, and organic matter. Pyrite, calcite, and organic matter are weathered products of marine deposition and shallow (several hundred feet) burial diagenesis, whereas gypsum and ferric oxyhydroxide are oxidation products of pyrite. Pyrite and organic matter are closely associated, whereas gypsum and calcite commonly occur in mineralized fractures or other secondary features, having been mobilized some distance from their source. Of importance, the presence of high concentrations of sodium on ion exchange sites is critical to producing the sodium sulfate major ion compositions that are ubiquitous in many Mancos Shale seeps.

Our conceptual model for the release of constituents from the Mancos Shale involves the irreversible incongruent dissolution of organic matter, the irreversible dissolution of pyrite, and the addition of sodium-filled ion exchange sites (NaX). Equilibrium is maintained among all aqueous speciation, ion exchange, and mineral precipitation and dissolution reactions. Reaction progress modeling can be thought of by considering a liter of water in a beaker to which we gradually add small increments of solid components (pyrite, organic matter, and shale with ion exchange sites) and compute the chemical composition at each addition. This has a similar effect as considering the evolution of water chemistry as this liter of water migrates along a flow path in the Mancos Shale and progressively reacts with the aquifer solids. Because we lack knowledge of the flow regime and have no groundwater data from various locations along a flow path, we cannot explicitly test chemical interactions in a predictive way. However, the model is useful in providing a numerical (and thermodynamically consistent) verification of the reasonableness of our conceptual model. Reaction progress modeling used the PHREEQC computer code (Parkhurst and Appelo 1999).

Thermodynamic data for all aqueous complexation, ion exchange, and mineral precipitation/dissolution reactions are from the database provided with the PHREEQC program. For computational simplicity, solid-phase organic matter in geologic systems is often presented as CH_2O (Stumm and Morgan 1981), and we used that simplification. We also simplify the

dissolved organic phase as carboxyl ion; thus, the following equation depicts the irreversible hydrolysis of organic matter:

$$CH_2O + H_2O = HCOO^- + 3H^+ + 2e^-$$

where $HCOO^-$ is used as a proxy for DOC. Because the groundwater is in the near-surface weathered Mancos Shale, oxygen was maintained at equilibrium with 10^{-7} atmosphere of O_2 (approximately 8 mg/L dissolved oxygen). Iron oxyhydroxide was simulated with amorphous $Fe(OH)_3$. Calcite, gypsum, and $Fe(OH)_3$ were maintained at equilibrium throughout the simulation. Ion exchange sites are considered to be highly charged with sodium, as indicated by the presence of concentrated sodium chloride groundwater in the deep borings of unweathered Mancos Shale. Our chemical analysis of a pristine (specific conductivity of 114 µS/cm) Delta Reservoir (DR) water sample on November 8, 2010, was used as the initial solution. Our goal was to seek a reasonable match to the seep chemistry at Delta Reservoir seeps DRS1 and DRS3 by adjusting the phase mixture within reasonable limits. A mixture of pyrite, CH_2O, and NaX in the molar amounts 0.0008, 0.0003, and 1.0, respectively, provided a reasonable match as shown in Table 9. This mixture was added in 1,000 steps of 0.005 mole each to the initial solution. The modeled value for sodium is higher than observed, because only sodium was considered to occupy ion exchange sites; calcium, potassium, and magnesium loading on ion exchange sites was probably minimal and was ignored. As an additional simplification, the carbon contained in DOC was not allowed to exchange with inorganic carbon. This condition is justified by the observation that DOC is at high concentrations in many of the groundwater samples despite oxidizing conditions that would cause its complete conversion to CO_2 if it reacted to thermodynamic equilibrium.

Table 9. Delta Reservoir Reaction Progress Model Results Compared to Chemistry Measured in Samples from Seeps DRS1 and DRS3, November 8, 2010 (mg/L). Five moles of reactive mixture were added.

	DIC	DOC	SO$_4$	Na	Fe	pH
DRS1	222	44	18,497	7,600	<1	7.16
DRS2	251	2.9	15,087	5,900	<1	7.25
Model	199	18	18,453	8,884	<1	7.17

DIC = dissolved inorganic carbon; DOC = dissolved organic carbon

Figure 32 shows the trends in constituent concentrations as the model progresses toward the final values shown in Table 9. Proton generation from the addition of pyrite, oxidized by the oxygenated atmosphere, causes a gradual decrease in pH. The pH would decrease much faster if not buffered by calcite dissolution. Iron generated by pyrite dissolution is taken up by $Fe(OH)_3$ precipitation. Calcium generated by calcite dissolution exchanges with sodium on the Mancos clay minerals; the lack of dissolved calcium prevents precipitation of gypsum. Thus, the system evolves to a dominantly sodium sulfate system.
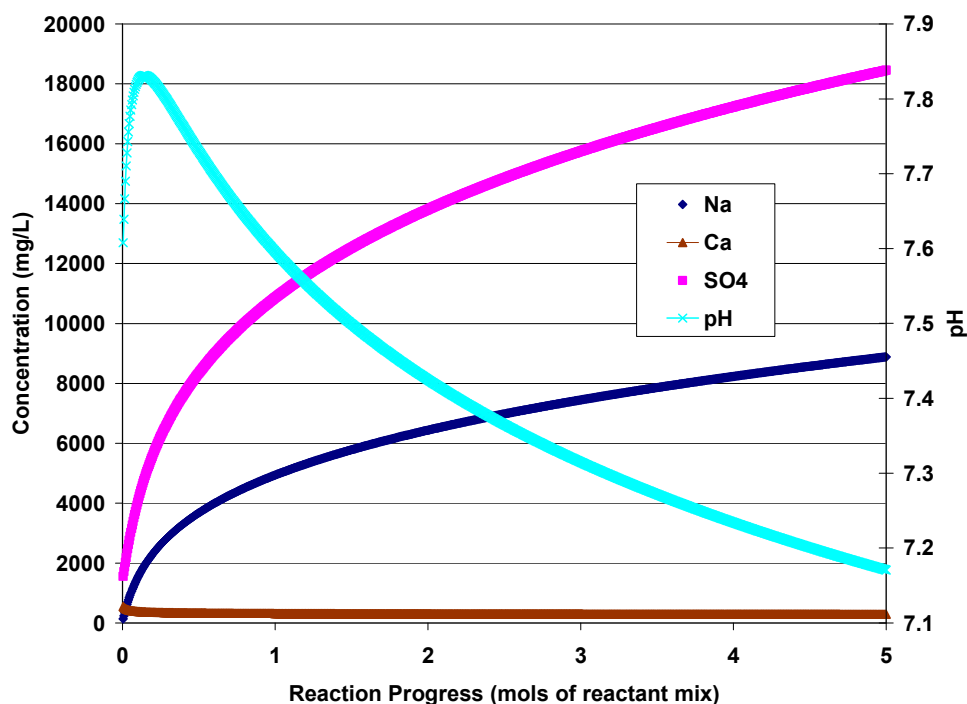
Figure 32. Calculated Concentrations for a Reaction Progress Model Simulation of the Delta Reservoir Seeps. Reaction progress is defined by a mixture of 1, 0.0008, and 0.0003 mole of NaX, pyrite, and CH_2O, respectively.

Uranium and other trace constituents were not modeled because too little is known about their mode of occurrence both in the solid and dissolved states. Based on literature data presented above, it is likely that uranium resides in the organic matter and is perhaps complexed by DOC in the aqueous phase.

7.0 Conclusions and Recommendations

This study identified groundwater seeping from the Mancos Shale that was contaminated by naturally occurring processes. The results indicate that high concentrations of major ions, nitrate, selenium, and uranium are likely to occur as a natural process of interaction between groundwater and Mancos Shale. The high concentrations are apparently limited to groundwater associated with shale beds, and concentrations of these constituents in groundwater associated with sandstone were much lower. High contaminant concentrations occurred throughout the study areas and were not correlated with geographic area, stratigraphic position, or source of water. Some of the samples were influenced by irrigation, but others were collected from locations in remote areas with no significant anthropogenic input. In the interest of developing reasonable and achievable cleanup goals, the effects of naturally occurring concentrations of nitrate, selenium, and uranium should be considered when evaluating groundwater contaminant plumes beneath and downgradient of disposal cells constructed on Mancos Shale.

Groundwater contacting shale beds of Mancos Shale can have concentrations of nitrate, selenium, and uranium that exceed regulatory standards. Many of the groundwater samples were highly saline, as indicated by specific conductivity values ranging from 418 to 70,002 µS/cm

with a geometric mean of 9,226 µS/cm. Samples collected at nine locations had specific conductivity values of more than 30,000 µS/cm. Nitrate concentrations exceeded 250 mg/L at 13 locations, and selenium concentrations exceeded 1,000 µg/L in eight samples. Uranium concentrations were also high, having a range of 0.2 to 1,922 µg/L with a geometric mean of 48.8 µg/L, and samples from 18 locations had concentrations more than 100 µg/L. The groundwater can also have DOC concentrations exceeding 100 mg/L, which commonly colors the water yellow to red. Boron (a possible indicator of marine shale) concentrations exceeding 1,000 µg/L were common in groundwater from shale beds, but lower values were observed in groundwater from sandstone. Vanadium and arsenic concentrations were low in the seep samples, and thus are not natural contaminants in the Mancos.

All uranium-234 to uranium-238 AR values were greater than the secular equilibrium value of 1.0. All but three of the AR values were more than 1.5, and about half of the values exceeded 2.0. Thus, high AR values may be a common characteristic of groundwater that has interacted with Mancos Shale.

Chemical reactions driven by the irreversible oxidation of organic matter and pyrite offer a plausible explanation for the evolution of groundwater chemistry. Pyrite oxidation generates sulfate, selenium, and protons, whereas organic matter yields DOC and liberates nitrate and uranium. These reactions occurred after the Mancos Shale had been uplifted sufficiently such that atmospheric oxygen was available to drive weathering processes.

The current study is based on a single set of samples from a wide geographic area encompassing much of the Mancos Shale depositional basin. It would be useful to sample the same seeps at least one additional time, during the main irrigation season, to help evaluate seasonal variation. Because of time limitations, several large areas of Mancos Shale outcrops were not investigated in the field. It would be beneficial to extend the study to include groundwater sampling in these areas. These areas include the Kaiparowits Plateau; Black Mesa Basin; areas of the southern San Juan Basin near Gallup, New Mexico; an area near Show Low Arizona; and areas in Colorado near Steamboat Springs and Pagosa Springs; and area near Vernal, Utah. Extending the investigation to include the Pierre Shale, Niobrara Formation, and other Mancos equivalent strata in eastern Colorado, Kansas, Montana, Nebraska, South Dakota, and Wyoming would also be of interest.

The main purpose of the current study was to evaluate groundwater chemistry in the Mancos Shale caused by natural processes. To meet this purpose, a limited set of chemical parameters was selected for study. Because some seeps were relatively nonproductive, obtaining a suitable volume of groundwater for extensive chemical analysis was not possible. However, most locations produced groundwater in sufficient quantity to facilitate additional analyses. Potentially useful data that were not included in this study are $\delta^{18}O$ and δD, which could help confirm the sources of groundwater and provide a more quantitative assessment of evaporation effects. More detailed work, including coring and analysis and installation of a groundwater monitoring array in an area that has well-defined groundwater control such as Daly Reservoir could help to understand groundwater chemistry as it evolves along flow lines. Determination of the nature of the DOC could lead to a better understanding of the processes responsible for its occurrence in the groundwater.

8.0   Acknowledgements

9.0   References

40 e-CFR 141. U.S. Environmental Protection Agency, "National Primary Drinking Water Regulations," *Code of Federal Regulations*, January 31, 2011.

Adams, J.A.S., and Weaver, C.E., 1958. "Uranium-to-thorium ratios as indicators of sedimentary processes: Example of concept of geochemical facies," *Bull. Amer. Assoc. Petrol. Geol.*, 42: 387−430.

Adams, S.S., H.S. Curtis, and P.L. Hafen, 1974. "Alteration of detrital magnetite-ilmenite in continental sandstones of the Morrison Formation, New Mexico," *Formation of Uranium Ore Deposits*, International Atomic Energy Agency, Vienna, Austria, pp. 219–253.

Aravena, R., and L.I. Wassenaar, 1993. "Dissolved organic carbon and methane in a regional confined aquifer, southern Ontario, Canada: Carbon isotope evidence for associated subsurface sources," *Applied Geochemistry*, 8: 483–493.

Berman, A.E., D. Poleschook Jr., and T.E. Dimelow, 1980. "Jurassic and Cretaceous systems of Colorado," in Kent, H.C., and K.W. Porter (eds.), *Rocky Mountain Association of Geologists 1980 Symposium Guidebook*, Denver, pp. 111–128.

Berner, R.A., 1987. "Models for carbon and sulfur cycles and atmospheric oxygen: Application to Paleozoic geologic history," *Amer. J. Sci.*, 287: pp. 177–196.

Broxton, D.E., W.A. Morris, and S.L. Bolivar, 1979. *Uranium Hydrogeochemical and Stream Sediment Reconnaissance of the Montrose NTMS Quadrangle, Colorado, Including Concentration of Forty-Three Additional Elements,* Informal Report LA-7507-MS, Los Alamos Scientific Laboratory, Los Alamos, New Mexico.

Buckau, G, R. Artinger, S. Geyer, M. Wolf, P. Fritz, and J.I. Kim, 2000. "Groundwater in-situ generation of aquatic humic and fulvic acids and the mineralization of sedimentary organic carbon," *Applied Geochemistry,* 15: 819–832.

Butler, D.L., R.P. Krueger, B.C. Osmundson, A.L. Thompson, and S.K. McCall, 1991. *Reconnaissance Investigation of Water Quality, Bottom Sediment, and Biota Associated with Irrigation Drainage in the Gunnison and Uncompahgre River Basins and at Sweitzer Lake, West-Central Colorado, 1988–89*, U.S. Geol. Survey Water-Resources Investigations Report 91-4103, 99 pp.

Butler, D.L., W.G. Wright, D.A. Hahn, R.P. Krueger, and B.C. Osmundson, 1994. *Physical, Chemical, and Biological Data for Detailed Study of Irrigation Drainage in the Uncompahgre Project Area and in the Grand Valley, West-Central Colorado, 1991–92*, U.S. Geol. Survey Open-File Report 94-110, 146 pp.

Butler, D.L., W.G. Wright, K.C. Stewart, B.C. Osmundson, and R.P. Krueger, 1996. *Detailed Study of Selenium and Other Constituents in Water, Bottom Sediment, Soil, Alfalfa, and Biota Associated with Irrigation Drainage in the Uncompahgre Project Area and in the Grand Valley, West-Central Colorado, 1991–93*, U.S. Geol. Survey Water-Resources Investigations Report 96-4138, 136 pp.

Butler, D.L., and K.J. Leib, 2002. *Characterization of Selenium in the Lower Gunnison River Basin, Colorado, 1988–2000*, U.S. Geol. Survey Water-Resources Investigations Report 02-4151, 26 pp.

Clayton, J.L., and P.J. Swetland, 1978. "Subaerial weathering of sedimentary organic matter," *Geochim. et Cosmochim. Acta*, 42: 305–312.

Cowart, J.B., and J.K. Osmond, 1977. "Uranium isotopes in groundwater: Their use in prospecting for sandstone-type uranium deposits," *J. Geochem. Exploration*, 8: 365–379.

Cross, W., and C.W. Purington, 1899. *Geologic Atlas of the United States, Telluride, Colorado*, U.S. Geol. Survey Folio 57, Washington, D.C.

Curtis, P.J., and D.W. Schindler, 1997. "Hydrologic control of dissolved organic matter in low-order Precambrian Shield lakes," *Biogeochemistry*, 36: 125–138.

Deverel, S.J., and S.P. Millard, 1988. "Distribution and mobility of selenium and other trace elements in shallow groundwater of the western San Joaquin Valley, California," *Environ. Sci. Technol.*, 22: 697–702.

Deyo, A.E., 1984. *Salinity Investigations of Mancos Landforms and Springs in the Upper Colorado River Basin*, Ph.D. Dissertation, University of California, Davis, 184 pp.

DOE (U.S. Department of Energy), 2000. *Final Site Observational Work Plan for the Shiprock, New Mexico, UMTRA Project Site,* GJO-2000-169-TAR, Grand Junction Office, Grand Junction, Colorado, November.

DOE (U.S. Department of Energy), 2007. *Revised Draft Remedial Action Plan and Site Design for Stabilization of Moab Title I Uranium Mill Tailings at the Crescent Junction, Utah Disposal Site*, DOE-EM/GJ1270-2006, U.S. Department of Energy Office of Environmental Management, Grand Junction, Colorado (unissued document).

Droycon Bioconcepts Inc., 2004. *BART User Manual*, Regina, Saskatchewan, Canada.

Eaton A. D., L.S. Clesceri, and A.E. Greenberg (eds), 1995. *Standard Methods for the Examination of Water and Wastewater, 19th Edition.* American Public Health Assoc., American Water Works Assoc., Water Environment Federation, Washington, D.C.

Erickson, R.L., Myers, A.T., Horr, C.A., 1954. "Association of uranium and other metals with crude oil, asphalt, and petroliferous rock," *Bull. Amer. Assoc. Petrol. Geol.*, 38: 2200–2218.

Evangelou, V.P., 1981. *Chemical and Mineralogical Composition and Behavior of the Mancos Shale as a Diffuse Source of Salts in the Upper Colorado River Basin*, Ph.D. Dissertation, University of California, Davis, 198 pp.

Evangelou, V.P., L.D. Whittig, and K.K. Tanji, 1984. "Dissolved mineral salts derived from Mancos Shale," *J. Environ. Qual.*, 13: 146–150.

Evangelou, V.P., L.D. Whittig, and K.K. Tanji, 1985. "Dissolution and desorption rates of calcium and magnesium from Mancos Shale," *Soil Science*, 139: 53–61.

Faure, G., 1977. *Principles of Isotope Geology*, John Wiley & Sons, New York, 464 pp.

Fisher, D.J., C.E. Erdmann, and J.B. Reeside Jr., 1960. *Cretaceous and Tertiary Formations of the Book Cliffs, Carbon, Emery, and Grand Counties, Utah, and Garfield and Mesa Counties, Colorado*, U.S. Geol. Survey Professional Paper 332, 80 pp.

Foster, M.D., 1950. "The origin of high sodium bicarbonate waters in the Atlantic and Gulf Coastal Plains," *Geochim. et Cosmochim. Acta*, 1: 33–48.

Gilbert, R.O., 1987. *Statistical Methods for Environmental Pollution Monitoring*, Van Nostrand Reinhold Company, New York, 320 pp.

Gerner, S.J., L.E. Spangler, B.A. Kimball, D.E. Wilberg, and D.L. Naftz, 2006. *Hydrology and Water Quality in the Green River and Surrounding Agricultural Area near Green River in Emery and Grand Counties, Utah, 2004–05*, U.S. Geol. Survey Scientific Investigations Report 2006-5186, 42 pp.

Golder Associates, 2004. *Results of the Investigation for the Devil's Thumb Area Delta County, Colorado*, prepared for Delta County, 501 Palmer St, Suite 227, Delta, Colorado (Unpublished document).

Grauch, R.I., M.L. Tuttle, B. Ball, J.G. Elliott, J.J. Kosovich, G.W. Chong, J. Fahy, K. Tucker, D. Murphy, and J. Belnap, 2005. "Mancos Shale landscapes: science and management of black shale terrains—a multi-agency project," Geol. Soc. Amer. Annual Meeting (October 28–31, 2007, Denver, Colorado), *Geol. Soc. Amer. Abstracts with Programs,* 39: 195.

Harder, H., 1970. "Boron content of sediments as a tool in facies analysis," *Sedimentary Geology*, 4: 153–175.

Helgeson, H.C., 1979. "Mass transfer among minerals and hydrothermal solutions," in Barnes, H.L. (ed.), *Geochemistry of Hydrothermal Ore Deposits, Second Edition*, John Wiley & Sons, New York, pp. 568–610.

Hem, J.D., 1985. *Study and Interpretation of the Chemical Characteristics of Natural Water*, U.S. Geol. Survey Water-Supply Paper 2254, U.S. Government Printing Office, Alexandria, Virginia, 263 pp.

Holloway, J.M., and R.L. Smith, 2005. "Nitrogen and carbon flow from rock to water: Regulation through soil biogeochemical processes, Mokelumne River watershed, California, and Grand Valley, Colorado," *J. Geophy. Res.*, 10: 1–12.

Hussain, N., and S. Krishnaswami, 1980. "U-238 series radioactive disequilibrium in groundwaters: implications to the origin of excess U-234 and fate of reactive pollutants," *Geochim. et Cosmochim. Acta*, 44: 1287–1291.

Hyden, H.J., 1956. "Uranium and other trace metals in crude oils of the western United States," in L.R. Page, H.E. Stocking, and H.B. Smith (compilers), *Contribution to the Geology of Uranium and Thorium by the United States Geological Survey and Atomic Energy Commission for the United Nations International Conference on Peaceful Uses of Atomic Energy, Geneva, Switzerland 1955*, Geol. Survey Professional Paper 300, U.S. Government Printing Office, Washington, D.C., p. 511–519.

Jackson, W.L., and R.P. Julander, 1982. "Runoff and water quality from three soil landform units on Mancos Shale," *Water Resources Bull.*, 18: 995–1001.

Jacobs, J., and K. Fagrelius, 1978. "Salt Creek Dakota [oil field]," in J.E. Fassett (ed.), *Oil and Gas Fields of the Four Corners Area, Volume 2*, Four Corners Geol. Society, Durango, Colorado, pp. 480–481.

Johnson, R.C., 2003. *Depositional Framework of the Upper Cretaceous Mancos Shale and the Lower Part of the Upper Cretaceous Mesaverde Group, Western Colorado and Eastern Utah*, U.S. Geol. Survey Digital Data Series DDS-69-B, 24 pp.

Jurinak, J.J., J.C. Whitmore, and R.G. Wagenet, 1977. "Kinetics of salt release from a saline soil," *Soil Sci. Soc. Am. J.*, 41: 721–724.

Kakouros, E., Y.K. Kharaka, and J.A. Oberdorfer, 2006. "Leaching rates and forms of selenium in cores from an agricultural area in middle Green River Basin, Utah, USA," *Earth Science Frontiers*, (China University of Geosciences, Beijing: Peking University), 12: 86–97.

Kauffman, E.G., 1969. Cretaceous marine cycles of the Western Interior, *The Mountain Geologist*, 6: 227–245.

Kauffman, E.G., 1977. "Geological and biological overview: Western Interior Cretaceous Basin," in E.G. Kauffman (ed.), Cretaceous Facies, Faunas, and Paleoenvironments Across the Western Interior Basin, *The Mountain Geologist*, 14: 75–99.

Kigoshi, K., 1971. "Alpha-recoil thorium-234: dissolution into water and the uranium-234/uranium-238 disequilibrium in nature," *Science*, 173: 47–48.

Knight, W.C., 1898. "Bentonite," *Eng. Mining J.*, 66: 491.

Laronne, J.B., 1977. *Evaluation of the Storage of Diffuse Sources of Salinity in the Upper Colorado River Basin*, Ph.D. Dissertation, Colorado State University, Fort Collins, Colorado, 111 pp.

Laronne, J.B., and H.W. Shen, 1982. "The effect of erosion on solute pickup from Mancos Shale hillslopes, Colorado, U.S.A.," *J. Hydrol.*, 59: 189–207.

Laronne, J.B., and S.A. Schumm, 1982. "Soluble mineral content in surficial alluvium and associated Mancos Shale," *Water Resources Bull.*, 18: 27–35.

Leckie, R.M., J.I. Kirkland, and W.P. Elder, 1997. "Stratigraphic framework and correlation of a principal reference section of the Mancos Shale (Upper Cretaceous), Mesa Verde, Colorado," in O.J. Anderson, B.S. Kues, and S.G. Lucas (eds.), *Mesozoic Geology and Paleontology of the Four Corners Region*, New Mexico Geological Society Fall Field Conference Guidebook, New Mexico Geological Society, Socorro, New Mexico, 48: 163–216.

Leythaeuser, D., 1973. "Effects of weathering on organic matter in shales," *Geochim. et Cosmochim. Acta*, pp. 113–120.

Littke, R., U. Klussmann, B. Krooss, and D. Leythaeuser, 1991. "Quantification of loss of calcite, pyrite, and organic matter due to weathering of Toarcian black shales and effects on kerogen and bitumen characteristics," *Geochim. et Cosmochim. Acta*, 55: 3369–3378.

Maher, K., D.J. DePaolo, and J.N. Christensen, 2006. "U-Sr isotopic speedometer: Fluid flow and chemical weathering rates in aquifers," *Geochim. et Cosmochim. Acta*, 70: 4417–4435.

Matthews, V., K. KellerLynn, and B. Fox (eds.), 2003. *Messages in Stone, Colorado's Colorful Geology*, Colorado Geol. Survey Special Publication 52, 157 pp.

McKelvey, V.E., D.L. Everhart, and R.M. Garrels, 1955. "Origin of uranium deposits," *Econ. Geol.*, 464–533.

Michel, J., 1990. "Relation of radium and radon with geological formations," Chapter 7, in C.R. Cothern and P.A. Rebers (eds.), *Radon, Radium and Uranium in Drinking Water*, Lewis Publishers, Chelsea, Michigan, 83–95.

Nadeau, P.H., and R.C. Reynolds Jr., 1981. "Burial and contact metamorphism in the Mancos Shale," *Clays and Clay Minerals*, 29: 249–259.

Noe, D.C., M.L. Morgan, P.R. Hanson, and S.M. Keller, 2007a. *Geologic Map of the Montrose East Quadrangle, Montrose County, Colorado*, Colorado Geol. Survey Open-File Report 07-02, scale 1:24,000.

Noe, D.C., J.D. Higgins, and H.W. Olsen, 2007b. "Steeply dipping heaving bedrock, Colorado: Part 2 - Mineralogical and engineering properties," *Environmental and Engineering Geoscience*, 13: 309−324.

Nolan, B.T., and M.L. Clark, 1997. "Selenium in irrigated agricultural areas of the Western United States," *J. Environ. Qual.*, 26: 849–857.

NPS, 2011. *Yucca House National Monument Visitor Guide*, U.S. Department of Interior National Park Service, http://www.nps.gov/yuho/historyculture/index.htm, accessed January 2011.

Osmond, J.K., and J.B. Cowart, 1976. "The theory and uses of natural uranium isotopic variations in hydrology," *Atomic Energy Review*, 144: 621–679.

Palsey, M.A., G.W. Riley, D. Nummedal, and R. Sassen, 1989. "Stratigraphic significance of organic matter variations—example from Mancos Shale and Tocito Sandstone, San Juan Basin, New Mexico," Abstract, *Amer. Assoc. Petrol. Geol. Bull.*, 73: 1169–1170.

Palsey, M.A., W.A. Gregory, and G.F. Hart, 1991. "Organic matter variation in transgressive and regressive shales," *Org. Geochem.*, 17: 483–509.

Parkhurst, D.L., and C.A.J. Appelo, 1999. *User's Guide to PHREEQC (Version 2)—A Computer Program for Speciation, Bath-Reaction, One-Dimensional Transport, and Inverse Geochemical Calculations*, U.S. Geol. Survey Water-Resources Investigations Report 99-4259, Denver, 321 pp.

Petit, J.C., Y. Langevin, and J.C. Dran, 1985. "^{234}U/^{238}U disequilibrium in nature: theoretical reassessment of the various proposed models," *Bull. Minéral.*, 108: 745–753.

Petsch, S.T., R.A. Berner, and T.I. Eglinton, 2000. "A field study of the chemical weathering of ancient sedimentary organic matter," *Organic Geochemistry*, 31: 475–487.

Pliler, R., and J.A.S. Adams, 1962. "The distribution of thorium, uranium, and potassium in the Mancos Shale," *Geochim. et Cosmochim Acta*, 26: 1115–1135.

Ponce, S.L., and R.H. Hawkins, 1978. "Salt pickup by overland flow in the Price River Basin, Utah," *Water Resources Bull.* 14: 1187–1200.

Pottorff, E.J., M.P. Wickham, J.S. Waples, and B. Bertram, 2005. "Case study of selenium mobilization from Mancos Shale: Relationship to nitrate contamination," Geol. Soc. Amer. Rocky Mountain Section, 57th Annual Meeting (May 23–25, 2005, Grand Junction, Colorado), *Geol. Soc. Amer. Abstracts with Programs,* 37: 45.

Quinby-Hunt, M.S., P. Wilde, C.J. Orth, and W.B.N. Berry, 1989. "Elemental geochemistry of black shales—Statistical comparison of low-calcic shales with other shales," in R.I. Grauch and J.S. Leventhal (eds.), *Metaliferous Black Shales and Related Ore Deposits-Program and Abstracts*, U.S. Geol. Survey Circular 1037, Denver, Colorado, 8–15.

Rao, B.K., D.S. Bowles, and G.J. Wagenet, 1984. "Salt efflorescence in Price River Basin," *J. Environ. Eng.*, 110: 457–471.

Reuter, J.H., and E.M. Perdue, 1977. "Importance of heavy metal-organic matter interactions in natural waters," *Geochim. et Cosmochim. Acta*, 41: 325–334.

Rosholt, J.N., W.R. Shields, and E.L. Garner, 1963. "Isotopic fractionation of uranium in sandstone," *Science*, 139: 224–226.

Schultz, L.G., 1964. *Quantitative Interpretation of Mineralogical Composition from X-ray and Chemical Data for the Pierre Shale*, U.S. Geol. Survey Professional Paper 391-C, 31 pp.

Schultz, L.G., H.A. Tourtelot, J.R. Gill, and J.G. Boerngen, 1980. *Composition and Properties of the Pierre Shale and Equivalent Rocks, Northern Great Plains Region,* U.S. Geol. Survey Professional Paper 1064-B, U.S. Government Printing Office, Washington, 114 pp.

Shannon, S.S., Jr., 1979. *Uranium Hydrogeochemical and Stream Sediment Reconnaissance of the Lamar NTMS Quadrangle, Colorado, Including Concentrations of Forty-Three Additional Elements*, Informal Report LA-7342-MS, Los Alamos Scientific Laboratory, Los Alamos, New Mexico.

Shawe, D.R., 1968. *Coincidence of fossil and lithologic zones in the lower part of Upper Cretaceous Mancos Shale, Slick Rock District, Colorado*, U.S. Geol. Survey Professional Paper 600-C, pp C66–C68.

Shawe, D.R., 1976. *Sedimentary Rock Alteration in the Slick Rock District, San Miguel and Dolores Counties, Colorado*, Geological Survey Professional Paper 576-D, U.S. Government Printing Office, Washington, D.C., 51 pp.

Spieker, E.M., and J.B. Reeside, 1925. "Cretaceous and Tertiary formations of the Wasatch Plateau, Utah," *Geol. Soc. Amer. Bull.*, 66: 177–202.

Stillings, L.L., M.L.W. Tuttle, R.I. Grauch, J.W. Fahy, B.A. Ball, and K.E. Livo, 2005. "Physical and chemical indicators of weathering in soils of the Mancos Shale, Gunnison Gorge National Conservation Area, CO, USA," Geol. Soc. Amer. Rocky Mountain Section, 57th Annual Meeting (May 23–25, 2005, Grand Junction, Colorado), *Geol. Soc. Amer. Abstracts with Programs,* 37: 45.

Stumm, W., and J.J. Morgan, 1981. *Aquatic Chemistry, 2nd Edition*, John Wiley & Sons, New York, 780 pp.

Suksi, J., K. Rasilainen, and P. Pitkänen, 2006. "Variations in $^{234}U/^{238}U$ activity ratios in groundwater—A key to flow system characterization?," *Physics and Chemistry of the Earth*, 31: 556–571.

Sunday, G.K., 1979. *Role of Rill Development in Salt Loading from Hillslopes*, M.S. Thesis, Colorado State Univ., Fort Collins, Colorado, 107 pp.

Swanson, V.E., 1961. *Geology and Geochemistry of Uranium in Marine Black Shales A Review*, Geol. Survey Professional Paper 356-C, U.S. Government Printing Office, Washington, 112 pp.

Thomas, C.L., R.M. Wilson, J.D. Lusk, R.S. Bristol, and A.R. Shineman, 1998. *Detailed Study of Selenium and Selected Constituents in Water, Bottom Sediment, Soil, and Biota Associated With Irrigation Drainage in the San Juan River Area, New Mexico, 1991–95*, U.S. Geol. Survey Open-File Report 98-4096 (also listed as Water-Resources Investigations Report 98-4096), Albuquerque, New Mexico, 84 pp.

Thomas, J.C., K.J. Leib, J.M. Mayo, 2008. *Analysis of Dissolved Selenium Loading for Selected Sites in the Lower Gunnison River Basin, Colorado, 1978–2005*, U.S. Geol. Survey, Scientific Investigations Report 2007-5287, Reston, Virginia, 25 pp.

Thomas, J.C., 2009. *Analysis of Dissolved Selenium Loading from Surface Water and Groundwater to Sweitzer Lake, Colorado, 2006–07*, U.S. Geol. Survey Scientific Investigations Report 2009-5048, Reston, Virginia, 17 pp.

Tourtelot, H.A., 1962. *Preliminary Investigation of the Geologic Setting and Chemical Composition of the Pierre Shale Great Plains Region*, U.S. Geol. Survey Professional Paper 390, U.S. Government Printing Office, Washington, D.C., 74 pp.

Tuttle, M.L., and R.I. Grauch, 2009. *Salinization of the Upper Colorado River-Fingerprinting Geologic Salt Sources*, U.S. Geol. Survey Scientific Investigations Report 2009-5072, 62 pp.

Tuttle, M.L.W., J.W. Fahy, R.I. Grauch, and L.L. Stillings, 2005. "Salt and selenium in Mancos Shale terrane on the Gunnison Gorge National Conservation Area, Western Colorado, USA," Geol. Soc. Amer. Rocky Mountain Section, 57th Annual Meeting (May 23–25, 2005, Grand Junction, Colorado), *Geol. Soc. Amer. Abstracts with Programs,* 37: 45.

Tuttle, M.L.W., J. Fahy, R.I. Grauch, K.E. Kivo, B. Ball, and L.L. Stillings, as listed in suggested citation (authors listed on report cover are M.L.W. Tuttle, J. Fahy, R.I. Grauch, B.A. Ball, G.W. Chong, J.G. Elliott, J.J. Kosovich, K.E. Livo, and L.L. Stillings), 2007. *Results of Chemical Analyses of Soil, Shale, and Soil/Shale Extract from the Mancos Shale Formation in the Gunnison Gorge National Conservation Area, Southwestern Colorado, and at Hanksville, Utah*, U.S. Geol. Survey Open-File Report 2007-1002D, Reston, Virginia, 24 pp.

USGS (U.S. Geological Survey), 2011a. *U. S. Geological Survey National Water Information Service Web Interface*, http://waterdata.usgs.gov/nwis/

USGS (U.S. Geological Survey), 2011b. *U.S. Geological Survey National Geochemical Database*, reformatted data from the National Uranium Resource Evaluation (NURE) Hydrogeochemical and Stream Sediment Reconnaissance (HSSR) Program, http://pubs.usgs.gov/of/1997/ofr-97-0492/

Vine, J.D., V.E. Swanson, and K.G. Ball, 1958. "The role of humic acids in the geochemistry of uranium," *Second Internat. Conf. on Peaceful Uses of Atomic Energy Proc.*, Geneva, Switzerland, 2: 187−191.

Wagenet, R.J., and J.J. Jurinak, 1978. "Spatial variability of soluble salt content in a Mancos Shale watershed," *Soil Science*, 126: 342–349.

Whittig, L.D., A.E. Deyo, and K.K. Tanji, 1982. "Evaporite mineral species in Mancos Shale and salt efflorescence, Upper Colorado River Basin," *Soil Sci. Am. J.*, 46: 645–651.

Whittig, L.D., K.K. Tanji, J.W. Biggar, V.P. Evangelou, and A.E. Deyo, 1983. *Salinity Investigation in the West Salt Creek Watershed, Colorado*, University of California, Davis, 160 pp.

Whittig, L.D. A.E. Deyo, K.K. Tanji, and C.G. Higgins, 1986. *Delineation and Correlation of Salinity to Landforms and Geologic Formation, Upper Colorado River Basin*, Land, Air and Water Resources Paper No. 100012, University of California, Davis, 143 pp.

Wright, W.G., and D.L. Butler, 1993. "Distribution and mobilization of dissolved selenium in groundwater of the irrigated Grand and Uncompahgre Valleys, Western Colorado," in *Management of Irrigation and Drainage Systems Integrated Perspectives*, American Society Civil Engineers, New York, 770–777.

Wright, W.G., 1995. "Nitrogen fertilizer as an oxidizing agent to mobilize trace constituents from soil," *Water Resource and Environmental Hazards: Emphasis on Hydrologic and Cultural Insight in the Pacific Rim,* Proc. of Summer Symp., Honolulu, Hawaii, June 1995, American Water Resources Assoc., Herndon, Virginia, 483–490.

Wright, W.G., 1999. "Oxidation and mobilization of selenium by nitrate in irrigation drainage," *J. Environ. Qual.*, 28: 1182–1187.

Wright, W.G., 2006. *Hydrology and Geochemistry of Yucca House National Monument and Surrounding Area, Southwestern Colorado*, Hydrological Studies Report 2006-1, Southwest Hydro-Logic, Durango, Colorado, 46 pp.

Zielinski, R.A., S. Asher-Bolinder, and A.L. Meier, 1995. "Uraniferous waters of the Arkansas River valley, Colorado: a function of geology and land use," *Applied Geochemistry*, 10: 133−144.

Zielinski, R.A., D.T. Chafin, E.R. Banta, and B.J. Szabo, 1997. "Use of ^{234}U and ^{238}U isotopes to evaluate contamination of near-surface groundwater with uranium-mill effluent: a case study in south-central Colorado, U.S.A.," *Environ. Geol.*, 32: 124–136.

Appendix A

Site Information

This page intentionally left blank

Location	ID	Latitude	Longitude	USGS Site No.	Geologic Unit	Region	Area
Seeps and Springs							
Bert Avery Spring	BAS	38.26847466	-110.8225768	381603110491901	Ferron Sandstone	Hanksville	
Blue Gate Spring	BGS	39.2207617	-110.9513918	391315110570301	Blue Gate	Price	
Buen Pastor Spring	BPS	38.70697125	-108.0353522		middle Smoky Hill	Delta	Sweitzer Lake
Bitter Spring Creek Spring	BSCS	37.91682206	-111.0217921	375458111011901	Emery Sandstone	Hanksville	
Bitter Spring Creek Upper Spring	BSCUS	37.916988	-111.021816		Emery Sandstone	Hanksville	
Browns Wash Seep	BWS	38.98516015	-109.9522626	385906109570601	Upper Blue Gate	Green River	
Cato Springs	CAS	39.13246669	-109.3674558	390758109220201	Upper Blue Gate	Green River	
Cedar Creek Seep	CCS	38.458021	-107.673677		upper or middle Mancos	Montrose	Cerro Summit
Cisco Springs	CIS	39.08870947	-109.3822425	390519109230001	Prairie Canyon	Green River	
Cottonwood Creek Spring	CWCS	38.27976	-110.861307	381639110513801	Ferron Sandstone	Hanksville	
Ditch 9 Spring	D9S	36.85511911	-108.7483559		Cortez	Shiprock	Shiprock
Daly Reservoir Spring 1	DARS1	38.97021006	-109.9710173		upper Prairie Canyon	Green River	Daly Reservoir
Daly Reservoir Spring 2	DARS2	38.97056543	-109.9711552		upper Prairie Canyon	Green River	Daly Reservoir
Delta Reservoir Dam Spring	DRDS	38.809687	-108.069081		Prairie Canyon	Delta	Delta Reservoir
Delta Reservoir Seep 1	DRS1	38.810393	-108.063758		Prairie Canyon	Delta	Delta Reservoir
Delta Reservoir Seep 3	DRS3	38.808375	-108.064455		Prairie Canyon	Delta	Delta Reservoir
Devils Thumb Seep 1	DTS1	38.79759965	-108.0544136		upper Smoky Hill	Delta	Devil's Thumb Golf Course
Devils Thumb Seep 2	DTS2	38.78388498	-108.053317		middle Smoky Hill	Delta	Devil's Thumb Golf Course
Devils Thumb Seep 3	DTS3	38.78344064	-108.0546702		middle Smoky Hill	Delta	Devil's Thumb Golf Course
Dutchmans Wash Seep	DWS	39.22153704	-110.9688968		Blue Gate	Price	
East Tributary Floy Wash	ETFW	38.96177	-109.904612		upper Blue Gate	Green River	
Green River Canal Return Seep	GRCRS	39.04252778	-110.1511944	390233110090401	upper Blue Gate	Green River	
Houston Gulch Seep	HGS	38.471966	-107.700601		upper or middle Mancos	Montrose	Cerro Summit
Houston Gulch Seep East	HGSE	38.471886	-107.700554		upper or middle Mancos	Montrose	Cerro Summit
Kannah Creek Flowline Spring	KCFS	39.006019	-108.462288		lower Smoky Hill	Delta	Whitewater
Little Grand Wash Seep	LGWS	38.88477648	-109.9658041		lower Blue Gate	Green River	
Loutsenhizer 11	LOUT11	38.544654	-107.7773699		upper or middle Mancos	Delta	Loutsenhizer Arroyo
Loutsenhizer 12 Lower	LOUT12L	38.5450158	-107.776946		upper or middle Mancos	Delta	Loutsenhizer Arroyo

Location	ID	Latitude	Longitude	USGS Site No.	Geologic Unit	Region	Area
Loutsenhizer 12 Upper	LOUT12U	38.545237	-107.776984		upper or middle Mancos	Delta	Loutsenhizer Arroyo
Loutsenhizer 13	LOUT13	38.543799	-107.778448		upper or middle Mancos	Delta	Loutsenhizer Arroyo
Loutsenhizer 14	LOUT14	38.540524	-107.784051		upper or middle Mancos	Delta	Loutsenhizer Arroyo
Loutsenhizer 3	LOUT3	38.5399	-107.787952		upper or middle Mancos	Delta	Loutsenhizer Arroyo
Loutsenhizer 8	LOUT8	38.544899	-107.784986	383242107470401	upper or middle Mancos	Delta	Loutsenhizer Arroyo
Loutsenhizer 9	LOUT9	38.55241793	-107.7799697	383307107454701	upper or middle Mancos	Delta	Loutsenhizer Arroyo
Many Devils Wash EF-22	EF-22	36.759505	-108.678292		Cortez	Shiprock	Shiprock
Mud Spring	MS	39.51934353	-110.5325294	393103110315901	middle Mancos	Price	
Mathis Wash Seep	MWS	39.44309801	-110.7881307		Blue Gate	Price	
Point Creek Seep	PCS	38.84549654	-108.1921318	385043108112901	upper Prairie Canyon	Delta	
Section 36 Spring	S36	38.93193402	-109.4255796		middle Blue Gate	Green River	
Salt Creek Wash Seep	SCWS	36.84469614	-108.6501375		Cortez	Shiprock	Shiprock
Sweitzer NE Seep	SNS	38.71654655	-108.0231702		upper Smoky Hill	Delta	Sweitzer Lake
Sweitzer NE Seep 1	SNS1	38.71649529	-108.0238606		upper Smoky Hill	Delta	Sweitzer Lake
Sweitzer NE Seep 2	SNS2	38.71656063	-108.0235525		upper Smoky Hill	Delta	Sweitzer Lake
Sweitzer NE Seep 3	SNS3	38.71684347	-108.0231466		upper Smoky Hill	Delta	Sweitzer Lake
Town Wash Spring	TWS	38.28946022	-110.84917	381721110505401	Ferron Sandstone	Hanksville	
Upper Eagle Nest Arroyo Spring	UENAS	36.80853481	-108.560075		Cortez	Shiprock	Shiprock
Upper Floy Wash Spring	UFWS	38.96103007	-109.9056714	385738109541901	upper Blue Gate	Green River	
USGS Seep 1	US1	38.71211716	-108.02314	*	upper Smoky Hill	Delta	Sweitzer Lake
Whitewater Creek Tributary Seep	WCTS	38.99507784	-108.3979729		Smoky Hill	Delta	Whitewater
Whitewater Ditch No. 2 Seep	WD2S	38.96777266	-108.4276475		Blue Hill	Delta	Whitewater
Yucca House Spring	YHS	37.250161	-108.686194	371500108410801	Juana Lopez	Shiprock	
Surface Water Bodies (Sources of Seeps or Springs)							
Bostwick Canal West Lateral	BCWL	38.54883569	-107.7753634		upper Mancos	Delta	Loutsenhizer Arroyo
Daly Reservoir	DAR	38.96965	-109.970598		upper Prairie Canyon	Green River	Daly Reservoir
Delta Reservoir	DR	38.810042	-108.068961		Prairie Canyon	Delta	Delta Reservoir
Sweitzer Lake	SL	38.711165	-108.033135		upper Smoky Hill	Delta	Sweitzer Lake
Sweitzer NE Garnet Canal	SNGC	38.716557	-108.02296		upper Smoky Hill	Delta	Sweitzer Lake
Whitewater Ditch No. 2	WD2	38.948979	-108.413333			Delta	Whitewater

Location	ID	Latitude	Longitude	USGS Site No.	Geologic Unit	Region	Area
Pools and Washes Near Seeps and Springs							
Cottonwood Wash at Cato Springs	CWC	39.132553	-109.367508		upper Blue Gate	Green River	
East Tributary Floy Wash Downstream	ETFWD	38.96161	-109.904595		upper Blue Gate	Green River	
Houston Gulch Red Pool	HGRP	38.471794	-107.700532		upper or middle Mancos	Montrose	Cerro Summit
Little Grand Wash	LGW	38.884758	-109.965785		lower Blue Gate	Green River	
Loutsenhizer 11 in Wash	LOUT11W	38.54464	-107.777341		upper or middle Mancos	Delta	Loutsenhizer Arroyo
Sweitzer Red Pool	SRP	38.71186071	-108.0233965		upper Smoky Hill	Delta	Sweitzer Lake
Town Wash Spring Pool	TWSP	38.289408	-110.84918		Ferron Sandstone	Hanksville	
Upper Floy Wash-30 ft from Spring	UFWS1	38.96095	-109.905626		upper Blue Gate	Green River	
Upper Floy Wash-50 ft from Spring	UFWS2	38.960901	-109.90559		upper Blue Gate	Green River	
Whitewater Creek Tributary Seep Pool 1	WCTSP1	38.995092	-108.397974		Smoky Hill	Delta	Whitewater
Whitewater Creek Tributary Seep Pool 2	WCTSP2	38.995119	-108.398076		Smoky Hill	Delta	Whitewater
West Fork Floy Wash	WFFW	38.974718	-109.90538	385829109541601	upper Blue Gate	Green River	

* USGS site referenced in Thomas (2009)

This page intentionally left blank

Appendix B

Calculation of Water Density from Specific Conductivity

This page intentionally left blank

Calculation of Water Density from Specific Conductivity

Salinity was derived from a relationship based on conductivity, which was in turn estimated from measurements of specific conductivity collected in the field. Conductivity is a direct measure of the ability of a solution to carry an electrical current normalized to the area of the conductor, whereas specific conductivity is conductivity that the solution would have at 25 °C.

Specific conductivity (SC) was converted to conductivity (C_t) using a relationship in Standard Method 2510 B:

$$C_t = SC \times [1 + 0.0191 \times (T - 25)], \text{ where T is temperature in °C.}$$

Salinity (S) was then calculated from conductivity using:

$$S = a_0 + a_1R_t^{1/2} + a_2R_t + a_3R_t^{3/2} + a_4R_t^2 + a_5R_t^{5/2} + f(T) \times (b_0 + b_1R_t^{1/2} + b_2R_t + b_3R_t^{3/2} + b_4R_t^2 + b_5R_t^{5/2}) - a_0/(1 + 1.5X + X^2) - b_0f(T)/(1 + Y^{1/2} + Y^{3/2})$$

where: $a_0 = 0.0080$, $a_1 = -0.1692$, $a_2 = 25.3851$, $a_3 = 14.0941$, $a_4 = -7.0261$, $a_5 = 2.7081$,
$b_0 = 0.0005$, $b_1 = -0.0056$, $b_2 = -0.0066$, $b_3 = -0.0375$, $b_4 = 0.0636$, $b_5 = -0.0144$, and
$R_t = C_t/(r_0 + r_1T + r_2T^2 + r_3T^3)$
$X = 400R_t$
$Y = 100R_t$
$f(T) = (T - 15)/[1 + 0.0162(T - 15)]$

where: $r_0 = 30332$, $r_1 = 844.33$, $r_2 = 3.8331$, $r_3 = -0.0282$

The constants r_0, r_1, r_2, and r_3 were determined in our laboratory from the temperature dependency of conductivity measured with our field sonde in artificial seawater simulated by a potassium chloride (KCl) solution containing 32.4356 g in a mass of 1 kilogram (kg) of solution (Standard Method 2520 B).

Density (ρ) in grams per cubic centimeter (g/cm^3) was calculated from salinity (S) using Standard Method 2520 C:

$$\rho = (\rho_0 + aS + bS^{3/2} + cS^2)/1{,}000$$

where:
$\rho_0 = 999.842594 + 0.06793952T - 0.00909529T^2 + 1.001685 \times 10^{-4}T^3 - 1.120083 \times 10^{-6}T^4 + 6.536332 \times 10^{-9}T^5$
$a = 0.824493 - 0.0040899T + 7.6438 \times 10^{-5}T^2 - 8.2467 \times 10^{-7}T^3 + 5.3875 \times 10^{-9}T^4$
$b = -0.00572466 + 1.0227 \times 10^{-4}T - 1.6546 \times 10^{-6}T^2$
$c = 0.00048314$

This page intentionally left blank

Appendix C

Analytical Data

This page intentionally left blank

ID	Sample	Temp	pH	Sp Cond	ORP	DO	Alk	Cl	NO3	SO4	NH3-N	U	Fe	Ca	Na	Mg	K	IRB	DOC	Color	pH	222Rn	Se	As	B	V	U233+234	U235	U238
	Date/Time	deg C		uS/cm	mV	mg/L	mg/L*	mg/L	mg/L	mg/L	mg/L	µg/L	mg/L	mg/L	mg/L	mg/L	mg/L	CFU/mL	mg/L	pt units		pCi/L	ug/L	ug/L	ug/L	ug/L	pCi/L	pCi/L	pCi/L
ACS	11/15/10 0:00	7.78	6.94	16362	**244**	0.3																							
BAS	11/17/10 14:00	10.75	7.29	418	-28	2.35	129	12	**0.5**	67		0.2	1.55	48	26	9.8	1.4	500	4.4	81	7.12	144	0.18	0.94	16	0.28	**0.284**	0.246	0.322
BCWL	11/4/10 12:30		8.53	197	201		64	0.9	1.7	27		0.4	**0.2**	22.1	5.8	4.6	2.4	35000	3.3	7	7.79	1.2	0.18	0.37	**3.1**	0.98	0.472	**0**	0.296
BGS	11/16/10 11:30	7.68	6.87	6203	-30	**7.16**	58	287	2.3	3911		1	0.57	412	780	400	14.8	9000	9.1	18	6.88	53	0.37	0.33	860	0.16	0.637	**0.159**	**0.081**
BPS	11/30/10 14:14	4.61	7.49	5639	33	7.09	365	62	1.9	3707		22.6	2	376	1200	210	15.8	35000	12.2	59	7.38	130	3.8	0.36	570	0.37	18.2	**0.168**	7.98
BSCS	11/18/10 13:40	8.58	7.05	2037	307	0.45						65.3																	
BSCUS	11/18/10 13:28	9.56	6.95	1079	198	**2.1**																							
BWS	11/12/10 10:20	4.78	7.74	10798	245	2.76	359	267	15	9853		26.6	1	468	3000	720	1.2	140000	19.5	65	7.67	316.3	25	0.48	240	0.47	16	0.484	8.54
CAS	11/11/10 10:25	10.97	7.58	2184	-65	0.34	625	21	1.7	762		7.6	2.03	73.2	355	135	3.6	9000	10.7	156	7.34	416.9	0.14	4.5	79	0.56	4.25	**0.0641**	1.83
CCS	11/3/10 10:30	10.85	6.55	16409	228	4.32	644	1430	2.9	9933		76.7	1	454	3300	1000	26.6	35000	25	23	7.32	1624.5	12	0.23	1200	**0.15**	38.9	1.44	23.5
CIS	11/11/10 12:18	9.28	7.56	3947	68	1.5						13.5																	
CWC	11/11/10 10:25	2.27	8.46	1112	218	12.38																							
CWCS	11/17/10 13:12	7.18	7.07	5965	-92	0.89	390	137	1.7	3532		15.4	0.79	392	870	210	4.1	35000	7.8	133	7.27	266	1.3	0.58	320	0.54	6.98	0.484	3.64
D9S	12/2/10 15:45	13.28	7.01	4045	174	1.66	329	33	38	2459		42	**0.2**	478	310	200	13.2	150	9.8	34	7.21	793	54	0.2	730	0.24	30	0.783	14.8
DAR	11/12/10 11:40	6.39	8.27	1720	168	9.56	55	24	3.7	941		0.8	**0.2**	256	120	15.5	12	9000	7.1	11	7.74	0.9	2.5	0.41	89	0.15	0.864	**0.0314**	0.282
DARS1	11/12/10 11:40	14.40	7.88	9187	149	0.47	305	97	150	5729		39.7	**0.2**	356	1860	250	23.6	500	17	202	7.79	715.4	110	0.36	570	0.52	24.9	1.12	12.5
DARS2	11/12/10 11:40	16.06	7.71	15377	124	0.8	335	175	449	9865		33.2	**0.2**	356	3650	320	33.6	140000	41	430	7.76	442	400	0.37	560	0.59	22.7	0.565	11.5
DR	11/8/10 11:24	9.77	8.71	114	193	7.82	47	2.8	**0.5**	4.1		0.2	**0.2**	14.1	2.4	4.1	1.5	9000	12.4	1	8.48	1	0.058	0.34	**3.1**	1.4	0.21	**-0.0512**	**0.131**
DRDS	11/8/10 11:44	14.58	7.97	793	145	5.55	101	1.1	8.2	312		3.2	**0.2**	146	9.3	9	1.2	9000	2.9	1	7.76	311.2	0.41	1.3	24	0.66	1.31	**0.0306**	1.07
DRS1	11/8/10 14:01	10.37	7.16	27250	174	1.75	925	1270	534	18497		119.1	1	377	7600	600	26.8	540000	16	170	7.25	233.3	950	0.2	550	0.35	108	1.9	41.5
DRS3	11/8/10 15:02	15.18	7.25	22840	198	3.58	1045	798	76	15087		137.2	1	410	5900	600	34.6	35000	44	350	7.48	352.9	100	3	690	0.84	98.6	3.74	47.9
DTS1	12/7/10 10:26	1.86	7.11	13503	227	1.82	407	388	413	7698		100.7	**0.2**	330	3000	440	19.5	2300	20.1	143	7.38	792	990	0.26	380	0.56	69.7	1.47	30.5
DTS2	12/7/10 14:11	11.59	7.25	8724	166	5.24	492	387	389	4905		58.4	**0.2**	424	1500	440	32	2300	23	184	7.44	208	600	0.43	760	1.2	44.9	1.26	19.1
DTS3	12/7/10 12:57	8.02	6.99	6576	172	0.4	338	146	6.1	4273		36.5	**0.2**	390	820	420	17.8	9000	13.3	95	7.24	1049	12	0.24	550	0.34	29.5	0.693	13.9
DWS	11/16/10 12:05	3.57	8.45	48519	108	8.1	882	1032	2.9	49063		329.1	2	426	15200	2150	71.5	150	81	380	8.21	1	10	1.2	430	1.4	253	5.74	101
EF-22	12/2/10 17:02	8.15	7.45	37064	230	0.57	662	1925	3189	22552		173.6	0.4	360	9200	1300	34	150	59	211	7.5	407	2300	0.91	510	3.3	139	2.87	57
ETFW	11/11/10 14:00	10.05	7.87	21315	139	2.25						38.1																	
ETFWD	11/11/10 14:00			6300																									
GRCRS	11/12/10 8:32	6.92	7.24	3847	191	5.6	370	45	1.9	2209		21.1	0.24	530	395	100	7.2	2300	28	136	7.5		3.6	0.69	310	0.64	13	**0.0813**	7.38
GS	12/2/10 12:15											34.2																	
HGRP	11/3/10 12:25	8.21	7.82	45645	166	**5.1**																							
HGS	11/3/10 12:10	19.45	7.36	22790	136	2.35	690	102	1371	22540	1	353.9	8	450	2550	3300	47	9000	67	575	7.78	119.4	890	1.8	940	1.4	201	8.97	135
HGSE	11/3/10 0:00	9.08	6.88	21658	169	3.4																							
KCFS	11/2/10 12:00	10.90	7.22	26250	221	**3.32**	417	927	2216	16012	1	26.6	**0.2**	404	7200	520	36.4	2300	24	142	7.6	544.3	1400	0.15	500	0.2	37.1	0.744	9.09
LGW	11/12/10 14:15	2.60	8	1326	107	7.18																							
LGWS	11/12/10 14:15	3.87	7.25	1637	**10**	0.98	75	20	9	616		1.5	**0.2**	161	96	6.2	14	9000	12.3	49	7.59	1	16	0.39	41	0.62	2.02	**0.157**	0.895
LOUT11	11/3/10 16:00			11600																									
LOUT11W	11/3/10 16:05			315																									
LOUT12L	11/3/10 15:20	11.20	7.04	6220	252	7.04																							
LOUT12U	11/3/10 15:00	13.36	6.13	5190	281	6.7	310	176	151	3014		89.1	**0.4**	410	640	230	9.9	9000	15.6	79	7.27	452.2	1300	0.24	810	0.65	48.3	1.48	27.2
LOUT13	11/3/10 16:15			5880																									
LOUT14	11/3/10 17:20			17700																									
LOUT3	11/3/10 17:30	11.97	7.03	15330	228	2.65		818	459	8820		102.6	2	480	3700	420	28.8	9000	53	309	7.62	107.4	2000	0.66	1100	3.1	59.8	1.97	35
LOUT3	11/4/10 8:05						384														1								
LOUT8	11/4/10 10:15	11.74	7.91	22130	250		428	928	3361	14942	1	135.2	2	448	6700	720	37	35000	112	605	7.8	433	4700	0.6	990	1.1	68.5	2.08	36.6
LOUT9	11/4/10 11:15	15.65	7.54	8844	197		633	79	342	5696		101.6	**0.4**	430	1220	680	28.8	9000	21	172	7.23	455.3	730	0.22	1200	0.36	58.1	2.01	34
MS	11/16/10 14:50	10.51	7.41	1650	66	3.72	351	53	3.9	553		9.7	**0.2**	72	166	110	1.8	9000	5.8	71	7.52	947	17	0.35	230	2.3	5.65	**0.0582**	4.06
MWS	11/16/10 13:35	7.69	7.77	70002	255	3	1295	3382	33.5	76922		480.5	0.53	600	22750	7000	14.4		265	1962	7.88								
PCS	11/8/10 8:46	9.82	7.56	10739	277	2.62	610	250	**0.5**	7282		217.6	1	436	1720	640	29	35000	15	60	7.47	216.9	1.5	0.75	1400	0.24	114	2.88	72.4
S36	11/11/10 14:00	12.41	7.67	24522	164	2.62	479	436	841	17695		122.9	1	396	6500	840	23.6	2300	24	84	7.92	256.2	4100	0.36	260	0.47	79.2	1.13	35.9
SCWS	12/7/10 11:33	1.97	7.39	48639	238	1.62	1090	7098	3614	23800		160.3	**0.4**	448	15000	1400	62	140000	183	462	7.53	258	2100	0.68	800	1.1	150	2.58	53.3
SL	11/4/10 15:45	12.94	8.63	1728	-62		124	15.4	2.3	892		11.3	**0.2**	142.5	172	50	5.6	500	8.5	1	8.26	8.1	8.9	0.88	170	1.4	6.54	**0.195**	4.36
SNGC	11/4/10 14:43	9.95	8.12	6529	108		334	79	92	4134		32.8	**0.2**	346	1160	200	12.6	35000	31	65	8.1	49.8	110	0.56	530	1.1	21.4	0.424	10
SNS	11/4/10 14:35	8.09	8.45	68114	126			1982	18	78003	3	694.8	2	520	25000	1950	45		280	2560	8.46		3500	12	2000	19	468	15	243
SNS	11/30/10 11:39	2.25	8.13	36546	187	6.29						800.4																	
SNS1	11/30/10 11:25	3.44	7.56	53320	239	1.15						984.5																	
SNS2	11/30/10 12:18	4.23	8.3	33489	197	4.41						1921.7																	
SNS3	11/30/10 11:54	2.11	7.44	55959	190	0.61	1726	1589	4.1	47251		821.6	2	484	19000	2700	20.5	500	134	520	7.44	193	13	5.3	3200	3.7	489	14.4	280
SRP	11/4/10 15:15	16.35	7.61	39380	-255																								
SRP	11/30/10 15:06	8.02	7.47	35984	**59**	0.54						113.1																	
TWS	11/17/10 11:25	3.36	7.34	10018	-19	1.36	293	171	2.4	6524		13.2	0.31	374	1300	700	6.2	500	6.6	76	7.56	221	1.7	0.62	89	0.28	7.34	0.354	2.61
TWSP	11/17/10 10:50	7.77	6.99	5630	**-40**	**1.3**																							
UENAS	12/2/10 10:00	8.42	7.3	26607	224	2.66	368	4172	1074	12839		53	0.3	474	5900	1050	21.5	150	161	24	7.37	403	540	0.23	700	0.3	31.3	0.794	14.7
UFWS	11/11/10 0:00	9.46	7.64	6514	100	3.14						9.5																	
UFWS1	11/11/10 0:00	10.57	7.75	2236	-75	0.07																							
UFWS2	11/11/10 0:00	8.92	7.47	2236	-119	0.72																							
US1	11/30/10 15:23	2.85	8.35	41615	127	6.42						361.9																	
WCTS	12/7/10 16:22											700								261	1504	7.74								
WCTS	12/7/10 16:26											487.7								126	570	7.87	76							
WCTSP1	12/7/10 16:26	3.85	8.49	47655	205																								
WCTSP2	12/7/10 16:26			67475																									
WD2	11/2/10 14:10	8.13	6.57	2185	234		221	18	2.5	1085		24.3	**0.2**	266	138	92	4.5	2300	7.9	24	8.03	12.6	15	0.69	310	0.63	10.2	0.526	6.39
WD2S	11/2/10 13:20	11.33	4.15	14285	258	4.06	**0**	171	**0.5**	10820		1	16.7	380	2950	720	20.2	**25**	36	272	4.48	316.8	5.6	2.8	1500	0.19	**0.249**	-0.0638	**0.19**
WFFW	11/11/10 16:30			21000								57.4																	
YHS	12/1/10 13:30	9.92	7	1442	130	1.9	317	29	2	463		9.4	**0.2**	164	92	56	0.9	140000	8.9	1	7.18	811	5.9	0.2	150	1	7.21	**0.105**	2.93

* Alkalinity in mg/L as CaCO3.

Bold = detection limit

This page intentionally left blank